Targeting the Brain in Brain-Computer Interfacing: The Effect of Transcranial Current Stimulation and Control of a Physical Effector on Performance and Electrophysiology Underlying Noninvasive Brain-Computer Interfaces

A Dissertation
SUBMITTED TO THE FACULTY OF
UNIVERSITY OF MINNESOTA
BY

Bryan Scott Baxter

IN PARTIAL FULFILLMENT OF THE REQUIREMENTS
FOR THE DEGREE OF
DOCTOR OF PHILOSOPHY

Advisor: Bin He, PhD

July 2017

Acknowledgements

First, I would like to thank Dr. Bin He for his support and encouragement over the course of my PhD while performing this research.

I would also like to thank the members of my committee: Dr. Matthew Johnson for his support in discussing the tDCS work of the course of my PhD and for the discussions of ethical issues in academia and neuromodulation; Dr. Hubert Lim for the committee discussions and the conference outings; Dr. Tim Ebner for allowing me to work in his lab on other aspects of neuromodulation and bringing a neuroscience perspective to this work; and Tay Netoff for his questions and recommendations to improve this work.

I would like to thank the members of the He lab and the Biomedical Engineering graduate program for their discussion and support. Rachel Jorgenson for her administrative support and responding to last minute deadlines. Dr. Xiaotong Zhang was always there with coffee when needed and support in MRI and modeling matters. Dr. Abhrajeet Roy for the experimental and moral support from the start and Brad Edelman for the hospitality and hours spent discussing the state of BCIs - it would have been a lot tougher without you two around. Abbas Sohrabpour for signal processing discussions and evening conversations on the quirks of the English language. I would also like to thank my undergraduate assistants, in particular, Andrew Decker for his help in programming the robotic arm, Albert You for experimentation assistance and for expanding my knowledge of Rubik's cubes, and Nick Nesbitt for experimentation and analysis assistance.

I would also like to thank my friends and family: AnnaMarie Vu for the support over these years and all the scientific discussions, and for always bringing a clinical and human-centered perspective when I get excited about over-engineering a solution. Trung Vu and Van Nguyen for their support and encouragement. Tim and Judy Baxter for fostering an interest in science and engineering from an early age. Amanda, Michael, and Rosemary Williams for their hospitality and support.

I would be remiss if I did not thank my previous mentors, in particular Drs. Winrich Freiwald, Gina Turrigiano, and Alexander Grunewald for teaching me how science should be done, which enabled me to get to get to this point.

Dedication

This thesis is dedicated to my family and friends.

Abstract

Brain-computer interfaces (BCIs) and neuromodulation technologies have recently begun to fulfill their promises of restoring function, improving rehabilitation, and enhancing abilities and learning. However, lengthy user training to achieve acceptable accuracy is a barrier to BCI acceptance and use by patients and the general population. Transcranial direct current stimulation (tDCS) is a noninvasive neuromodulation technology whereby a low level of electrical current is injected into the brain to alter neural activity and has been found to improve motor learning and task performance. A barrier to optimizing behavioral effects of tDCS is that we do not yet understand how neural networks are affected by stimulation and how stimulation interacts with ongoing endogenous activity. The purpose of this dissertation was to elucidate strategies to improve BCI control by targeting the user through two approaches: 1. Subject control of a robotic arm to enhance user motivation and 2. tDCS application to improve behavioral outcomes and alter networks underlying sensorimotor rhythm-based BCI performance. The primary results illustrate that targeted tDCS of the motor network interacts with task specific neural activity to improve BCI performance and alter neural electrophysiology. This effect on neural activity extended across the task network, beyond the area of direct stimulation, and altered connectivity unilaterally and bilaterally between frontal and parietal cortical regions. These findings suggest targeted neuromodulation interacts with endogenous neural activity and can be used to improve motor-cognitive task performance.

Table of Contents

List of Tables

List of Figures

Introduction

The brain is composed of hundreds of billions of cells communicating electrically through ions and chemically through neurotransmitters. The electrical properties of neurons allow for invasive and noninvasive bidirectional interfacing with the brain through neural decoding and neural stimulation. Noninvasive readout of electrical brain activity was first demonstrated in 1929 (Berger, 1929) and since then electroencephalography (EEG) has found uses in clinical applications, such as monitoring seizures, and basic and applied neuroscience to understand the response of the brain to external stimuli and internally generated states in health and disease (Schomer & Lopes da Silva, 2010). One of the primary proposed applications for decoding neural activity is to develop a brain-computer interface (BCI) that allows an individual to control any type of electronic device by thought alone (He, Gao, Yuan, & Wolpaw, 2013). The range of possibilities for this control spans from passive to active, from assistive to augmentative, and invasive to noninvasive (Wolpaw, Birbaumer, McFarland, Pfurtscheller, & Vaughan, 2002; Zander & Kothe, 2011). Interfacing a computer to the brain can be done through electrical stimulation to alter neural activity and behavior with proposed uses from enhancement to neuropsychiatric disorders (Coffman, Clark, & Parasuraman, 2014; Paulus, Nitsche, & Antal, 2016; Philip et al., 2017; Stagg & Nitsche, 2011). In this section, we give an overview of BCIs, then of noninvasive electrical stimulation of the brain, followed by a brief ethical discussion of the uses of these technologies.

Brain-Computer Interfaces

The field of brain-computer interfacing has two main branches: invasive

approaches that require surgery and noninvasive approaches that do not. Both have their advantages and disadvantages and they are useful in different situations, however the limits of each is unclear. Currently, invasive approaches in humans and non-human primates have higher information transfer rates than noninvasive approaches and have been demonstrated to allow dexterous movements of paralyzed or robotic limbs (Bouton et al., 2016; Collinger et al., 2012; Hochberg et al., 2006). The primary advantage of the noninvasive approach is applicability of these to a wide population of patients and healthy individuals, with no significant risks associated with their use. This allows rapid iteration of the technology including device design, control algorithm optimization, and evaluation of possible control signals (He, Baxter, Edelman, Cline, & Ye, 2015; Wolpaw et al., 2002; Wolpaw & Boulay, 2010). Because of these advantages, this dissertation is focused solely on noninvasive BCIs, though knowledge gained can be applied towards learning BCI control with invasive devices.

The primary clinical motivations for developing BCIs have been to restore function or improve rehabilitation following neural damage or disease with the aim of improving the patient's ability to interact with their environment and other people (He et al., 2015). Individuals with spinal cord injuries, neurodegenerative disorders, or post-stroke have difficulty interacting with their environment primarily due to impairments in motor control stemming from central or peripheral nervous system damage. As a single example of the diseases and disorders that could be alleviated with BCIs, stroke is the leading cause of disability in the United States with 795,000 people suffering a stroke each year. The cost of post stroke-care in 2010 was $73.7 billion with the standard of care

consisting of three to six months of outpatient rehabilitation (Moskowitz, Lo, & Iadecola, 2010). BCIs have been used to support rehabilitation post-stroke (Ramos-Murguialday et al., 2013; Soekadar, Birbaumer, & Cohen, 2011) though they are not currently FDA approved nor reimbursed by Medicare in the United States. Neurodegenerative disorders such as ALS and muscular dystrophy as well as spinal cord damage can confine individuals to wheelchairs while in some cases not directly affecting the brain. In patients with ALS, BCIs have been used in the clinic and in the home to allow patients to write text to communicate, paint, and control their environment (Kübler et al., 2005; Nijboer & Broermann, 2010; Sellers, Vaughan, & Wolpaw, 2010).

Commercial and low-cost EEG-based BCI products for the general population have been available for over a decade, but with the increased power of mobile processers to provide onboard signal processing and analog-to-digital conversion for inexpensive prices, these have expanded in recent years (Brunner, Bianchi, Guger, Cincotti, & Schalk, 2011; McCrimmon et al., 2017). An understanding of the usefulness of these for healthy people is unclear, though applications towards mindfulness and 'relaxation' have been advertised. Newer noninvasive BCI approaches using hemodynamic signals from functional Near-Infrared Spectroscopy (fNIRS) and other optical methods have been hyped and advertised to improve the information transfer rate to allow healthy users to augment their communication and control, though the ability of these technologies to deliver on these promises is unclear (Strickland, 2017). With each of these approaches, we must be careful not to make promises beyond the ability of the technology.

There have been a multitude of approaches to developing these interfaces from

using self-modulation of ongoing rhythms by mental tasks to using external stimuli to evoke a response on the brain based on user attention and task directions (Pfurtscheller et al., 2010; Scherer & Pfurtscheller, 2013; Wolpaw et al., 2002; Wolpaw & Wolpaw, 2012; Yuan & He, 2014). Sensorimotor rhythm modulation by motor task performance was first reported 40 years ago by Pfurtscheller in Germany (Pfurtscheller & Aranibar, 1977). This work found that executing a motor task produces a desynchronization in alpha band (8-13 Hz) activity in the sensorimotor cortical area that controls the task. Further work established a similar event related desynchronization to occur when motor tasks are purely imagined (Pfurtscheller, Neuper, Flotzinger, & Pregenzer, 1997). For example, when you imagine moving your right hand, the contralateral, left, sensorimotor cortex representing the hand area shows a desynchronization, and thus a decrease, in alpha power. This decrease in power is likely caused by altered firing of networks in the sensorimotor cortex. At rest, the sensorimotor cortex is synchronized in the alpha band and therefore shows a moderate amount of power in the alpha band. When a person executes or imagines a movement, the firing rate and patterns of neurons in the sub-network within the motor cortex that underlie the performance of the movement are altered. This differentiates the network activity from that of the resting motor cortex, and therefore the total synchronized alpha or beta band power decreases (Pfurtscheller & Lopes da Silva, 1999). Invasive and noninvasive reports have also shown that there is an increase in gamma band power during motor execution and imagination (Ball et al., 2008; Darvas et al., 2010; Kus, Ginter, & Blinowska, 2006; Pfurtscheller & Lopes da Silva, 1999). Motor imagination has interesting characteristics in that the controlling

network partially overlaps with that of the motor execution (Lotze et al., 1999; Lotze & Halsband, 2006) and there is a general stereotyped signature in electrophysiological recordings, but it also has no obvious output to the person performing the imagination; the subject does not intrinsically have feedback. Therefore, it is similar to many cognitive tasks that are internally generated via thought alone.

An intrinsic aspect of networks across the brain are oscillations, though there is debate as to whether they carry useful information or if they are epiphenomena related to biophysical aspects of neurons and their networks (Buzsáki, Anastassiou, & Koch, 2012; Engel & Fries, 2010; Joundi, Jenkinson, Brittain, Aziz, & Brown, 2012; Salari, Büchel, & Rose, 2012; van Wijk, Beek, & Daffertshofer, 2012). An understanding of the brain rhythms and interactions during sensorimotor rhythm performance can help us to further develop BCIs and improve BCI performance. This is important moving forward to clinical applications, as with any technology, if it is difficult to use or does not work reliably, people will not use it (Holz et al., 2013). In order to expand the use of BCIs to patients and healthy subjects, understanding how the brain uses BCIs to control different devices as well as how neural activity can be externally altered to improve performance is needed.

Transcranial Current Stimulation

Electrical stimulation of the brain to treat neurological symptoms has been performed for millennia, though a basic understanding of the effect of electrical stimulation on muscles and the nervous system has only been developed in the past few centuries and although an understanding of how the electrical current affects the brain

and neurons has only been extensively investigated over the past century (Priori, 2003). In modern times, with the dawn of psychiatry and neuroscience as a discipline, our understanding of how externally generated electric fields/current in the brain affects the brain has allowed for more scientific investigation into the behavioral, and electrophysiological, effects of electrical stimulation. Electroconvulsive therapy, using electrodes placed on the scalp to induce seizures, was introduced in the 1930s for mental health disorders and is still efficaciously in use today to treat treatment-resistant major depressive disorder (Priori, 2003). In the 1960s, neuroscientists began investigating how externally applied electrical fields influence neuron activity and at what levels of current neuronal effects occur in vivo and in humans (Lippold & Redfearn, 1964; Priori, 2003; Purpura & McMurtry, 1965). While the noninvasive brain stimulation technique of transcranial magnetic stimulation was pioneered in the early 1980s and was approved for treatment-resistant depression in 2008, transcranial current stimulation was reintroduced in the literature with work by Nitsche and Paulus (Nitsche & Paulus, 2001; Nitsche & Paulus, 2000). Since this time, there has been an explosion in publications examining the behavioral, electrophysiological, and cellular effects of current stimulation in vitro and in vivo in animals and humans (Brunoni, Fregni, & Pagano, 2011; Stagg & Nitsche, 2011).

The use of electrical neuromodulation to treat diseases and disorders through either the peripheral (PNS) or central (CNS) nervous system was branded as ‘electroceuticals’ (Famm, Litt, Tracey, Boyden, & Slaoui, 2013) to draw a parallel analogy to pharmaceuticals. The potential advantage of these over CNS or PNS affecting drugs is in their local and targeted network effects, compared to systemic effects of standard drug

delivery. Current approaches to noninvasive current stimulation are primarily characterized by the waveform of the current injected into the brain. The most studied version is directed current stimulation (tDCS), where a non-oscillating current is injected at an amplitude up to a few millamperes. Antal et al. (Antal et al., 2008; Antal & Paulus, 2013) first used alternating current stimulation (tACS) at specific frequencies to stimulate the motor cortex and found an effect on motor excitability. Other types of stimulation include random noise stimulation (tRNS), where the waveform is random noise with a frequency distribution within a specific frequency band, which was introduced by Terney and colleagues has been proposed to work through stochastic resonance (Terney, Chaieb, Moliadze, Antal, & Paulus, 2008). All forms of transcranial stimulation are thought to interact with endogenous firing activity, oscillations, and neural noise in some way, though the specifics of these effects in vivo are still being investigated.

On a cellular neural network basis, networks of interneurons generate the specific rhythms that influence how pyramidal neurons fire. The effect of tDCS in the cortex is thought to be on pyramidal neurons where, based on mathematical modeling and in vitro studies, there would be an expected slight hyperpolarization of the dendrites and a depolarization of the cell body and proximal axons for pyramidal neurons perpendicular to the anode of the tDCS electrode (Bikson et al., 2004; Kabakov et al., 2012; Radman, Ramos, Brumberg, & Bikson, 2009; Rahman, Toshev, & Bikson, 2013; Stagg & Nitsche, 2011). This depolarization of the cell body and axons would then lead to an increase in the firing rate due the affected neurons being closer to their firing threshold.

Cellular and molecular investigations have found multiple molecules and

receptors involved in the time-varying effects of tDCS. Acute effects have been eliminated using voltage sensitive sodium and calcium channel antagonists (Liebetanz, Nitsche, Tergau, & Paulus, 2002; Stagg & Nitsche, 2011). Long-term after-effects were abolished by an NMDA receptor antagonist (Brunoni et al., 2012; Fritsch et al., 2010; Stagg & Nitsche, 2011). These molecular effects and methods of action need to be considered when applying tDCS for investigational use into the treatment of neuropsychiatric disorders and neurodegenerative disorders. Commonly prescribed medication that targets neurotransmitters or neuromodulators can alter the effect of stimulation, for example selective serotonin reuptake inhibitors (SSRIs) used to treat anxiety and depression can alter the directional effect of stimulation on excitability (Kuo et al., 2016; Nitsche et al., 2009).

Many studies in both healthy humans and patients have been performed to examine the effect of tDCS on performance and learning of cognitive and motor tasks (Bestmann, de Berker, & Bonaiuto, 2015; Buch et al., 2017; Coffman et al., 2014; Kuo & Nitsche, 2012), as well as the effects to improve rehabilitation and reduce symptoms for mental illnesses or neurodegenerative disorders (Brunoni & Boggio, 2014; Flöel, 2014; Halko et al., 2011; Paulus, 2011; Philip et al., 2017; Zimerman & Hummel, 2014). The effects of TCS have been proposed to be a combination of effects directly on the brain and on somatosensory and cranial nerve inputs into the brain (Zaghi, Acar, Hultgren, Boggio, & Fregni, 2010). Extensive modeling studies have been performed with increasingly intricate and subject specific levels of detail to determine the distribution of current with differing electrode montages and the amount of current flowing through

different brain tissues (Kuo et al., 2013; Ruffini, Fox, Ripolles, Miranda, & Pascual-Leone, 2014; Sadleir, Vannorsdall, Schretlen, & Gordon, 2010). With these models, the expected magnitude of current is high enough to alter neuronal excitability based on in vitro studies. Recently, studies in both non-human primates and humans undergoing surgical procedures have examined, in vivo, the amount of current reaching cortical tissue using scalp stimulation electrodes (Opitz et al., 2016).

With the promotion of do-it-yourself TCS devices, the marketing of low-cost devices by numerous companies, and the portrayal in the media of these devices the treatment of neuropsychiatric disorders and improve learning (Dubljević, Saigle, & Racine, 2014), self-medication using TCS has been cautioned against in the literature (Wurzman, Hamilton, Pascual-Leone, & Fox, 2016). As our understanding of the effects of TCS on the brain, both beneficial and detrimental, continue to be investigated and new methods of targeting the regions and networks of interest continue to be developed, it is clear a cautious approach should be advocated for. Long-term effects, either direct or side-effects, with subjects followed for years after stimulation have not been thoroughly investigated. However there have been studies that have found motor performance improvements to subsist for months following learning with stimulation (Reis et al., 2009). At the same time, there have been few, if any, reports of significant side effects, with most side effects, including acute tingling or burning sensation during stimulation, and local scalp sensitivity under the electrodes following stimulation, being minimal (Brunoni et al., 2011; Poreisz, Boros, Antal, & Paulus, 2007). While many reports on the application of tDCS show improvements in motor learning, motor ability, or a reduction

in clinical symptoms, this is not always the case. Detrimental effects in task ability can occur based on the targeted location and polarity of stimulation (Iuculano & Cohen Kadosh, 2013) and is under-investigated due to the expansive parameter space that could be tested for detrimental side-effects. With these devices readily available and easily produced, and few demonstrated adverse effects, people will use them if there is a hope of cognitive improvement or enhancement.

Ethical Issues Surrounding BCIs and Neuromodulation

Neural engineering at its base involves large ethical issues as its purpose is to alter the nervous system, and the brain in a vast majority of cases, which defines us as a person (Hamilton, Messing, & Chatterjee, 2011). Both neural decoding through BCIs and neuromodulation have ethical quandaries inherent in their use, though the specifics of these arises with specific usage. These technologies have been proposed to restore deficits following damage or improve rehabilitation, but they may also be able to enhance function in healthy people.

The use of brain-computer interfaces raises ethical issues in terms of informed consent and medical determinations of minimally conscious state and potential recovery for this state, as well as recovery from other damage (Haselager, Vlek, Hill, & Nijboer, 2009; Nijboer, Clausen, Allison, & Haselager, 2013). When including subjects for at-home and in-lab experiments, consideration towards the psychological effects on subjects who regain abilities, or have the hope of regaining abilities, should be considered, particularly in light of the possible loss of these following experimentation or lab use (Mabe, 2017).

When considering enhancement with neuromodulation, we need to balance the known effects and possible side effects when performing experiments and when discussing the promise of the technology. Anecdotally, when asked, many people would likely say that they would prefer to learn some skill faster or perform some task better. I have asked this of elementary and middle school students when speaking to their classes about the brain; some want to learn mathematics or a foreign language faster, and they get very excited about it. Then I've asked: "What if you learn poorer in some other class?" They seem to have an idea if they can specifically pick which one, though their parents may have some other ideas. There have been reports of improvements in mathematical ability in children as well as improvements in creative problem solving though caution is suggested when performing neuromodulation on children (Cohen Kadosh, Levy, O'Shea, Shea, & Savulescu, 2012).

There are a multitude of reasons to improve learning and performance of motor or cognitive tasks, from learning new skills to rehabilitation and recovery from disease or damage (Cramer et al., 2011; Dayan & Cohen, 2011). Neuroplastic mechanisms such as long-term potentiation, long-term inhibition, and homeostatic plasticity allow us to learn throughout our lives but also allow stabilization of networks underlying this learning. During development there are specific neuroplastic time periods, generally referred to as critical periods, during development where there is increased reorganization of neural connections in local areas and across the brain (Berardi, Pizzorusso, & Maffei, 2000). However, there are other potential plastic time windows throughout the life, specifically, following damage or injury where changes are widespread with reorganization of the

brain happening on a rapid time-scale compared to regular plasticity. During this time the goal is to maximize rehabilitative outcomes to maximize quality of life following damage (Bütefisch, 2004; Cramer et al., 2011).

Both BCIs and TCS can be used by healthy and the individuals with neural damage or improper network activity to alter their brain states. These two categories of use raise differing at the concern as well as or have differing brains states. The main issue is how the brain state, brain anatomy, brain connectivity interacts with both brain computer interface performance and individuals with brain damage, CNS, or PNS technologies in the same way. There has been profound hope and some evidence for improving pathological symptoms of mental illness as well as rehabilitation following traumatic brain injury, stroke, and other neural damage using transcranial current stimulation to improve neuronal regrowth as well as reorganization both locally and across networks of the brain. Examining the combination of this with transcranial stimulation may allow us to maximize rehabilitation within a specified time to maximize rehabilitation and outcomes on an individual level. An emerging hypothesis is that combining noninvasive brain stimulation with the specific task performance being targeted is required to gain the most from the stimulation (Berker et al., 2013; Bikson & Rahman, 2013; Luft, Pereda, Banissy, & Bhattacharya, 2014; Reis & Fritsch, 2011).

Problem Statement:

Our approach to the outstanding challenge to improve noninvasive BCI performance and learning was to target the user, and the user's brain, to improve the signal generated at the source rather than through later signal processing. With this, we

targeted user motivation, with an initial set of experiments where the device controlled was a robotic arm rather than a cursor on the computer screen. Following the first set of experiments, we shifted the focus to directly targeting the users' brain with transcranial current stimulation to alter the underlying brain activity to improve performance and learning. We found promising results, particularly with the neuromodulation approach, which opens numerous possibilities to further enhance and improve targeting functional areas and networks of the brain in a task specific manner to develop safe, effective interventions to modulate brain functions.

Chapter 1 of this dissertation gives an overview of a project that examined noninvasive sensorimotor rhythm-based BCI continuous control of an assistive device robotic arm to evaluate the performance of subjects on move and grasp task, with the result illustrating the difficulty of performing a 1D/2D continuous control with grasping, even with subjects that perform well on standard tasks 1D/2D tasks. Additionally, one subject in the chronic post-stroke phase demonstrated their ability to use a standard BCI setup to perform equivalently to healthy subjects on these tasks.

Chapter 2 examines the combination of tDCS with sensorimotor rhythm-based BCI to investigate how these two technologies interact and their simultaneous effect on the brain during BCI tasks following localized stimulation of different polarities. Subjects receiving anodal stimulation demonstrated a reduced time to hit targets during imagination with the hand contralateral to the stimulated cortex. In addition, following cathodal stimulation, alpha power over the stimulated hemisphere was decreased compared to alpha and sham stimulation.

Chapter 3 examines connectivity during motor imagination and BCI performance in healthy subjects and how these connectivity patterns are altered following tDCS. We found that anodal stimulation increases connectivity in a task specific manner within the motor imagination network in alpha and beta frequency bands. In addition, we found that anodal and cathodal stimulation yield different connectivity changes and directions of changes when using within subject comparisons. Connections between regions in the motor imagination network were also found to correlate with behavioral measures, suggesting future approaches to targeted network neuromodulation.

Combining these studies, we found that targeting the user affects their performance, though it does not necessarily improve performance. While using physical devices may increase motivation to learn and perform the BCI task, the difficulty of dealing with physical constraints to arm movement velocity and translation, hand grasp closing speed, and perspective in real space decrease performance ability in a continuous complex task. Targeting task specific activity with simultaneous BCI control and tDCS yields changes in behavioral, electrophysiological, and neural network connectivity following stimulation and these changes underlie improved behavioral performance. These results suggest future work to optimize stimulation with the aim of altering task specific frequency bands of interest and network connectivity to improve behavioral performance.

Chapter 1 –

Noninvasive Control of a Robotic Arm by "Thoughts" as Decoded from Scalp Electroencephalogram

Chapter 1 Overview

Robotic limbs can enable individuals with impaired mobility and motor system output to interact with their environment. Many of these individuals do not have the motor control necessary to utilize their hands to control an assistive device. Invasive cortical BCIs have demonstrated 2D and 3D control of robotic arms in tetraplegia patients but the invasive approach greatly limits the number of individuals who can utilize the technology. We demonstrate EEG control of a human size robotic arm and hand to complete a multi-step grasping tasks. Four healthy and one post-stroke subject controlled the arm in two-dimensions to move to a target, grab the target block, and move it to a final location using motor imagery (MI) recorded through scalp EEG. Subject performance was a maximum of 25% correct for completing two steps, and a maximum of 12% for completing all three steps of the task. This demonstrates both successful control of a robotic arm in 2D performance of a multi-step task in a time-limited manner and the difficulty of this control for all subjects. The primary results of this work were published in the *Proceedings of the IEEE Engineering in Medicine and Biology – Neural Engineering* conference in 2013 (Baxter, Decker, & He, 2013).

Introduction

The promise of brain-computer interfaces for studying the brain and developing integrated human-machine systems has yet to be fulfilled. BCI technology has been successfully used to empower individuals with impaired motor abilities, following stroke, neurodegenerative diseases, and spinal cord injuries, to increase their interaction with their environment (Jackson & Zimmermann, 2012; Mak & Wolpaw, 2009; Silvoni et al., 2011). Ongoing research into signal processing (Krusienski et al., 2011), training (Green & Kalaska, 2011), novel applications (Daly et al., 2009; Mak & Wolpaw, 2009), and new signals and hybrid systems (Allison et al., 2010; Pfurtscheller et al., 2010) continues to illustrate the range of possible uses and improvements to the BCIs. Physical manipulators are one of the most promising outputs from a BCI because they allow impaired individuals to interact with their immediate physical surroundings without assistance (McFarland & Wolpaw, 2010).

Humans have used implanted electrode arrays to control robotic arms in three dimensions using an invasive BCI (Collinger et al., 2012; Hochberg et al., 2012). These implants have been used for up to five years in humans, though a decrease in the signal quality occurs over time (Hochberg et al., 2012). The implantation procedure of this approach limits the usefulness to patients that are willing and able to have an electrode array implanted into their cortex, and are presently only used in the laboratory as a support team is needed to care for and set up the devices.

EEG-based BCIs are an attractive alternative to invasive recording systems. EEG control in three dimensions has been recently shown in virtual cursor (McFarland,

Sarnacki, & Wolpaw, 2010) and virtual helicopter tasks (Doud, Lucas, Pisansky, & He, 2011). These virtual objects have been controlled using motor imagination of the arm, leg, and tongue combined to control all dimensions simultaneously. Control in a virtual task is useful for navigating a cursor or a virtual game, and as a proof of concept for control of physical objects, but does not insure an individual will be able to control an object in physical space in their immediate surroundings.

Controlling and interacting with physical objects is vital to allow a patient to be independent in their environment. Interacting with the physical environment is more difficult, and is fundamentally different, than controlling a virtual object because physical objects need be maneuvered in space with all the physical laws that entails (Green & Kalaska, 2011). Numerous studies have examined BCI control of physical objects (McFarland & Wolpaw, 2010). Galan and colleagues (Galán et al., 2008) utilized imagery for two-dimensional (2D) control of a virtual wheelchair and a remotely controlled physical wheelchair using intelligent control strategies. Motor imagery (MI) was combined with steady-state visual evoked potentials (SSVEPs) to develop a hybrid control system for a two degree-of-freedom robotic arm and hand (Horki, Solis-Escalante, Neuper, & Müller-Putz, 2011). Other work with robotic arms has included control in 1D and 2D translation tasks, though primarily using a remote control setup compared to an arm proximal to the user (Horki et al., 2011; McFarland & Wolpaw, 2010; Wang et al., 2011).

Motor imagery has been shown to improve motor rehabilitation following stroke (de Vries & Mulder, 2007) and post-stroke subjects have demonstrated MI-BCI control of

a virtual cursor in 1D (Bundy et al., 2012; Soekadar et al., 2011). As stroke subjects regain function, more complex tasks are required to continue to improve recovery as a function of their abilities. Complex task planning and implementation for the control of a physical object allows for this increased difficulty and further rehabilitation. The use and interaction of physical objects with a robotic hand can lead to an engagement of embodiment (Velliste, Perel, Spalding, Whitford, & Schwartz, 2008) which causes the user to attribute the control or the robotic arm differently than to that of the virtual cursor.

We utilized a grasp task experimental setup to evaluate performance when subjects perform real-world tasks. The subject was required to maintain control of the hand and arm while moving the robotic hand to the target, grasping the block, and then moving the block to the final target. We utilized a reduced set of electrodes to examine control performance in the situation where an individual would utilize BCI control frequently, where the use of fewer electrodes reduces setup time as well as user discomfort, both important considerations when designing a system for use in the home.

Subjects demonstrated control of a robotic arm along three dimensions using five motor imagery combinations. Extending our reductionist approach followed in previous work, subjects used motor imagery to control three-dimensions of a robotic arm; two-dimensions of translation, horizontal and vertical, and opening/closing of the hand, to pick up and move blocks. Subjects could control the robotic arm and hand with a minimum of five total hours of BCI training. This is demonstrated in both healthy subjects and in a single subject post-stroke.

Methods

Experimental Setup

*Subjects***:** 5 subjects (3 female) were recruited to participate in these experiments (Ages: 22-56 years). All procedures and protocols were approved by the University of Minnesota Institutional Review Board. Four subjects were healthy individuals (S1-S4); one subject previously had a subcortical stroke with residual limb impairments (S5). Subjects S1-S3 were trained subjects recruited following 5 (1 hour) sessions of 1D and 2D virtual cursor training. These subjects were able to translate their previous training into moving the arm in both 1 and 2 dimensions with a short learning phase. S5 had undergone 5 hours of previous virtual cursor BCI training primarily in 1D. One naive subject was recruited who was trained using solely the arm task for feedback. All subjects participated in at least seven sessions using the arm (**Table 1**).

Hardware Setup: A 64 channel Neuroscan cap with SynAmps2 headbox, and SynAmps RT amplifier (Neuroscan Inc., Charlotte, NC) were used to record the EEG signal. A bipolar EMG setup located on the subject's right extensor digitorum muscle (Ramoser, Müller-Gerking, & Pfurtscheller, 2000) was used on at least one experimental session per subject to insure subjects were not moving the arms or hands during motor imagery.

Robotic Arm: The JACO arm (Kinova Robotics, Montreal, Canada), a seven degree of freedom human-sized arm with three fingered hand, was used output feedback for all experiments. This arm was designed for wheelchair use and thus has safety features that enable it to be used in close proximity to a user. The arm was securely mounted on a table 72 cm above the ground and the work envelope was restricted to the table with a

width of 72 cm depth of 72 cm, and height of 100 cm above the table surface. The arm was prevented from hitting the table surface by limiting the work envelope to 2 cm above the surface. The arm was controlled in the Cartesian coordinate system and the company supplied API was used to calculate the kinematics of arm and hand movement.

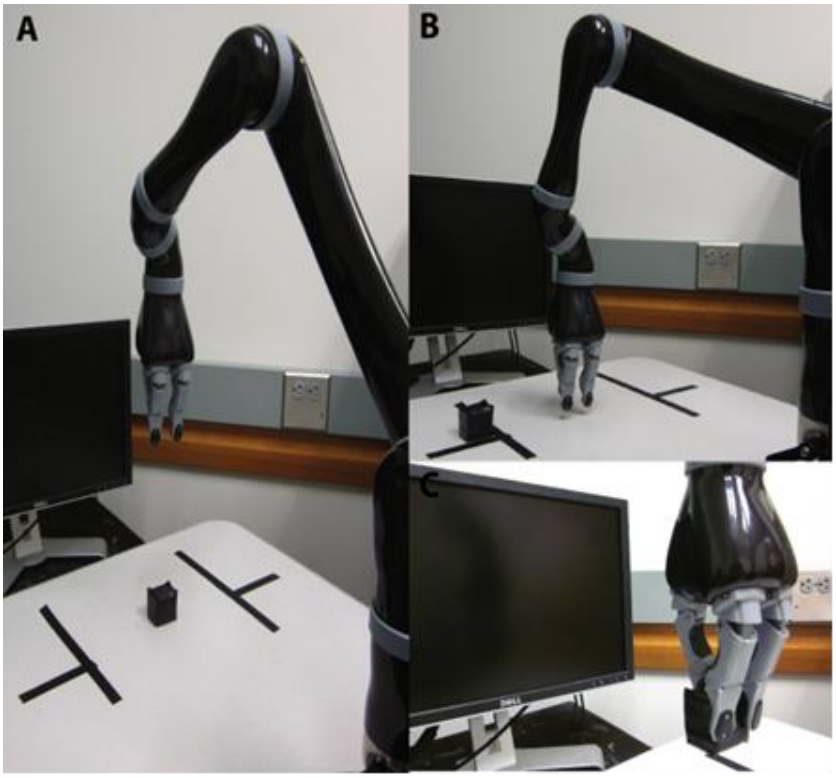

Fig. 1. Robotic Arm Setup. Anthropomorphic robotic arm with 6 degrees of freedom and 3 finger hand during task performance. A. Illustrates the position at the start of the vertical claw task. B. Illustrates the arm position and target position at the start of the horizontal claw task. C. Illustrates the hand grasping the target cube and raising it above the table.

Experimental Procedure

Subjects were seated comfortably in a chair located adjacent to the robotic arm facing a computer screen (**Fig. 1**). They were instructed to relax, keep their head still, and to blink as little as possible during the trials. Subjects were free to move their eyes, as would be used in the real world when moving a physical effector throughout the environment. To control left and right movement, subjects were instructed to imagine continuously opening and closing their left or right hand, respectively. To control vertical movement, subjects were instructed to imagine continuously opening and closing both their left and right hands simultaneously to move up and to relax to move down. To control the opening and closing of the hand, subjects were instructed to imagine tapping their right foot; this dimension was used as a switch. When a threshold was reached, and the hand was in an open state, it closed to a predefined distance, enough to grasp the target block. Likewise, if the hand was closed and the threshold was reached, it opened a predefined distance. This control design was more straightforward for the user than continuous control (Royer & He, 2009) and, with compliant hands, it allowed robust grasping of the target object.

Training: The naive subject was trained solely using the robotic arm movement as feedback. Initial robotic arm training for all subjects was on targets composed of colored plastic balls. Balls were placed 28 cm left or right of the hand and 28 cm above and below the hand. Training consisted of 3 minute runs of 7 second trials; the inter-trial interval was 4 seconds and pre-feedback time was 1 second to allow the subject to plan their movements prior to the trial starting. The target was randomly selected out of the four possible choices and displayed as a colored square on an LCD screen located

approximately 90 cm from the subject. Initial training was in 1D horizontal movement. Once the subject achieved greater than 70% correct on 4 runs of 3 minutes in one day, they were trained in 1D vertical movement. Subjects were considered 'trained' following performance of 1D horizontal and vertical control of greater than 80% accuracy on a run of each type. Trained subjects then performed simultaneous 2D control and claw tasks.

Tasks: For two-dimensional control tasks, subjects controlled vertical and horizontal dimensions simultaneously. Determination of target hit was computed by comparing the position of the hand acquired from the arm to the known position of the targets. When targets were hit, the trial ended, the arm was reset to the center position and a new trial was initiated. 2D control of the claw task were interspersed with simultaneous 2D translation tasks.

Claw Tasks: 2D claw task consisted of either vertical or horizontal movement of the arm plus hand opening and closing. Claw tasks consisted of three steps performed in a specified order to correctly complete the task. A partial completion of two of the steps for a correct trial was recorded. Closing the hand prior to moving to the target position did not allow completion of the task. Grasp and translation were controlled simultaneously to allow the subject to parallel naturalistic limb movement when reaching for an object. The target was a 4cm by 4cm by 4cm, 25g weighted foam cube. Trials were 13 seconds long with a 4 second inter-trial interval to allow the arm to reset to the starting position. Following each trial, the arm was reset to the initial starting position and the target cube was manually placed back at its starting position. Runs were 3 minutes long. Each of these claw trials was a timed 2D, three step task, and allowed the subject the ability to

error correct.

Horizontal Claw Task: The hand was centered on the of the workspace table 36 cm from the edges and 2 cm above the table with a target located 15 cm to the left or right of the center position. During each run, the target block was on the same side, either the left or the right. To fully complete the task, the subject was required to: 1. Move the arm from the center position to the left or right so the hand can grasp the target. 2. Maintain the position of the hand and close the hand. 3. Hold the target block while moving the arm 30 cm in the opposite direction.

The area to successfully grab the target was 6 cm as the opposing finger was 2 cm wide and the target was 4 cm wide, with a required 1 cm of the finger to contact the target in order to successfully grab the cube.

Vertical Claw Task: The hand was located in the center of the workspace table located 25 cm from the surface of the table, with a target placed directly below the hand on the surface of the table. To fully complete the task, the subject was required to: 1. Move the arm from the raised position down to the target 24 cm below the starting position. 2. Maintain the position of the hand and close the hand. 3. Hold the block while moving the arm 24 cm up.

Signal Processing

Online: BCI2000 (Schalk, McFarland, Hinterberger, Birbaumer, & Wolpaw, 2004) generated the control signal for a robotic arm. BCI2000 output a position signal through UDP to custom C# software where the arm position was controlled by the virtual cursor

position in 2D/3D space. The robotic arm was controlled by the provided API and custom C# software.

Electrode Selection: All individuals initially used a 3Hz window around 12Hz for all controls. Vertical movement was controlled by the subtraction of C3 and C4; horizontal movement was controlled by a subtraction of C3 from C4 and hand grasp was controlled by either the addition or subtraction of Cz. This was manually optimized for each individual based on performance during their 1D and 2D training sessions (Table 1). 16th order autoregressive moving average algorithm as developed for BCI2000 (McFarland & Wolpaw, 2008) was used to model the signal in each frequency band (4-30Hz) with 300 millisecond time windows. The control signal was normalized for unit variance and zero mean to insure the correct learning of the linear classifier.

Offline: Raw data collected with BCI2000 was processed using custom software utilizing EEGLAB (Delorme & Makeig, 2004) in MATLAB (The Mathworks, Inc., MA, USA). Data were bandpass filtered from 2 to 110 Hz and the mean was removed. Claw trials were analyzed time locked to the correct grasping of the target cube. Full (3-step) correct trials were epoched 4 seconds before and 2 seconds after the hand close to include the times of interest. Two-step correct trials were epoched 2 seconds before to 0.1 seconds after the correct closing of the hand to include the time of interest. Time-frequency power over the correct trials was compared to baseline power of the selected channel 1 second prior to the start of the trial. 300 millisecond time windows with 75% overlap were used to generate the spectrograms.

TABLE 1
Electrode Selection and Performance Data for all Subjects

Subject	Electrodes and Frequency Used (H:Horizontal Control V:Vertical Control G:Grasp Control)	2D	Vertical Claw - 2 Step	Vertical Claw - 3 Step	Horizontal Claw - 2 Step	Horizontal Claw - 3 Step	Total Arm Performance Sessions
S1	H:C3/12Hz C4/12Hz V:C3/12Hz C4/12Hz G:Cz/12	40.2	29.6	23.8	14.2	5.3	9
S2	H:C3/12Hz C4/12Hz V:C3/12Hz C4/12Hz G:Cz/12	46.6	19.7	12.4	9.8	1.4	10
S3	H:C3/12Hz C4/12Hz V:C3/12Hz C4/12Hz G:Cz/12	39.5	30.9	21.8	11.7	4.4	7
S4	H:C3/12Hz C4/12Hz V:C3/12Hz C4/12Hz G:Cz/12	44.4	28.7	2	7.8	0	7
S5	H:C3/12Hz C4/12Hz V:C3/21Hz C4/21Hz G:Cz/21	46.9	14.1	0	9.1	2.2	7

Subject specific electrodes and frequency displayed. Subjects S1-S3 and S5 had 5 previous sessions of virtual cursor task training. All task values are in percent correct.

Results

All subjects correctly completed the 2D translation task and could correctly perform at least one of the three-step claw tasks (**Table 1**). Mean task performance for the 2D translation task across all subjects was 42.7% correct (**Fig. 2**).

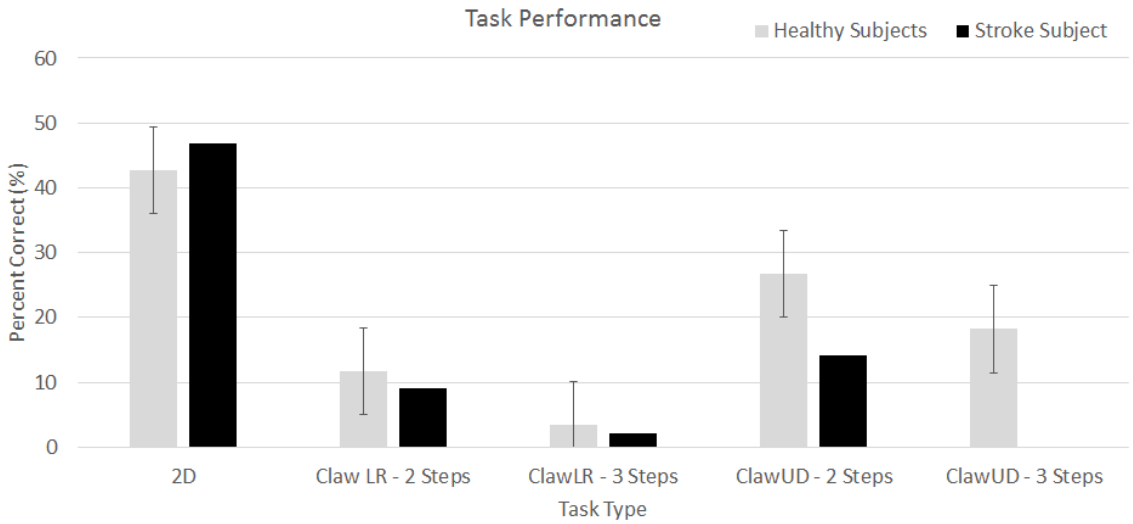

Fig. 2. Robotic arm performance across all subjects. Right graph illustrates mean across all healthy subjects. Left graph illustrates the performance of the stroke subject. The healthy subjects had more accurate performance than the stroke subject on the complex claw tasks.

Vertical Arm Claw: Mean percent correct on the vertical claw task for completion of two steps for all subjects was 26.7 (+/- 5.0%) and three steps had a mean of 18.2 (+/-5.4% SD) (**Fig. 2**). Mean time to grasp for two-step correct trials was 7.616 seconds and for three-step correct trials was 7.706 seconds. To correctly complete these trials, the subject was required to rapidly switch neural states from 'rest', to lower the arm, to 'foot tap', to close the hand, to 'both hand grasp', to raise the arm to the final target position. These state switches are illustrated across the control electrodes in the time-frequency plots over the four seconds prior to the correct grasp and two seconds after the grasp. This subject used 12Hz ERD as the vertical control with electrodes C3 and C4 and 12Hz CZ to signal the hand to close. Consistent ERDs were found when averaging an individual's correct trials together. An example of this is shown in the time-frequency plot for subject S1

(Fig. 3) of 32 merged correct trials time-locked to the hand closing shows the intentional rest state from 0-2.5 seconds characterized by increased synchrony at 12Hz compared to baseline. Following this, there was a decrease in synchrony one second prior to correct grasp in Cz and the ERD is present on both C3 and C4 post-grasp to move the hand up to correctly complete the trial. The topograph plots of the EEG power over the entire scalp illustrates the shifting desynchronization over the entire time of interest.

Horizontal Arm Claw: Mean percent correct for the horizontal claw task for completion of two steps for all subjects was 11.7 (+/- 1.9%) and three steps had a mean of 3.5 (+/- 1.7%) (**Fig. 2**). Chance level is 2% for full completion and 4% for 2 step completion. Mean time to grasp was 8.021 seconds. The time-frequency plot for subject S3 (**Fig. 4**) of 5 merged correct trials with the target on the right-side time-locked to the hand closing shows the initial desynchronization on C4 to initiate movement to the right, followed by a synchronization at Cz initiating a hand close, and synchronization in C4 following the target grab leading to movement to the left.

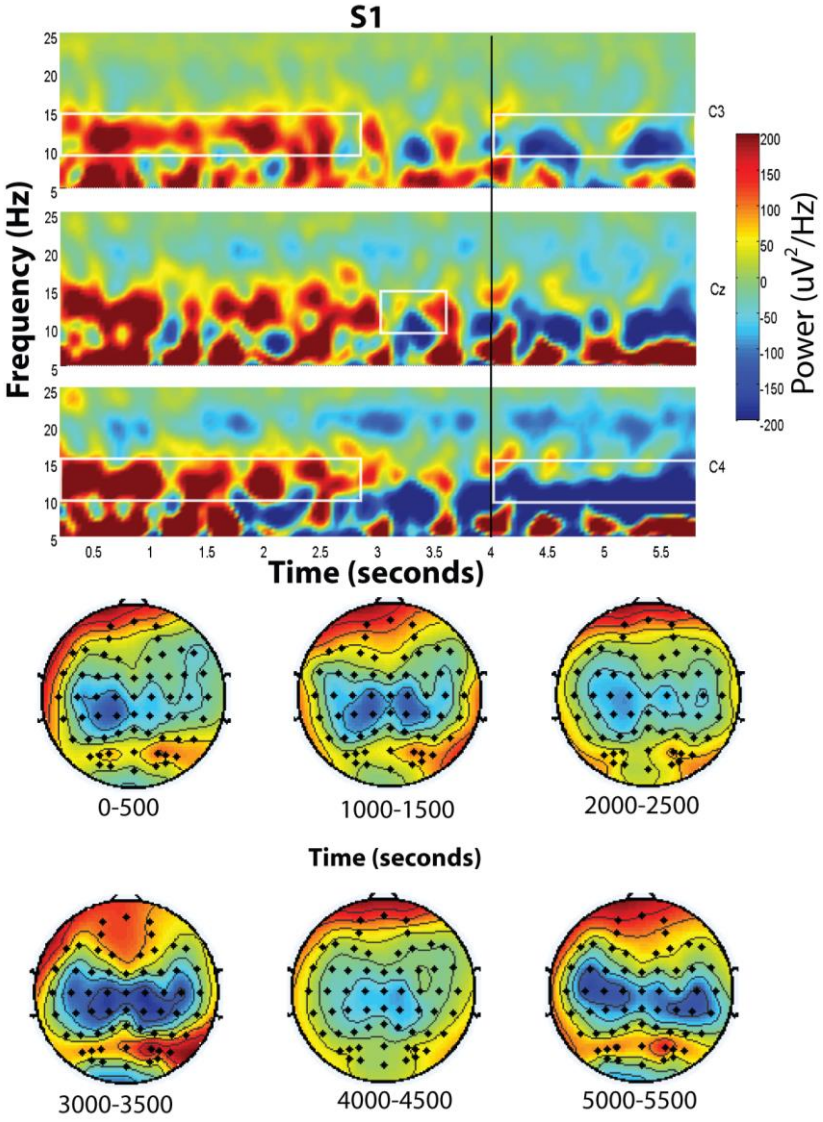

Fig. 3. Electrophysiology of up-down robotic arm control. Time-Frequency plot of mean event-related power over thirty-two trials of the vertical claw task for a single subject (Top). Black line at 4s indicates when the hand closed around the target block in the correct position due to the power decrease in Cz ~800ms prior to the grasp. Both C3 and C4 desynchronized following grasping of the block indicating the intention to move the hand up to complete the task. Topographs of power over 500ms time windows corresponding to the time-frequency plot (Bottom).

Subject Control: Three subjects could move the arm in the target direction and close the hand simultaneously onto the target with maximum hand movement speed and without error, resulting in a fluid motion of grasping directly onto the target directly. This was performed in two percent of the correct trials. Subjects successfully completed trials both by going directly to the target, grasping it, and moving to the end position and by overshooting the target, moving the arm back to the target, and back to the end position, illustrating the ability to correct errors online in time limited situations (**Fig. 5**). Time range to grasp for correct trials was 1.830 to 11.97 seconds illustrating that subjects could both move directly to the target and grasp the cube as well as correct their errors in translation and move to grasp the cube after initial translational movement errors. All subjects that had previously performed cursor control stated that the physical arm was more difficult to control than the virtual cursor. Everyone mentioned that it was difficult to focus when the arm was going in the opposite of their intended direction or when they were trying to hold the arm in place while grasping.

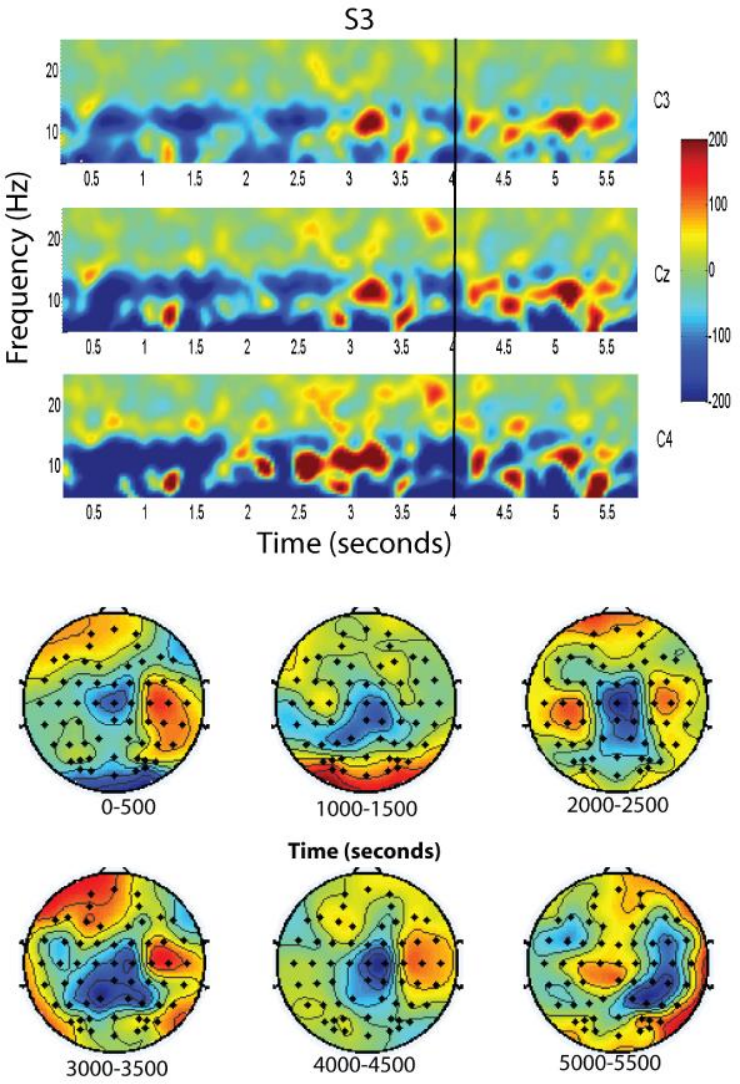

Fig. 4. Electrophysiology of right-left robotic arm control. Time-frequency transform during a trial (Top). The ERD for right movement is present from 0-2.5s on C4. From 3-3.5s there is an increase in synchronization in Cz initiating the closing of the hand on the target block at 4s. At 4s there is an increase in synchronization in C3 which moves the arm to the left target area. Color indicates event-related change in power. Topographs of power over 500ms time windows corresponding to the time-frequency plot (Bottom)

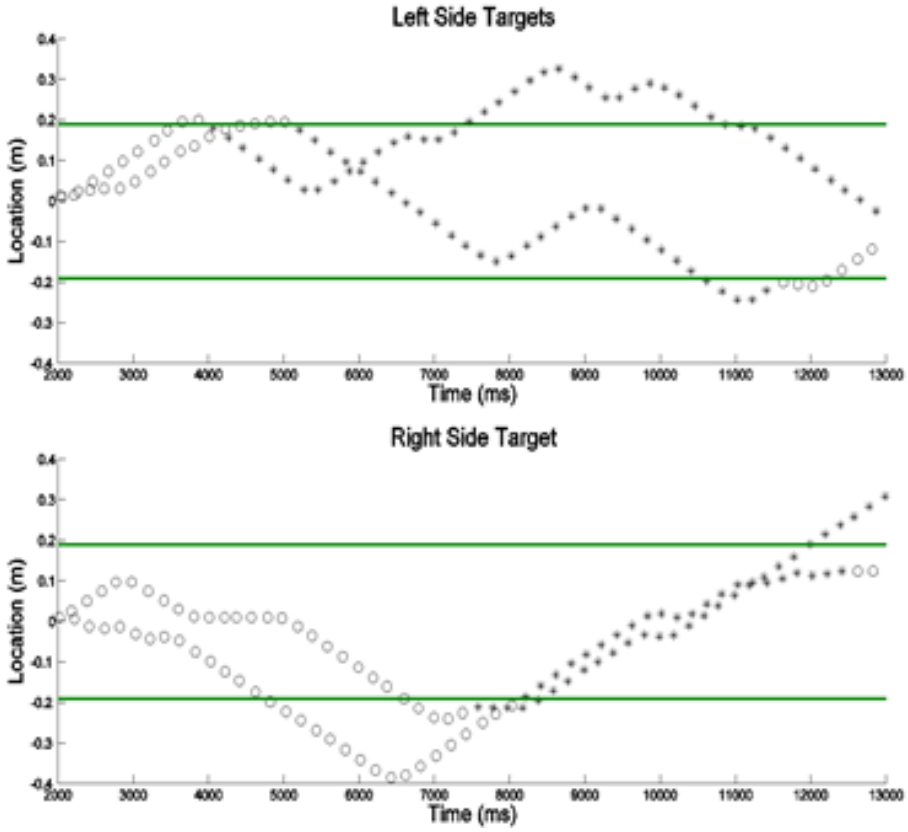

Fig. 5. Trajectory examples during the horizontal claw task for left and right side targets. Right side target example illustrates trials where the subject overshot the block, then moved the hand back to the block, successfully grabbed it, and moved it to the final target location. ‘o’ indicates hand is open. ‘*’ indicates hand is closed. Green lines indicate the location of the target block and the final target.

Discussion

We are extending the field of BCI control from virtual control of digital objects (Doud et al., 2011; Yuan, Doud, Gururajan, & He, 2008) to physical devices and effectors (LaFleur et al., 2013). In this study, we demonstrated user control of three-dimensions of

a human sized robotic arm with EEG based MI-BCI. This work extends previous work showing robotic arm control through motor imagery control of translation and using hybrid systems (Horki et al., 2011; McFarland & Wolpaw, 2010). We also report subjective and objective measures of the difficulty of controlling a physical effector in a physical environment, as subjects have a more difficult time controlling the arm than previously controlling the virtual cursor in a similar task. One factor to consider when controlling an arm in 3D physical space is user perspective and the effects of user placement and viewing angle on performance and neural activity. For two trials of the horizontal claw task, we placed S3 on the opposite side of the arm and this resulted in reduced performance, while performance returned to the initial state upon moving back to the original position. Further studies are needed to study the human-computer interaction while controlling an object in the physical environment.

Patients have utilized invasive electrode arrays to successfully maneuver robotic arms and hands in three dimensions of translation and grasp (Collinger et al., 2012). As control algorithms are trained on the information from the high density electrode arrays, and signals are from single and sets of neurons, which both non-human primates and humans (Fetz, 2007) can control volitionally, the higher density of information allows for faster training and more accurate control compared to noninvasive systems. Noninvasive systems have the advantage in not needing a neurosurgical procedure to use thus allowing them to be implemented in a more of the population. This work demonstrates the need to develop improved control signal discrimination to allow subjects to control increased dimensions of arm control, as the completion of real world tasks requires a high

dimensionality of accurate control. Current BCI signal processing algorithm development primarily focus on demonstrations in one dimensional control (Krusienski et al., 2011). Further testing of promising algorithms for 2D and more complex tasks is needed to evaluate which may be useful for controlling assistive and prosthetic devices.

We demonstrated, for the first time, healthy and stroke subject motor imagery control of a human sized robotic arm in two-dimensions in a multi-step task. Electrophysiological analysis using time-frequency plots illustrated the rapid sequential switching of task performance to complete the task in the required time. Control was performed by both healthy subjects and a stroke subject illustrating the feasibility of EEG-based robotic arm control in two-dimensions. The use of BCI control for a robotic arm proximally to a subject would be of great use to individuals that are unable to extend their arms to reach to interact with objects in their environment. In addition, the use of an anthropomorphic arm could increase motivation and rehabilitative potential for post-stroke subjects that are undergoing motor imagery rehabilitation training. Recent work decoding 2D and 3D limb movements noninvasively (Bradberry, Gentili, & Contreras-Vidal, 2010; Presacco, Goodman, Forrester, & Contreras-Vidal, 2011) combined with this work could be combined for the initial control of a prosthetic limb. Further work with prosthetic limb users to understand underlying electrophysiology while subjects control a prosthesis is needed to optimize EEG based MI-BCI control.

Chapter 2 –

Sensorimotor Rhythm BCI with Simultaneous High Definition-Transcranial Direct Current Stimulation Alters Task Performance

Chapter 2 Overview

Transcranial direct current stimulation (tDCS) has been used to alter the excitability of neurons within the cerebral cortex. Improvements in motor learning have been found in multiple studies when tDCS was applied to the motor cortex before or during task learning. The motor cortex is also active during the performance of motor imagination, a cognitive task during which a person imagines, but does not execute, a movement. Motor imagery can be used with noninvasive brain computer interfaces (BCIs) to control virtual objects in up to three dimensions, but to master control of such devices requires long training times.

The objective of this study was to evaluate the effect of high-definition tDCS on the performance and underlying electrophysiology of motor imagery based BCI. We utilized high-definition tDCS, to investigate the effect of stimulation on motor imagery-based BCI performance across and within sessions over multiple training days.

We report a decreased time-to-hit with anodal stimulation both within and across sessions. We also found differing electrophysiological changes of the stimulated sensorimotor cortex during online BCI task performance for left vs. right trials. Cathodal

stimulation led to a decrease in alpha band power during task performance compared to sham stimulation for right hand imagination trials. In addition, anodal and sham subjects had an increase in discriminability between left and right trials following stimulation. These results suggest that unilateral tDCS over the motor cortex differentially affects cortical areas based on task specific neural activation. These findings were published in *Brain Stimulation* in 2016 (Baxter, Edelman, Nesbitt, & He, 2016).

Introduction

Transcranial direct current stimulation (tDCS) is a noninvasive neuromodulation approach wherein a low level of current is applied through scalp electrodes into the brain (Nitsche & Paulus, 2001). Essentially, tDCS is considered to modulate the resting membrane potential of neurons within the generated electric field. This results in an increase or decrease in excitability based on neuron location and orientation with respect to the field (Stagg & Nitsche, 2011). Initial studies characterized polarity specific differences in cortical effects utilizing transcranial magnetic stimulation (TMS) to elicit motor evoked potentials (MEPs) in the hand. Nitsche and Paulus (Nitsche & Paulus, 2001) examined the effects of anodal tDCS over the motor cortex and found MEPs elicited by TMS were increased in amplitude, suggesting greater cortical excitability following the stimulation, while cathodal stimulation decreased MEP amplitude, suggesting decreased cortical excitability (Nitsche & Paulus, 2001). Other studies have since characterized the effects of electrode polarity and electrode placement using in vitro and in vivo models (Dmochowski, Datta, Bikson, Su, & Parra, 2011; Johnson et al.,

2013; Kabakov et al., 2012; Stagg & Nitsche, 2011). In studies with healthy humans, tDCS has been found to improve (or impair) task performance based on stimulation parameters with applications involving numerical learning (Iuculano & Cohen Kadosh, 2013), memory (Javadi, Cheng, & Walsh, 2012), and attention (Pope & Miall, 2012). tDCS has exhibited both acute effects lasting an hour and longitudinal effects lasting from several days to months when examining performance measures as outcome at follow-up (Nitsche & Paulus, 2001; Reis et al., 2009).

The BCI field has developed noninvasive online systems that utilize sensorimotor rhythms (SMRs) modulated by motor imagination to control virtual and physical objects with the goal of expanding this control to clinical populations (Cassady, You, Doud, & He, 2014; Doud et al., 2011; Edelman et al., 2015; He et al., 2015, 2013; LaFleur et al., 2013; McFarland et al., 2010; Wolpaw & McFarland, 2004; Yuan & He, 2014). Importantly, many people with motor neuron damage are not able to control their limbs due to loss of motor control pathways, but can still generate cortical activity corresponding to the hand or limb movement by performing motor imagery (MI) (Kübler et al., 2005; Wolpaw & McFarland, 2004). Motor Imagery is a cognitive task consisting of kinesthetically imagining a motor movement while not executing the movement. The electrophysiological signature of MI performance is an event related desynchronization (ERD), a decrease in power relative to baseline, in the alpha (8-13 Hz) and/or beta (13-30 Hz) bands in the hemisphere contralateral to the imagined movement, and an event related synchronization (ERS) in the ipsilateral hemisphere (Pfurtscheller & Lopes da Silva, 1999). These alpha and beta oscillations over the motor and sensorimotor cortex

are referred to as sensorimotor rhythms SMRs. However, MI-based BCI is not without its challenges including lengthy training times which increases user burden and findings indicating 20% of healthy subjects may not be able to learn to self-modulate SMRs to control BCIs with current technology (Blankertz et al., 2010).

The brain networks underlying motor execution overlap with those that underlie motor imagery (Lotze & Halsband, 2006) and motor learning tasks have been extensively used to evaluate the behavioral effects of tDCS. Anodal stimulation over the motor cortex has resulted in a faster learning rate for implicit (Nitsche et al., 2003) and explicit motor learning (Stagg et al., 2011) as well as retention of a learned motor paradigm (Galea, Vazquez, Pasricha, de Xivry, & Celnik, 2011; Reis et al., 2009). Using cathodal stimulation, Nitsche and colleagues and Stagg and colleagues found an opposite or no effect in using these same motor learning paradigms. As a result, these studies and others (see Madhavan & Shah, 2012; Reis & Fritsch, 2011) conclude that applying anodal tDCS over the motor cortex can improve behavioral motor learning across motor tasks.

The effects of tDCS on motor imagination are largely unknown due in part to inconsistent findings in the literature. Initial studies suggested increased ERD resulting from MI performance following anodal stimulation in small cohorts of both healthy (Matsumoto et al., 2010) and stroke subjects (Kasashima et al., 2012). More recently, Lapenta and colleagues combined tDCS stimulation with MI found an opposite effect; anodal stimulation decreased the ERD (Lapenta, Minati, Fregni, & Boggio, 2013). Combining high-definition tDCS (HD-tDCS) with EEG of MI before and after high-

definition anodal tDCS found similar results, a decrease in beta band ERD in the stimulated hemisphere (Roy, Baxter, & Bin He, 2014). In addition to the effect of tDCS on motor imagery, there have been multiple studies examining MI-BCI performance with tDCS. An initial study of anodal tDCS prior to BCI performance found an increased ERD over the stimulated motor cortex during BCI performance of contralateral hand motor imagination following stimulation, but no change in performance within a single session (Wei, He, Zhou, & Wang, 2013). Using trained subjects, Soekadar and colleagues found no change in performance within a session for those who received anodal stimulation compared to the sham group (Soekadar, Witkowski, Cossio, Birbaumer, & Cohen, 2014). Given the current state of this research, further work needs to be done to clarify how tDCS acutely and longitudinally affects subjects' ability to modulate their SMRs.

Recently, the electrophysiological network effects of tDCS have begun to be evaluated using simultaneous EEG and MEG (Roy et al., 2014; Soekadar et al., 2013). HD-tDCS systems use more electrodes, and smaller electrodes, than the standard two electrode tDCS configuration to improve the targeting of the cortical area of interest (Edwards et al., 2013; Kuo et al., 2013). These characteristics allow for online recording of the EEG during stimulation and online BCI performance (Edwards et al., 2013; Roy et al., 2014). Pharmacological and behavioral evidence suggests that tDCS application during, as compared to before or after, the learning of a new motor task results in an increased learning rate and increased performance.

With these technical developments, our aim is to better understand stimulation timing and task performance on MI-based BCI ability and the underlying

electrophysiology by combining EEG and HD-tDCS. We utilized HD-tDCS to examine the effect of multiple sessions of simultaneous high-definition tDCS and SMR-BCI on subject learning of right and left hand BCI tasks within and across sessions in BCI-naïve healthy subjects. We hypothesized that simultaneous anodal tDCS over the left primary motor cortex will improve BCI performance during and after stimulation compared to sham and cathode subjects. In addition, we hypothesize that within a session, anodal and cathodal HD-tDCS will differentially alter SMR power during task performance.

Methods

Experimental Setup

Subjects: 29 healthy subjects (14 female; 26 right handed) naïve to MI-BCI control were recruited to participate in these experiments (Age: 18-44 years; Mean: 24.1 years; SD: 5.6 years). Subjects were blinded to their group condition and were pseudo-randomized into three groups: anodal, cathodal, and sham stimulation. Subjects participated in three experimental sessions of their assigned condition. All procedures and protocols were approved by the University of Minnesota Institutional Review Board.

Hardware Setup: A 64-channel Biosemi EEG cap with active electrodes and an ActiveTwo amplifier were used to record the EEG signal at 1024 Hz (BioSemi, Amsterdam, Netherlands). A tDCS device with a high-definition (4x1) tDCS adapter was used to deliver 2 mA of current to the center electrode with four return electrodes (Soterix Medical, NY, USA). Conductive gel (Signa Gel, Cortech Solutions) was applied to reduce electrode offsets to below 30 mV for EEG electrodes and impedances under 1 kΩ for tDCS electrodes. The EEG cap was adapted to fit HD-tDCS electrodes adjacent to

EEG electrodes arranged per the international 10/20 system. The polarity of the center electrode is indicated by the subject group condition; the combined surround electrodes received the opposite current. The center electrode was placed between C3/CP3 and surround electrodes were placed between CP3/P3, C1/FC1, C5/FC5, and C3/FC3 at a radius of 3.5 cm from the center electrode (Figure 6). For anodal and cathodal conditions the stimulation consisted of a 30 second ramp up, 20-minute constant current and 30 second ramp down. For the sham condition, the device ramped up over 30 seconds and then immediately ramped down over 15 seconds. At the end of the 20-minute stimulation window, the device was ramped up and down over 45 seconds.

Experimental Procedure

Subjects were seated in a chair 90 cm from an LCD monitor where experimental stimuli were displayed. Subjects were instructed to remain still during the experimental trials. BCI2000 software was used to present experimental stimuli and record EEG data. Subjects were instructed to kinesthetically imagine opening and closing their respective hand, or a similar action such as squeezing a ball, unilaterally based on the target location. The trial structure was the same for all BCI trials and allowed for baseline rest (3 second inter-trial interval), planning (3 seconds), and online performance recordings (6 seconds maximum) (**Fig. 6**). Subjects performed four runs of 18 trials of the left/right BCI task before stimulation (Pre-Stim). Following this pre-stimulation block, the tDCS system was turned on and stimulation was started. During stimulation, subjects performed 5-6 runs depending on individual resting time (During Stim). The tDCS device was then turned off and the subject immediately performed four runs of BCI trials (I-Post

Stim) followed by a visual oddball task for 13 minutes to engage the subject while allowing a rest from the BCI task. Finally, subjects performed a final four runs of the session (D-Post Stim). Time between sessions was at least 48 hours.

Data Collection/BCI Control

The autoregressive filter implemented in BCI2000 was used to calculate the power in the frequency band of interest using a 16^{th} order model with a time window of 160 ms (McFarland & Wolpaw, 2008). Power in the 11-13 Hz range at C3/C4, when possible, was used to control the cursor with the control signal calculated based on a linear classifier with inputs composed of the positively weighted power in C4 and the negatively weighted power in C3. During stimulation, using C3 was not possible on all experimental days due to stimulation artifacts, and therefore one of the 9 surround electrodes was used instead of C3 to increase the signal-to-noise ratio in the controlling electrodes. Electrodes saturated by stimulation were removed on a session by session basis and voltages were later spherically interpolated during offline processing.

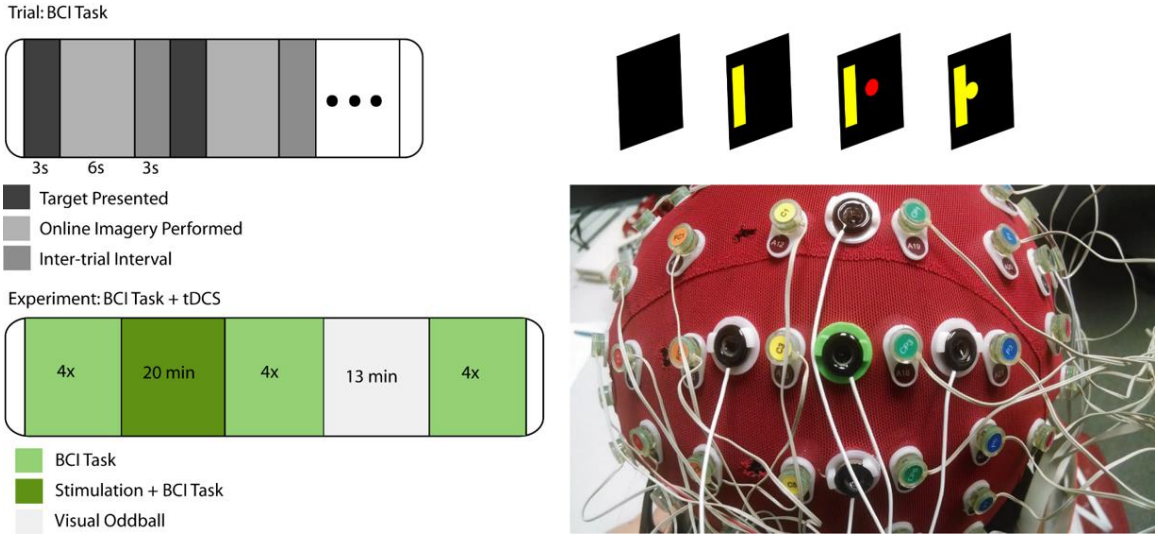

Fig. 6. Simultaneous BCI and tDCS task design and experimental setup. Experimental session: the subject performs 4 runs of 18 trials before stimulation, undergoes 20 minutes of stimulation and BCI trials, performs 4 runs after stimulation, performs a 13-minute visual oddball experiment with right hand response, and performs 4 runs delayed after stimulation (lower left). Setup of HD-tDCS electrodes (black circles) embedded within the 64 channel EEG cap (lower right). Single trial sequence of events: after the target is presented for 3 seconds, a red ball appears on the screen and moves based on the SMR control signal for a maximum of 6 seconds, and followed by a 3 second inter-trial interval (upper panel).

Signal Processing

Raw data were high pass filtered within hardware at 1Hz and 60Hz notch filtered. Offline processing was performed with custom scripts utilizing the EEGLAB toolbox (Delorme & Makeig, 2004) in MATLAB (The Mathworks, Inc., MA, USA). Data was low pass filtered at 110 Hz and the mean of each channel was removed. Electrodes were

re-referenced to the common average reference and downsampled to 250 Hz. Independent Component Analysis (fast-ICA) (Hyvarinen, 1999) was run on concatenated data from all non-stimulation blocks. Components corresponding to eye movement, eye blink, and muscle artifact were removed. Data was then epoched into trials; those contaminated with artifacts during baseline or task performance not removed by ICA were discarded. Data from each channel were then transformed into their time-frequency representation using a 1Hz band Morlet wavelet and the power in each time window and frequency band was computed (Qin & He, 2005). For the EEG collected during stimulation, ICA did not completely remove all stimulation artifacts in surrounding electrodes and resulted in a difference between the during-stimulation block and the pre-/post-stimulation block power that could not be solely attributed to electrophysiological responses to stimulation. Therefore, we do not directly compare left hemisphere electrophysiological results between these time blocks.

Analysis

For analysis of pre-stimulation data, we removed the first run as the control signal normalizer was not yet adapted to the subject for that day. Therefore, we included 54 left/right trials for Pre-Stim, 90-108 trials for During Stim, 72 for I-Post Stim, and 72 for D-Post Stim.

Primary performance outcome measures include percent valid correct (PVC) and time-to-hit (TTH) the correct target. The PVC is defined as the number of trials in which the subject hit the correct target divided by the sum of hit and miss trials, with the aborted trials not included. The time-to-hit was defined for correct trials as the time elapsed from

the appearance of the ball to when the ball hit the correct target.

Primary electrophysiological outcome measures include electrode baseline power, electrode online power during task performance, and the event-related power in the alpha (8-13 Hz) band. Analysis of electrophysiological data was only performed on correct trials. We specifically examined sensorimotor electrodes C3/C4/CP3/CP4 for each of the electrophysiological measures. In addition, we calculated the pseudo-online control signal (C4 power - C3 power) during the task performance period. The trial-by-trial event-related power change, normalized to the baseline power (Gert Pfurtscheller & Lopes da Silva, 1999; Yuan et al., 2008). The baseline was defined as the 1 second of the inter-trial interval prior to the target appearing. The online power used was the mean power over the task window. We calculated the correlation value between the power and right vs. left hand trials as a measure of the discriminability for individual electrodes (Muller, Krauledat, Dornhege, Curio, & Blankertz, 2004).

When the measure was normally distributed, we utilized a three-level hierarchical linear model (HLM) with random effects across subjects, groups, and blocks. ANOVA and t-test analyses were performed post-hoc. When non-normally distributed, we collapsed the data along specific dimensions (session or block) and used Kruskal-Wallis tests, with Wilcoxon rank-sum tests Bonferroni corrected for post-hoc analysis. To measure longitudinal effects, we defined each block within a session as the mean of the subject values within each group for each time-point. To measure within session effects, we corrected values to the pre-stimulation values for that session. Depending on the measure, this correction was either normalization to or a subtraction of the pre-

stimulation value from the post-stimulation values.

Results

Effects of tDCS on Performance Measures

Percent valid correct (PVC) is a measure of the accuracy of performance. Using a hierarchical linear model, we found an initial difference in PVC performance between stimulation groups for right hand trials (p = 0.002) and left hand trials (p = 0.019). For right hand trials, post-hoc analysis resulted in an overall difference between anodal stimulation and cathodal stimulation groups (p = 0.048) and an interaction effect of session by group for anode and cathode (p = 0.002). For left hand trials, post-hoc analysis resulted in a significant interaction effect of session by group for anodal and cathodal stimulation groups (p = 0.018). Anodal subjects had higher baseline performance and had higher performance overall, therefore we baseline subtracted the pre-stimulation value of first session. With this correction, there was no significant difference in PVC based on condition for either left or right hand trials (**Fig. 7**).

The absolute time-to-hit (TTH) was not significantly different between stimulation groups in either left or right hand trials (**Table 2**). When normalizing the time-to-hit to each group's initial baseline value, there was a significant difference in right hand trials between the three groups (p = 0.039). Post hoc analysis found a difference between the anodal group and the cathodal group (p = 0.01); the anodal group had a significantly decreased time-to-hit for right hand trials (**Fig. 8**). For right hand trials within a session there was a significant difference between groups at the delayed post-stimulation time block (p = 0.003); post-hoc pairwise comparison resulted in a significant

difference between anodal and cathodal groups (p = 0.003), and anodal and sham groups (p = 0.004) (**Fig. 9**). There was no significant difference for left hand trials.

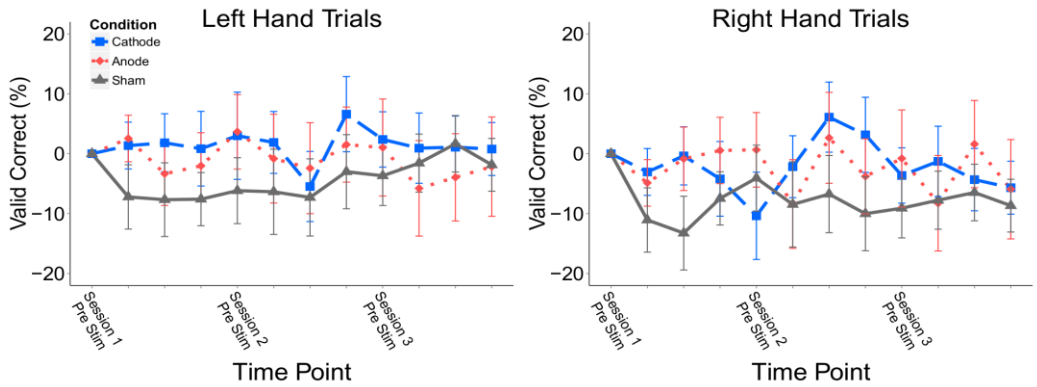

Fig. 7. Longitudinal baseline subtracted percent valid correct. Percent valid correct across time for left and right hand trials with the baseline from each individual first session pre-stimulation block subtracted from the values at later time points. Group PVC did not significantly change over the three sessions. Values: Mean +/- S.E.

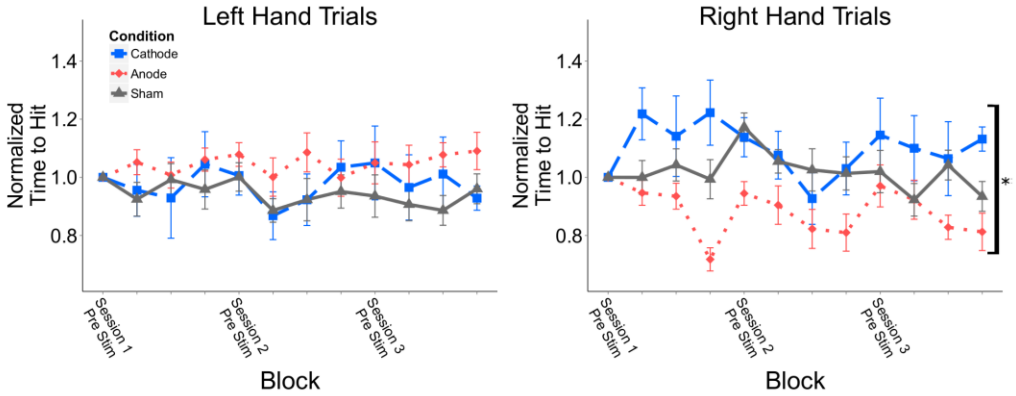

Fig. 8. Longitudinal normalized time to hit. Time to successfully hit right and left hand targets within experimental sessions normalized to subject initial baseline prior to stimulation. The anodal group displayed a reduced time-to-hit for right hand trials compared to the cathodal group. There was no difference for left hand trials. Values: Mean +/- S.E. *p<0.05 for Kruskal Wallis test.

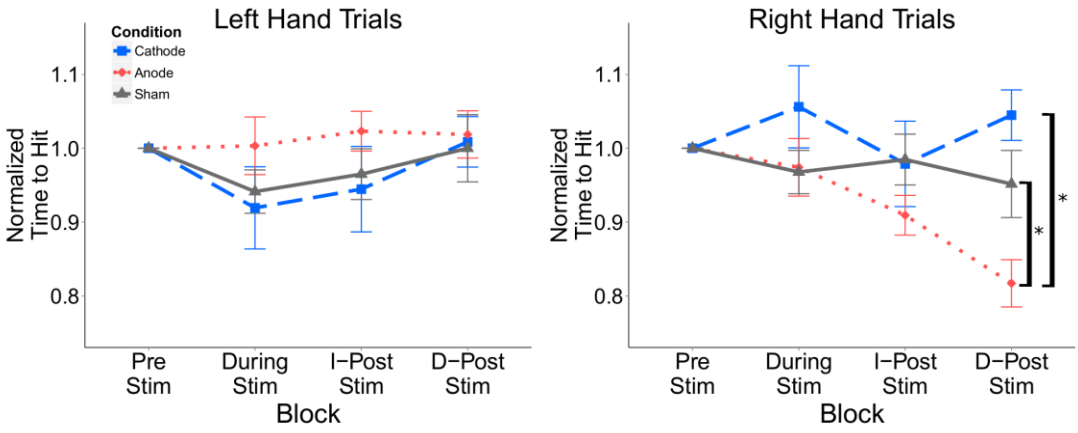

Fig. 9. Acute normalized time to hit. Time to successfully hit right and left hand targets within experimental sessions normalized to the pre-stimulation baseline for each session. The anodal group had a reduced time-to-hit for right hand trials following stimulation at the delayed time point for right hand but not left hand trials. Values: Mean +/- S.E. *p<0.05 for Wilcoxon rank sum test.

Right Hand Time-To-Hit (ms)	Pre-Stim	I-Post Stim	D-Post Stim
Anode	3325 ± 167	2933 ± 87	2686 ± 163
Sham	3191 ± 142	3005 ± 160	2906 ± 90
Cathode	3130 ± 173	2946 ± 116	3165 ± 193

Table 2: Mean time to successfully hit right hand imagination trials across blocks. Values: Mean +/- S.E.

Effects of tDCS on Electrophysiological Measures

We examined the event-related power following stimulation within sessions and across sessions and found no significant difference between stimulation groups at C3, CP3, C4 or CP4 for both left hand and right hand trials. We examined trial baseline alpha power within and across sessions normalized to the pre-stimulation power between

stimulation groups and found no significant difference within sessions at C3, C4, or CP4 following stimulation. When normalized to the pre-stimulation baseline power, there were within session differences between groups at CP3 at the delayed time point (p = 0.023), but no significant pairwise comparisons with post-hoc testing.

There were changes in alpha power during task performance across all groups over the course of a session. To visualize these changes bilaterally across the motor strip, we normalized the power at each electrode to the pre-stimulation value within each session (**Fig. 10**). We quantitatively characterized these changes at each electrode by directly comparing the values across groups at the post-stimulation time points. There were group differences in alpha power within sessions in the C3 and CP3 electrodes for right hand trials. For electrode C3, there was a difference in alpha power between cathode and sham groups immediately following stimulation (p = 0.0125). At the delayed time point there was a difference between all groups (p = 0.04) (**Fig. 11**). Post-hoc analysis resulted in a significant difference between the sham and cathodal groups at the delayed time point (p = 0.007). There was also a significant difference between groups over all blocks (chi-squared = 6.67, p = 0.036) with a post-hoc difference between sham and cathodal groups (p = 0.004). For left hand trials, there is no significant difference between the stimulation groups at any time points (immediate post-stim, p =.20; delayed post-stim, p = 0.07), but there was a trend for the cathodal group to have lower power than the sham and anode groups. Similar results are found in electrode CP3 for right hand trials with a significant group difference at the delayed post-stim time point (p = 0.04) with post-hoc difference between sham and cathode (p = 0.007). We did not find any

difference in C4/CP4 electrodes for right or left hand trials, respectively, immediately post-stimulation (C4: p = 0.34; p = 0.64) or delayed post-stimulation (C4: p = 0.43; p = 0.65).

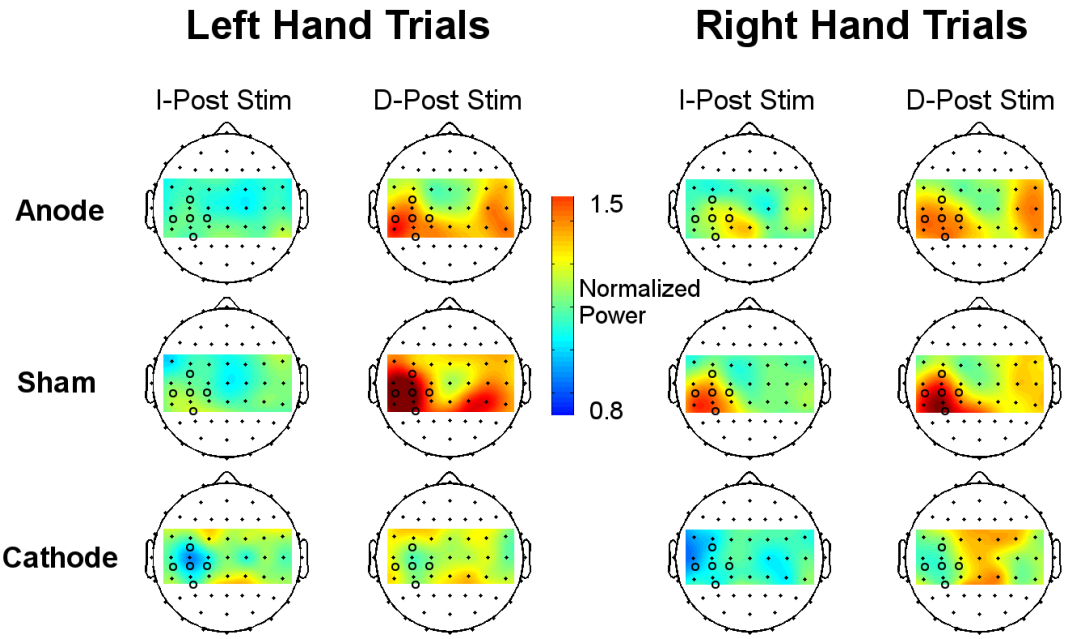

Fig. 10. EEG topograph of alpha band power changes. Mean alpha power during task performance in the task blocks after stimulation normalized to the pre-stimulation power for left and right hand trials. For right hand trials, cathodal stimulation decreased the alpha power in the stimulated hemisphere during task performance immediately following stimulation compared to the anodal and sham groups. Colors represent power normalized to pre-stimulation baseline. Black circles represent tDCS electrodes located over the left sensorimotor cortex.

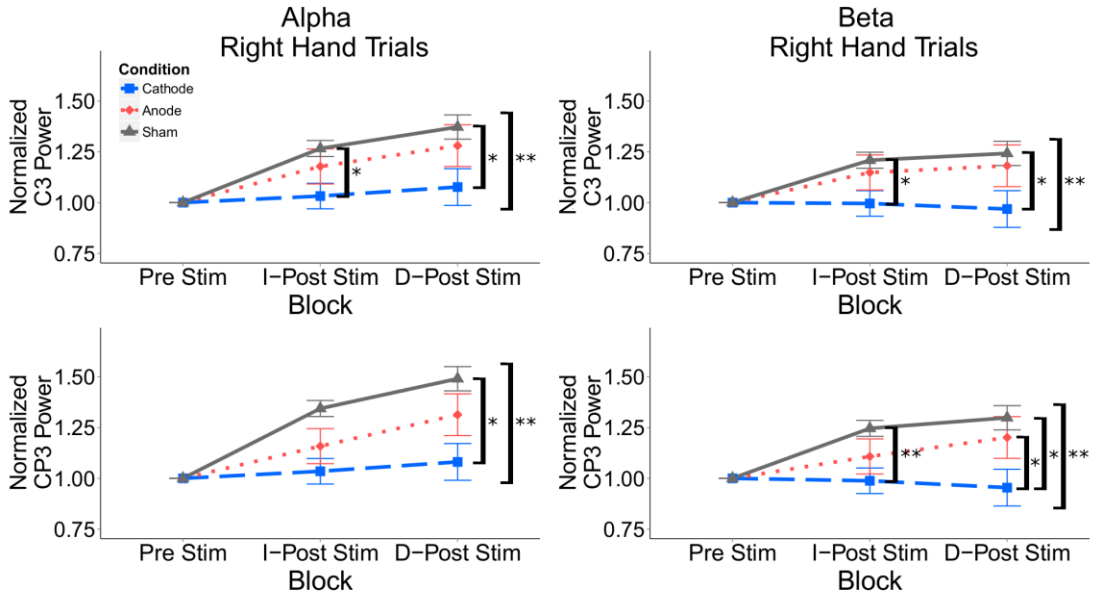

Fig. 11. Acute changes in alpha power following HD-tDCS. Mean alpha power during task performance normalized to pre-stimulation trial power for successful right hand and left hand trials in the C3 electrode. There is decreased alpha power in the cathodal group compared to the sham group during right hand task performance in the C3 electrode immediately after stimulation and at the delayed time point. There is no significant difference for left hand trials. Values: Mean +/- S.E. *p<0.05 for Wilcoxon rank sum test. **p<0.05 for Kruskal Wallis test.

We found a difference between stimulation groups with measures combining electrodes and trial directions. For the pseudo-control signal, we examined the change over time within a session and found that there was a significant difference immediately following stimulation between the groups for right hand trials when normalized to the pre-stimulation baseline (p = 0.047). Though there was no difference in post-hoc pairwise comparisons when correcting for multiple comparisons, a trend towards an increased

control signal for the anode group compared to sham was present ($p = 0.025$). There were no differences for left hand trials between groups. There was an increase in discriminability in C3 for anodal subjects at delayed post-stimulation ($p = 0.008$), and an increase for sham subjects immediately post-stimulation ($p = 0.014$) and delayed post-stimulation ($p = 0.003$). For C4 we found a similar pattern for the sham and anode groups, respectively, at the delayed time point (Anode: $p = 0.012$; Sham: $p = 0.005$). Cathodal subjects did not show any increase in discriminability for either of these electrodes.

Discussion

We report the results of the first study, to our knowledge, of motor imagery-based BCI with simultaneous left sensorimotor HD-tDCS on behavioral and electrophysiological measures across multiple learning sessions. Stimulation alters electrophysiology and behavior during BCI performance based on task specific neural activation within and across experimental sessions.

The primary behavioral effect of anodal HD-tDCS over the left sensorimotor cortex was a reduced time to acquire right hand imagination targets both within sessions after stimulation and across three sessions on multiple days. Previous studies did not report the effect of tDCS on BCI task timing as timing was not variable (Soekadar et al., 2014; Wei et al., 2013). For motor learning tasks examining the speed of performance, Nitsche et al. (Nitsche et al., 2003) used a serial reaction time task with left M1 stimulation and right hand movement and found anodal subjects to have a decreased reaction time compared to cathodal and sham stimulation. Our results parallel this result,

though in a different paradigm where timing is not the specific target of training. In addition, similar to previous studies, we found no direct effect on the accuracy for either left or right hand trials.

Anodal tDCS is thought to depolarize pyramidal neurons that generate the synchronous signal recorded with EEG. Two ways this may affect the sensorimotor network utilized during MI-BCI include: the depolarization leads to greater overall synchrony as more neurons are likely to fire together, or that this resting synchrony is not significantly affected by tDCS, but nonsynchronous firing, which yields the ERD, may be affected. To evaluate the support for these hypotheses, we examined baseline power changes, task based power changes, and the ERD/ERS.

We found no difference in the mean ERD/ERS at the primary electrodes of interest (C3/CP3/C4/CP4) across groups following stimulation when normalized to the pre-stimulation event-related power. Previous electrophysiological studies found mixed effects on the ERD following tDCS stimulation. Initial MI work found an increase in ERD of the stimulated hemisphere (left M1) when performing MI (Kasashima et al., 2012; Matsumoto et al., 2010) and MI-BCI (Wei et al., 2013) whereas others found no change in the ERD for MI, MI-BCI, or motor observation (Lapenta et al., 2013; Soekadar et al., 2014). Our study design differed from these previous studies in multiple ways; we applied stimulation during learning over three sessions, and in the context of a single session, subjects performed the BCI task before, during, directly after, and thirty minutes after stimulation. The specific timing of stimulation relative to task performance has been found to have a significant effect on the outcome of the stimulation for motor tasks;

simultaneous performance and stimulation have yielded the greatest effect (Reis & Fritsch, 2011).

We found differing effects on the baseline power and online power during task performance. There was no significant difference post-stimulation in the baseline period of the trials which would suggest that tDCS is not affecting this alpha activity prior to task performance. We found a difference in alpha power between the stimulation groups during right hand task performance across blocks at electrodes C3 and CP3. This difference was composed of a decreased alpha power during right hand trials for cathodal stimulation compared to sham stimulation, where anodal and sham stimulation both increased following the stimulation block. We also found an increase in discriminability for the sham and anode groups in C3 and C4, but no increase in the cathodal group. Combined, these results suggest that cathodal stimulation reduces a subject's ability to modulate their SMR during task performance compared to sham stimulation. This also suggests there is not an overall change in alpha power following stimulation but rather a task specific effect. In addition, when calculating our pseudo-control signal, we found a difference in the control signal for right hand trials between groups with a trend for an increased control signal in the anodal group compared to the sham group. For right hand imagination, we expect the left sensorimotor cortex to have decreased power relative to the right and anodal stimulation resulted in an increase in this signal compared to the sham stimulation.

There is a large degree of individual variability for both MI-BCI performance and responses to non-invasive brain stimulation (Berker et al., 2013; Bestmann et al., 2015;

Blankertz et al., 2010; Hammer et al., 2012). We did not individually target the tDCS based on subject specific anatomy or functionality, targeting the area of maximum ERD/ERS during motor imagination. This could have resulted in inaccurate targeting of the stimulation area on the individual level, particularly with HD-tDCS which restricts the stimulated area compared to the standard two electrode tDCS configuration. Others have found subject specific targeting of non-invasive neuromodulation to be vital for treating neurological disorders (Fox et al., 2014). For the BCI learning, we did not individualize parameters for each subject, rather we used the 11-13 Hz frequency band and fixed electrodes (C3/C4) for all subjects, though there can be variability in electrodes or frequencies bands that subjects use to control the BCI. Additionally, we did not use a source-analysis based filter the EEG control signal which may lead to improvements in performance by solving the inverse problem (Edelman, Baxter, & He, 2016; Kamousi, Liu, & He, 2005; Qin, Ding, & He, 2004).

We may see differing effects compared to previous studies due to a host of parameters, including the stimulation time, the amplitude of stimulation, the timing of stimulation, as well as the electrode montage (Moliadze, Atalay, Antal, & Paulus, 2012). The variability across study design and parameters within MI and BCI performance, and across tDCS studies, in general, suggest significant avenues for future investigation to optimize stimulation for the target task. Overall, the behavioral and electrophysiological results combined suggest that anodal tDCS is differentially affecting right and left hand motor imagination. Using noninvasive electrophysiological recordings during and after stimulation is a promising way of further understanding the effects of tDCS stimulation

on brain networks, as without these recordings, we cannot understand the underlying physiological changes that result in the vast number of behavioral changes reported in the literature.

Chapter 3 –

Transcranial Direct Current Stimulation Alters Brain Connectivity during Motor-Imagery Based Brain-Computer Interface Control

Chapter 3 Overview

Transcranial direct current stimulation has been shown to affect motor and cognitive task performance and learning when applied to brain areas involved in the task. Targeted stimulation has also been found to alter connectivity within the stimulated hemisphere during rest. However, the connectivity effect of the interaction of endogenous task specific activity and targeted stimulation is unclear. Here we examined this interaction during a 1D sensorimotor rhythm-based BCI task combined with high-definition tDCS. We collected two sets of data from healthy subjects who participated in three BCI-tDCS sessions. Analysis of the first set investigated the effect of anodal stimulation over multiple session. Analysis of the second set investigated intersubject variability between anodal, cathodal, and sham stimulation. Connectivity analysis showed altered connections bilaterally between frontal and parietal regions, and these alterations occur in a task specific manner; this difference is illustrated by connections between similar cortical regions altered differentially during left and right imagination trials. Using finite element modeling we show that current flow from HD-tDCS is focused under the stimulation electrodes with limited current flowing to the contralateral

hemisphere, which suggests the stimulation connectivity effects are due to anatomical or functional connections between affected regions rather than the direct effect of tDCS current on non-targeted regions. In addition, we found that connectivity correlates with behavioral measures. These results suggest that targeting tDCS to affect connectivity and understanding how the stimulation this interacts with task specific endogenous activity should be combined to maximize the targeted effect.

Introduction

Transcranial direct current stimulation (tDCS) of the human brain has been increasingly investigated since the resurgence of research into the effects of noninvasive electrical brain stimulation in the late 1990s (Bestmann et al., 2015; Nitsche & Paulus, 2000; Paulus & Opitz, 2013). tDCS consists of injecting current of a maximum of 4 mA into the head of a subject through multiple electrodes located on the scalp or extracephalically. Modeling studies using both standard two-electrode and multi-electrode configurations have found that a low level of current reaches the cortex, and depending on electrode configuration, deeper structures, with levels that have been shown in vitro to affect neuronal firing (Bikson et al., 2004b; Kabakov et al., 2012; Kuo et al., 2013; Opitz et al., 2016; Sadleir et al., 2010). These neuronal effects most likely stem from a variety of sources including membrane depolarization and hyperpolarization of the dendrites and axons of pyramidal cells as well as secondary effects on membrane resistance (Paulus & Rothwell, 2016; Stagg & Nitsche, 2011). Behaviorally, the effects of tDCS on the motor system has been extensively studied and has been found to affect motor performance and learning when stimulating the motor network (Buch et al., 2017;

Reis et al., 2009; Reis & Fritsch, 2011). The in vivo effects of tDCS on endogenous resting and task specific brain oscillations is less well-understood, and has only recently begun to be investigated with EEG and MEG (Bergmann, Karabanov, Hartwigsen, Thielscher, & Siebner, 2016; Notturno, Marzetti, Pizzella, Uncini, & Zappasodi, 2014; Roy et al., 2014; Soekadar et al., 2013, 2014).

An emerging hypothesis relating the effect of noninvasive neuromodulation to brain activity utilizes a long-term potentiation rationale for targeting brain areas that are specifically active during a task or rest (Bikson & Rahman, 2013). Previous work found specific effects based on task related activation found using functional magnetic resonance imaging (fMRI). Fox et al examined the effects of transcranial magnetic stimulation (TMS) targeting and found specifically that if the areas targeted overlapped with correlated or anticorrelated resting state networks, there was an effect on neurological symptoms in patients (Fox et al., 2014). Further work targeting resting state activity in the motor network with tDCS found increased stimulation efficacy with anodal stimulation of correlated areas as compared to anodal-cathodal stimulation of correlated areas (Fischer et al., 2017). Clark and colleagues found effects during task performance, targeting areas that show increased BOLD signal with anodal stimulation and those areas with a decreased BOLD signal with cathodal stimulation and have found improvements in visual attention tasks targeting parietal, prefrontal, and temporal areas, with activation and polarity specific effects (Clark et al., 2012).

Simultaneous stimulation of involved areas during motor performance and learning has specifically led to improvements in performance compared to stimulation

prior to, or after, task performance (Buch et al., 2017). Recent work by our group found a decrease in time to hit and an increase in alpha and beta band power following simultaneous tDCS over the sensorimotor cortex during motor imagery based BCI performance (Baxter et al., 2016). We found acute differences between stimulation types over three groups of subjects, with each subject receiving a single stimulation type over three sessions. While these results demonstrated the effects of anodal and cathodal stimulation over multiple days, significant intersubject variability in response to stimulation has been reported due to neurotransmitter levels, genetics, brain geometry, and ongoing individual brain states (Antal et al., 2010; Krause & Cohen Kadosh, 2014); this variability remains a significant issue in neuromodulation (Ammann, Lindquist, & Celnik, 2016; Mordillo-Mateos et al., 2012; Wiethoff, Hamada, & Rothwell, 2014).

The development of noninvasive brain computer interfaces has allowed individuals with motor dysfunctions to control computers and devices in the lab (He et al., 2015; Mak & Wolpaw, 2009; Millán et al., 2010; Scherer & Pfurtscheller, 2013; Wolpaw, McFarland, Neat, & Forneris, 1991) and in the home (Sellers, Mcfarland, Vaughan, & Wolpaw, 2010) in real-time using self-modulated brain rhythms or external stimuli. A predominant paradigm for continuous control of an output device is using motor imagination with sensorimotor rhythm modulation. To voluntarily modulate their sensorimotor rhythms, subjects kinesthetically imagine moving a body part without executing the movement. This imagination engages similar networks to motor execution and generates an event related desynchronization in alpha (8-13 Hz) or beta (15-30 Hz) frequencies in the sensorimotor cortex underlying the imagined body region which

corresponds to a local decrease in power in the affected frequencies (Lotze & Halsband, 2006; Pfurtscheller & Lopes da Silva, 1999). An event related synchronization also may occur in contralateral sensorimotor regions. A recent meta-analysis of fMRI data found premotor and somatosensory regions predominantly active during motor imagination as well as more distributed areas in the frontal and parietal cortices including the inferior frontal gyrus, premotor cortex, supplementary motor area, primary motor cortex, primary somatosensory cortex, and superior parietal cortex (Hétu et al., 2013). While fMRI yields precise localization of indirect measure of neural activity, the temporal resolution is on the order of seconds which does not allow us to examine most oscillatory dynamics. The temporal resolution of EEG is on the order of milliseconds however standard analysis of EEG data on the sensor level does not allow for high spatial resolution.

Source imaging which involves solving the inverse problem of mapping EEG sensor activity to the brain using Maxwell's equations and the physical properties of head tissues has been developed in the last few decades (Cincotti et al., 2008; Hamalainen & Sarvas, 1989; He et al., 1987). Based on the specific algorithm for performing this transformation, modeling and event-related potential studies have found localization errors of 7 mm or less (Im, Gururajan, Zhang, Chen, & He, 2007; Michel et al., 2004). Source imaging analysis of motor imagination both without and with feedback has been demonstrated to have higher signal-to-noise ratio than sensor data, which can lead to improved motor imagination classification (Edelman et al., 2016; Kamousi, Amini, & He, 2007; Kamousi et al., 2005; Qin & He, 2005; Yuan et al., 2008). While source based analysis allows us to examine how brain areas are active over time, more explicit analysis

of the interaction of different brain areas are needed to functionally understand how information flows within the network.

There are multiple families of methods that have been used to examine undirected and directed connectivity during cognitive tasks using both direct EEG/MEG and indirect fMRI/functional near-infrared spectroscopy (fNIRS) measurements. These include models with underlying assumptions regarding the cortex and anatomical connections, such as dynamic causal modeling, as well as data driven approaches where a model is fit to the data, and the model is analyzed, such as multivariate autoregressive model analysis using Granger Causality time-based methods (Friston, Moran, & Seth, 2013), or frequency based methods such as the directed transfer function (DTF) and partial directed coherence (PDC) (Astolfi et al., 2007; Kamiński & Blinowska, 1991; Sameshima & Baccala, 2001).

Electrophysiological and hemodynamic techniques have been used to evaluate changes in brain connectivity during and following tDCS (Luft et al., 2014). Connectivity analysis using EEG following transcranial current stimulation was initially performed by Polania et al. found that after tDCS during a motor task, there was an increase in intrahemispheric connectivity in the alpha, beta and high gamma frequencies (Polanía, Nitsche, & Paulus, 2011). Further studies examining effects on the motor network found brain state dependent effects following stimulation (Feurra et al., 2011; Notturno et al., 2014). fMRI studies have examined stimulation based changes in cortical and subcortical connectivity. Polania et al. found increased functional connectivity between the left motor cortex and the ipsilateral thalamus and caudate nucleus following anodal

stimulation (Polanía, Paulus, & Nitsche, 2012). Hunter et al. found an increase in connectivity strength across the default mode networks that included the superior parietal region following stimulation of the parietal region (Hunter et al., 2015). Sehm et al. found resting state networks effects of unilateral and bilateral primary somatosensory anodal stimulation both during and after stimulation (Sehm et al., 2012). Further work examining both task specific (Meinzer et al., 2012) and resting state has shown similar effects due to anodal stimulation (Amadi, Ilie, Johansen-Berg, & Stagg, 2014; Keeser et al., 2011; Peña-Gómez et al., 2012). Combined, these results suggest anodal stimulation increases connectivity near the stimulation electrode as well as to more distant sites intra- and interhemispherically, though the specific effects and regions affected are dependent on the task being performed, the networks involved in the task, and the regions connected to the stimulated area.

The regions underlying motor imagination have been evaluated using connectivity methods to examine the interaction of frequency bands in areas of interest, though generally confined to the sensorimotor cortex (Hamedi, Salleh, & Noor, 2016; Kus et al., 2006). Previous work examined time and frequency based measures such as Granger causality and coherence metrics and found connections both unilaterally and bilaterally between sensory motor cortex and frontal areas during motor imagination (Hamedi et al., 2016). There may be specific differences between motor imagination as performed in these studies and motor imagery brain computer interfaces performance in later studies and in the present study due to the visual feedback based on performance, as the feedback will change the brain states and the time course of brain patterns. More recent work has

examined sensor-based and source based connectivity using independent components in order to examine at the discriminatory ability for BCI control of connectivity features, in comparison to power and frequency based features and found little to no improvement using connectivity features (Billinger, Brunner, & Müller-Putz, 2013).

There is a disconnect between the work performed early on looking at a neuroscientific basis of motor imagination and how features develop while subjects are performing motor imagination and classification and discrimination used for online BCIs. Sensorimotor rhythm-based BCIs are a useful experimental protocol as unilateral hand imaginations generally yield different bilateral signals generated by the sensorimotor cortex and if stimulation interacts with ongoing oscillations it can be evaluated by comparing the laterality of imagination.

The aim of this study was to determine connectivity changes during sensorimotor rhythm-based BCI control following simultaneous HD-tDCS of the sensorimotor cortex. We analyzed data recorded during sensorimotor rhythm BCI performance while subjects controlled a moving cursor on the screen prior to and following anodal stimulation of the left sensorimotor cortex. We collected two data sets to evaluate this effect: data set one consisted of five subjects who received anodal stimulation over three sessions; data set two consisted of eight subjects who received anodal, cathodal, and sham stimulation over three sessions; this set enabled subject specific effects of tDCS and reduce variability by eliminating intersubject differences between stimulation groups.

We used a data-driven approach to determine regions-of-interest during BCI control across the cortex, calculated the connectivity between these regions, and

determined the changes that resulted from the tDCS. In addition, we examined the relationship between performance and connectivity measures to inform how information flow and connectivity of networks underlying motor imagination correlate with behavioral outcomes. By combining the connectivity changes after stimulation and the correlations of connectivity values with performance, we aim to inform the functional targeting of networks of interest to maximize stimulation effects and develop multifocal closed loop-noninvasive stimulation on a subject specific level.

Methods

Experimental setup

Data set one: Data analyzed was a subset from a set of experiments previously reported (Baxter et al., 2016). In short, five right-handed healthy subjects (3 female) naive to MI-BCI control participated in these experiments (Age: 22-24 years; Mean: 22.6 years; SD: 0.8 years). These subjects were selected because they performed proficiently and achieved >70% accuracy. Each subject attended three experimental sessions where they received anodal stimulation according to the experimental setup described below.

Data set two: Eight healthy subjects (3 male; ages: 19-55, mean: 27.7; 7 right handed) participated in this study. Four subjects had previous BCI and tDCS experience, four subjects were naïve to tDCS and BCI. Each subject participated in three stimulation sessions during which twenty minutes of 2 mA anodal, cathodal, and sham stimulation was delivered while subjects performed sensorimotor rhythm-based BCI control.

Data set three: Ten healthy subjects participated in this study. All subjects were naïve to BCI, motor imagination, and tDCS. Each subject participated in three stimulation sessions during which twenty minutes of 2 mA anodal, cathodal, and sham

stimulation was delivered while subjects performed motor imagination without feedback. All other aspects of the task were consistent with the BCI setup and methods were identical therefore in the rest of this section we do not differentiate between MI and BCI.

All procedures and protocols were approved by the University of Minnesota Institutional Review Board.

A 64-channel Biosemi EEG cap with active electrodes and an ActiveTwo amplifier were used to record the EEG signal at 1024 Hz (BioSemi, Amsterdam, Netherlands). A tDCS device with a high-definition (4x1) tDCS adapter was used in a Laplacian configuration to deliver 2 mA of current to the center electrode with four return electrodes (Soterix Medical, NY, USA). Conductive gel (Signa Gel, Cortech Solutions) was applied to reduce electrode offsets to below 30 mV for EEG electrodes and impedances under 1 kΩ for tDCS electrodes. The EEG cap was adapted to fit HD-tDCS electrodes adjacent to EEG electrodes arranged per the international 10/20 system. The center electrode (anode/cathode) was placed between C3/CP3 and surround electrodes (cathodes/anodes) were placed between CP3/P3, C1/FC1, C5/FC5, and C3/FC3 at a radius of 3.5 cm from the center electrode. Active anodal and cathodal stimulation consisted of a 30 second ramp up, 20-minute constant current and 30 second ramp down. For the sham condition, the device ramped up over 30 seconds and then immediately ramped down over 15 seconds. At the end of the 20-minute stimulation window, the device was ramped up and down over 45 seconds.

Subjects were seated in a chair 90 cm from an LCD monitor where experimental stimuli were displayed. Subjects were instructed to remain still during the experimental

trials. BCI2000 software was used to present experimental stimuli and record EEG data. Subjects were instructed to kinesthetically imagine opening and closing their respective hand unilaterally based on the target location. The trial structure consisted of a baseline rest period (3 seconds), planning phase (3 seconds), and online performance (6 seconds maximum). Subjects performed 72 trials of the left/right BCI task before stimulation (Prestim); the first 18 trials were removed as at the start of each session the normalizer needed to adjust for the subject and session. Following this, the tDCS system was turned on and stimulation was started. During stimulation, subjects performed 90-108 trials depending on individual resting time between runs. The tDCS device was then turned off and the subject immediately performed 72 trials ($Post_0$) followed by a visual oddball task for 13 minutes to engage the subject in a controlled task, while allowing a rest from the BCI task. Finally, subjects performed 72 trials during the delayed time period from approximately 25 to 37 minutes post-stimulation ($Post_{25}$). Subjects participated in three sessions with the time between sessions at least 48 hours.

The BCI control system used the autoregressive filter implemented in BCI2000 was used to estimate the 11-13 Hz power at C3/C4 which was used, when possible, to control the cursor with the control signal calculated based on a linear classifier with inputs composed of the positively weighted power in C4 and the negatively weighted power in C3. A normalizer was used with the classifier to reduce any directional bias in the cursor movement due to a subject's difference in relative power between C3 and C4. After each trial, the normalizer removed the offset by subtracting the mean and scaling

the classifier output to unit variance based on the weighted sum of C3 and C4 during the online period of the preceding 30 seconds. For further details see Chapter 2.

Signal processing

Raw data were high pass filtered within hardware at 1Hz and 60Hz notch filtered. Offline processing was performed using custom scripts utilizing the EEGLAB toolbox (Delorme & Makeig, 2004) in MATLAB (The Mathworks, Inc., MA, USA). Data was low pass filtered at 110 Hz and the mean of each channel was removed. Electrodes were re-referenced to the common average reference and downsampled to 250 Hz. Independent Component Analysis (fast-ICA) (Hyvarinen, 1999) was run on concatenated data from all non-stimulation blocks for each session. Components corresponding to eye movement, eye blink, and muscle artifact were removed (Jung et al., 2000). Data was then epoched into trials. We visually examined the EEG time course data and removed electrodes that displayed a drift from their mean over time and spherically interpolated their activity (Delorme & Makeig, 2004); these were primarily prefrontal or temporal electrodes. Those trials that were contaminated with artifacts during baseline or task performance, respectively, not removed by ICA were discarded. Following removal and interpolation of bad channels, and removal of trials with significant artifactual activity, we referenced the data to a common reference and removed channel means.

For the mean baseline values used to characterize the noise for source imaging, we included all clean trials remaining after artifact rejection and preprocessing. The one second prior to the appearance of the target, during the inter-trial interval, was used as the baseline. It is unlikely that subjects performed motor imagery accurately for the entire control period during every trial, therefore the peak control period for each trial was

selected and analyzed. For each correct trial, we calculated the difference in power between C3 and C4 in the alpha band within a sliding 500ms time window when subjects were controlling the BCI. For analysis, we removed the first 500ms of the trial, as there was frequently an ERP artifact due to the cursor appearance, as well as the final 250ms of the trial, as there was frequently an additional artifact. The data within the 500ms time window that contained the largest power difference was then used for the analysis of the online data. The time courses were detrended and standardized prior to model fitting and further analysis.

Source analysis

The BEM forward model was calculated using OPENMEEG (Gramfort, Papadopoulo, Olivi, & Clerc, 2010) with relative conductivity values of Skin/Skull/Brain: (1/.0125/1) using a quasistatic approximation mapping 64 electrodes to 15002 dipoles covering the entire cortical surface. A common head model based on the Colin27 head was used for all source analysis with electrodes located in the Biosemi 64 channel EEG configuration. $M = GD,$ with M indicating the EEG sensor measured values, G indicating the gain matrix from the forward problem mapping of noiseless data from the dipole sources to the sensors, and D indicating the dipole current source density. As this is an underdetermined problem, we employed Tikhonov regularization with the weighted minimum norm approach to estimate the dipole current density distribution using Brainstorm (Tadel, Baillet, Mosher, Pantazis, & Leahy, 2011). The weighted minimum norm solution is given by

$$\hat{D} = (W^T W)^{-1} G^T (G(W^T W)^{-1} G^T + \lambda I)^{-1} M$$

where $\widehat{D}$ is the estimated dipole cortical current density, W is the weight matrix, λ is the regularization parameter, and I is the identity matrix (Grech et al., 2008). Where $W = \Omega \otimes I$ with $\otimes$ denoting the Kronecker product and Ω being the norm of the columns of G.

The alpha power during the trial and baseline period was computed using 1 Hz resolution Morlet wavelets. The real and imaginary components were separately used to calculate the inverse for each set of values for each trial. To calculate the noise covariance matrix for the inverse calculation, the baseline data from one second prior to the start of the trial was mean subtracted on a trial by trail basis. The noise covariance was calculated for each trial and the final matrix was the mean of all artifact free trial matrices for each specific block. To increase the robustness of the solution, we assumed covariance between channels was zero and used the diagonal of the matrix. The orientation of dipoles on the cortical surface were constrained perpendicular to the surface under the assumption that the primary source of the EEG is coherent postsynaptic potentials across populations of pyramidal neurons that are arranged perpendicular to the cortical surface (Buzsáki et al., 2012).

ROI Selection

Our ROI selection method utilized pipeline similar to our previous work (Yuan et al., 2008). The time courses of each electrode was transformed into its time-frequency representation using a 1Hz band Morlet wavelet and the power in each time window and frequency band (from 1-50 Hz) was computed (Qin & He, 2005). Mean amplitude at each sensor in the alpha band (8-13 Hz) was calculated. The real and imaginary parts were separated. Source imaging was then performed with the source amplitudes calculated for

the real and imaginary parts separately. The real and imaginary cortical current density (CCD) amplitudes were combined to compute a total frequency-specific CCD.

Group level ROI selection was performed iteratively based on the mean CCD across all subjects for all sessions in each data set separately. First, all dipoles were assigned an alpha-band score based on the mean CCD across subjects and sessions which was calculated at each dipole over the 500ms of maximum control signal for each trial. The dipole with the largest alpha-band score was taken as the center of the first ROI. The extent of the ROI was taken as other dipoles within a 2 cm radius that had an alpha-band score of at least one-quarter of the center dipole. The alpha-band score of all dipoles within a 3 cm radius was then set to zero, and the largest alpha-band score of those remaining was selected and this proceeded iteratively until the top ten ROIs were determined. ROIs to analyze further for connectivity were selected from the aforementioned set based on knowledge of active areas during motor imagination and BCI task performance (Hétu et al., 2013; Lotze & Halsband, 2006) and were limited to the frontal and parietal cortices. ROI were determined separately for left and right hand imagination.

Data set one (**Fig. 12**): For left hand imagination, the center of the ROIs were located in: 1. Left premotor cortex (pM), encompassing sections of the premotor and primary motor cortices; 2. Left lateral primary somatosensory cortex (LS1), encompassing sections of the lateral primary motor and somatosensory cortices; 3. Left medial primary motor cortex (mM1), encompassing sections of the medial primary motor cortex and posterior supplementary motor/premotor cortex; 4. Right lateral primary

motor cortex (M1), encompassing sections of the lateral primary motor, primary somatosensory, and premotor cortices; 5. Left posterior parietal cortex (PPC); 6. Left supplementary motor area (SMA), encompassing sections of the SMA bilaterally. For right hand imagination, the center of the ROIs were located in: 1. Right lateral primary motor cortex (M1), encompassing sections of primary motor, primary somatosensory, and posterior premotor cortices; 2. Left premotor cortex (pM), encompassing sections of the premotor and lateral primary motor cortices; 3. Right posterior parietal cortex (PPC), encompassing sections of the posterior parietal and medial primary somatosensory cortices; 4. Left primary somatosensory cortex (S1), encompassing primary somatosensory and motor cortices; 5. Left posterior parietal cortex (PPC); 6. Right supplementary motor area (SMA), encompassing sections of SMA bilaterally. ROIs were similar for data set two and are illustrated in the results.

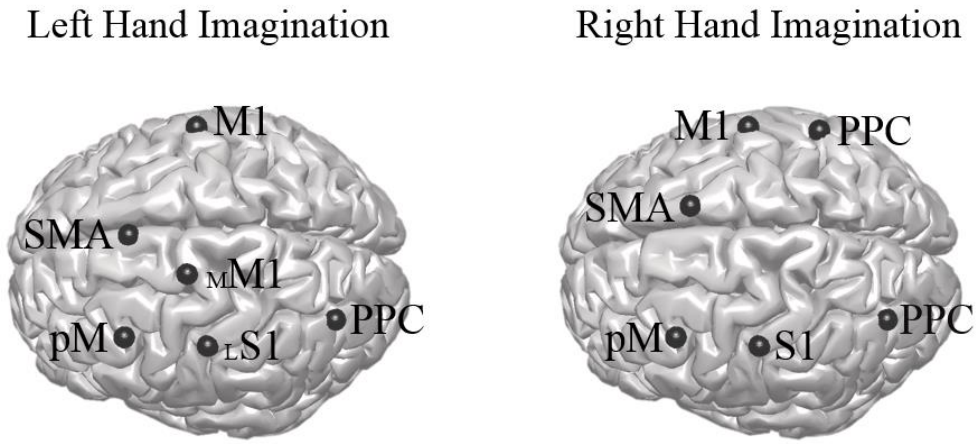

Fig. 12. Group regions of interest for left and right hand imagination. Black sphere indicates the center of the ROI. M1: primary motor cortex; MM1: medial primary motor cortex; SMA: supplementary motor area; pM: premotor cortex; S1: primary

somatosensory cortex; LS1: lateral primary somatosensory cortex; PPC: posterior parietal cortex

Subject specific ROIs on a session by session basis were determined by calculating the largest alpha-band scores across cortical dipoles for each subject within each session, within each of the global ROIs. The ROI activity time course was calculated by taking the mean of the dipoles within a 5 mm radius around the peak dipole. These time courses were used as a source-based virtual channels for analysis. These virtual channels were utilized for fitting the multivariate autoregressive model (MVAR) followed by analysis using the non-normalized and normalized directed transfer function. An overview of the processing pipeline is illustrated in **Fig. 13**.

Connectivity analysis

The multivariate autoregressive model is defined by

$$X(t) = \sum_{j=1}^{p} A(j)X(t-j) + E(t)$$

Where $X(t) = [X_1(t), X_2(t), \dots X_k(t)]^T$ are the k time series at time t and $E(t) = [E_1(t), E_2(t), \dots E_k(t)]^T$ are the k white noise values at time t, and $A(j) = \begin{pmatrix} A_{11}(j) \dots & A_{1k}(j) \\ A_{k1}(j) \dots & A_{kk}(j) \end{pmatrix}$ for j = 1,…,p are model parameters derived from the data

E(t) is the uncorrelated white noise input driving the system with zero mean. The number of channels, k, was determined based on the number of ROIs chosen for connectivity. Model order, P, was determined using the AIC with the ARfit toolbox (Schneider & Neumaier, 2001) with each trial in each block being independently fit, then the mean of

all trials per block taken as the order for all trials in that block, and each trial refit using the specified model order for that block. For most trials, cross and autocorrelation across 20 time lags exceeded the 2/sqrt(t) threshold, which is a measure of the goodness of fit of the MVAR model, under ten percent of the time (Ding, Bressler, Yang, & Liang, 2000).

The directed transfer function calculates the connectivity between regions of interest for each frequency of interest. The directed transfer function evaluates the directed influence from one channel to another based on MVAR model fit to the data (Kamiński, Ding, Truccolo, & Bressler, 2001; Kamiński & Blinowska, 1991).

$$X(f) = H(f)E(f)$$

Where H is the transfer matrix defined in the frequency domain as

$$H(f) = \left(\sum_{m=0}^{p} A(m) e^{-2\pi i m f \Delta t} \right)^{-1}$$

This can then be normalized to the total inflow to each channel yielding the normalized directed transfer function

$$\gamma_{ij}^2(f) = \frac{|H_{ij}(f)|^2}{\sum_{m=1}^{k} |H_{im}(f)|^2}$$

To assess the significance of the connectivity on a trial by trial basis, we used a surrogate phase shuffling method (Theiler et al. 1992, He et al. 2011). In short, we transformed the time domain data into the frequency domain using a fast Fourier Transform, normalized the power at each frequency, and shuffled the phase across frequencies, multiplied these shuffled phases by the original frequency power, and applied the DTF to the inverse FFT of this shuffled data with the same model order as the original data. This procedure was repeated 1000 times for each trial to calculate a

distribution of DTF values, and a significance of 0.05 was used to compare the original data to the shuffled phase distribution data.

Statistics

Data set one:

To evaluate changes in connectivity following stimulation, we used a generalized linear model with fixed effects of block, and random effect of subject with session and block nested within each subject. A Gamma link function was used as it was found to empirically fit the data better than Gaussian or logit functions using the Akaike information criterion (AIC). P values were corrected for each measure using the false discovery rate to correct for the number of comparisons which was calculated as the number of connections with significant differences across blocks multiplied by two, for the planned comparison of Prestim to $Post_0$ and Prestim to $Post_{25}$.

To evaluate changes in the number of statistically significant trials, we applied the Freidman test, with post-hoc Wilcoxon-signed rank for pairwise comparisons FDR corrected for planned comparisons between pre-stimulation and post-stimulation conditions.

A generalized linear model with the fixed effects of each connectivity value and random effect of subject with levels by session and block was used to examine the relationship between behavioral measures and connectivity. A Poisson link function was used when analyzing the number of correct trials; for time to hit, a Gamma link function was used as this empirically fit the data well. The p value was adjusted for multiple comparisons across all fixed effects using the false discovery rate.

Data set two:

The pre-stimulation normalized DTF value was subtracted from the post-stimulation values for each session. The mean of the change of $Post_0$ and $Post_{25}$ was used for analysis to evaluate the change between pre-and post-stimulation. To evaluate changes in connectivity following stimulation between different stimulation polarities, we used a general linear model with fixed effect of session, and random effect of subject with session and block nested within each subject. Single sample t-tests were calculated for each condition to evaluate if the change was nonzero.

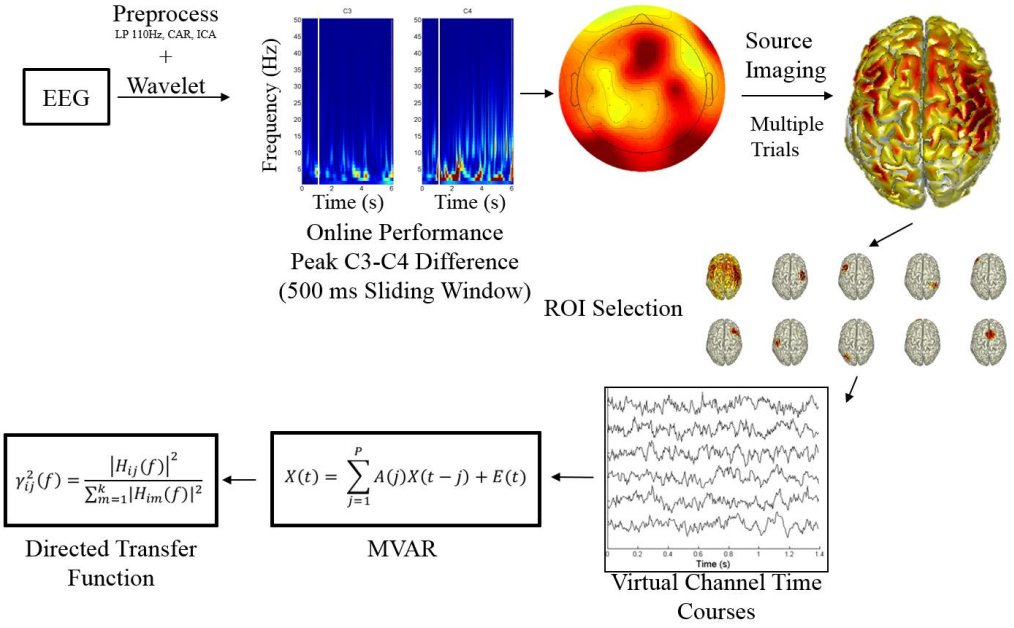

Fig. 13. Data analysis processing pipeline. The included time frequency transform is an example of a correct trial of right hand imagination, the white bar indicates when online feedback began. The sensor level topograph illustrates alpha band activity during an example trial. The source imaging distribution illustrates the mean alpha power distribution across all subjects for right hand imagination. ROI selection is then performed based on previous studies. The peak ROIs are found for each subject each

session and trial specific time courses are extracted and fit with a multivariate autoregressive model to which the directed transfer function is applied.

Finite Element Model of HD-tDCS

ANSYS version 14 (ANSYS Inc., PA, USA) was used for 3D modeling and Finite Element Method (FEM) based electromagnetic simulation (Silvester & Ferrari, 1996; Zhang, Zhu, & He, 2010). The DUKE head model from the Virtual Family (Christ et al., 2010) was imported and constructed in ANSYS, by a hexahedral element with the mesh size of $2\times2\times2$ mm^3. Head segmentation (19 head tissues) was provided along with the head model, and their corresponding conductivity values were taken from literature (Sadleir et al., 2010) and assumed to be isotropic. Electrodes were localized on the scalp surface in the configuration as performed in our experiments with the surround electrodes located 3.5cm from the center electrode. 2.0 mA of current was injected into the center electrode while surround electrodes each had -0.5 mA of current injected.

Results

Data set one

Across frequency bands, there were more changes in connectivity for right hand imagination than for left hand imagination following left sensorimotor HD-tDCS. Total inflow to and outflow from ROIs in the alpha band changed based on laterality of hand imagination as measured by the normalized DTF. Ipsilateral pM and S1 for left hand imagination and ipsilateral M1 and PPC for right hand imagination contributed greater outflow compared to other ROIs (**Fig. 14**). There was a trend towards an increase in the

outflow following anodal stimulation from the sensorimotor cortex ipsilateral to the imagined hand irrespective of stimulated hemisphere for both left and right hand imagination; however, this was only significant for right hand imagination. For left hand imagination, there were significant increases in inflow to the left PPC and SMA following stimulation. For right hand imagination, there was increased inflow to the left pM, S1, and PPC following stimulation at both $Post_0$ and $Post_{25}$, and an increase to the right PPC post-stimulation. There was an increase in inflow in the beta band to the left PPC, right M1 and PPC following stimulation (**Fig. 15**). There was also an increase in outflow from the SMA at $Post_0$. For left hand imagination in the beta band, there was a difference in outflow from right M1 and left PPC but there were no significant post-hoc comparisons between pre- and post-stimulation.

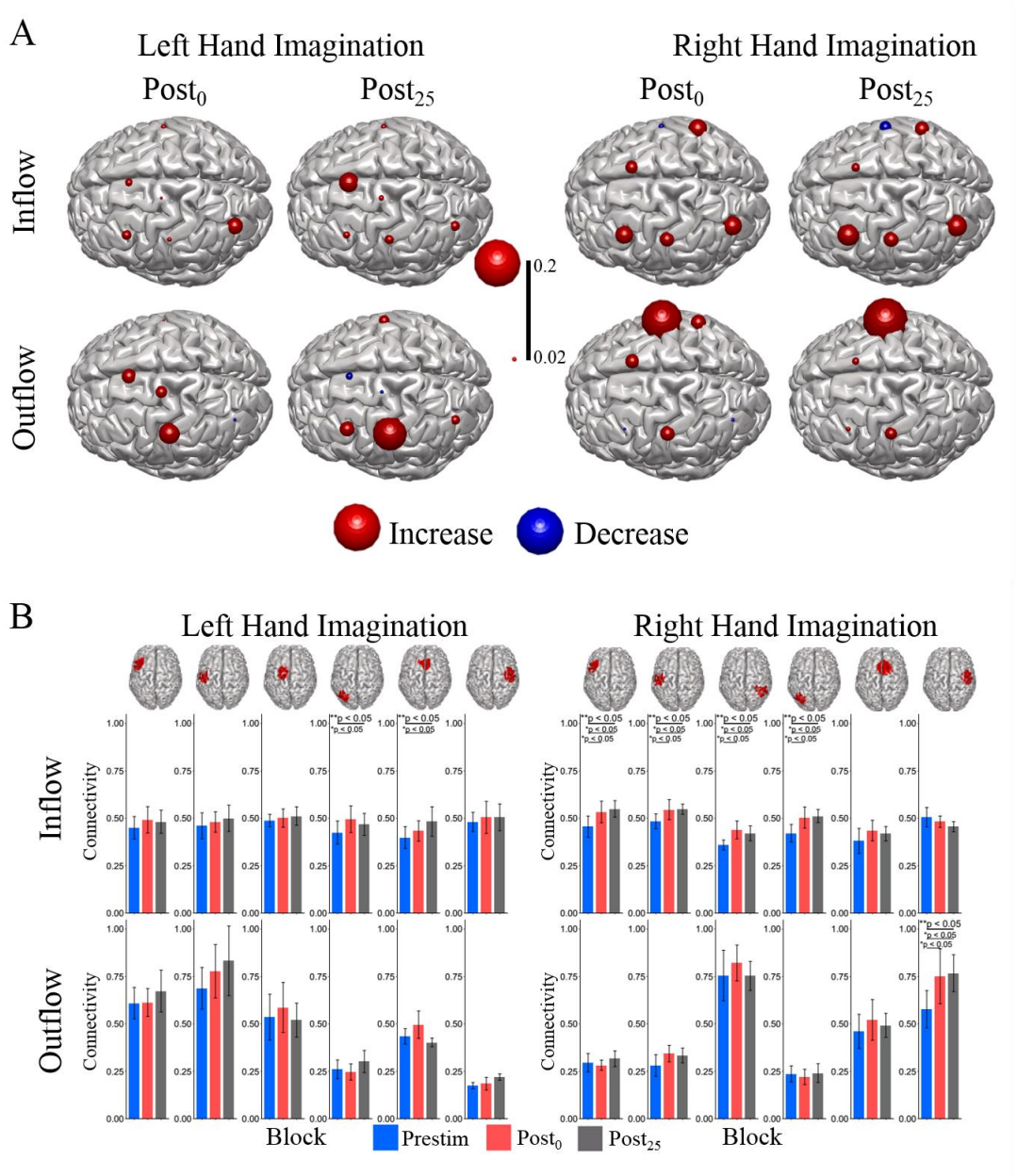

Fig. 14. Alpha band normalized DTF total flow for each ROI. (A) Change in connectivity from the pre-stimulation time point mapped onto the peak dipole of each ROI. (B) Absolute connectivity values for each block within each session. For left hand

imagination (Left) there was a significant increase in the left PPC and SMA inflow following stimulation at the indicated time points. For right hand imagination (Right) there was increased inflow to left pM, S1, and PPC, and to right PPC following stimulation at both the immediate post and delayed post time points. There was a significant increase in right M1 outflow following stimulation. Total inflow to the ROI (top) and total outflow from the ROI (bottom). Bar color indicates the block: pre-stimulation (blue), $Post_0$ (red), and $Post_{25}$ (black). Values are mean across subjects across blocks; error bars are standard error across subjects. ** $p<0.05$ across blocks, * $p<0.05$ FDR corrected post-hoc between pre-stimulation and post-stimulation blocks.

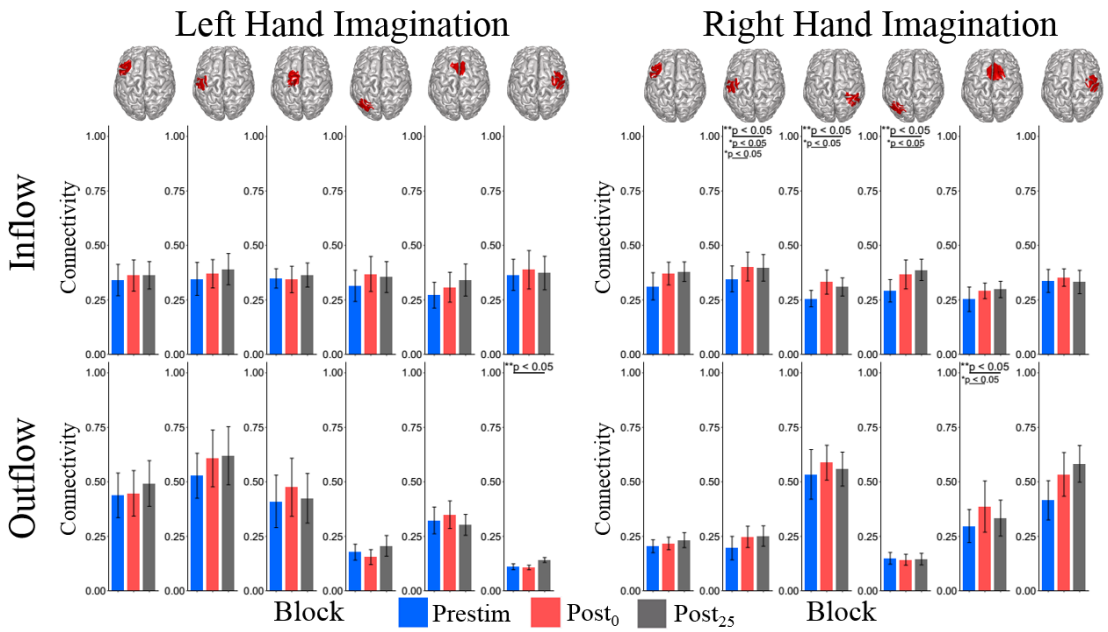

Fig. 15. Beta band normalized DTF total flow for each ROI. For left hand imagination (Left) there was a significant difference in outflow from the right M1 and left PPC. For right hand imagination (Right) there was increased inflow to the left S1 and PPC and to the right PPC following stimulation. The SMA showed increased outflow directly

following stimulation. Bar color indicates the block: pre-stimulation (blue), $Post_0$ (red), and $Post_{25}$ (black). Values are mean across subjects across blocks; error bars are standard error across subjects. ** $p<0.05$ across blocks, * $p<0.05$ FDR corrected post-hoc between pre-stimulation and post-stimulation blocks.

Directed connections between the ROIs in the alpha band display further differences due to HD-tDCS based on the laterality of hand imagination (**Fig. 16**). For left hand imagination, there was a significant difference between SMA and left PPC but there were no significant post-hoc difference between pre- and post-stimulation. For right hand imagination, there was a significant increase in connectivity from the right M1 to the right PPC and from the right M1 to left pM. There was also a significant increase in connectivity between the SMA and left pM at both post-stimulation time points. In the beta band for both left and right hand imagination, there was increased connectivity from right M1 to the left pM at $Post_{25}$ (**Fig. 17**). For right hand imagination, there was an increase from SMA to the left pM at both post-stimulation time points.

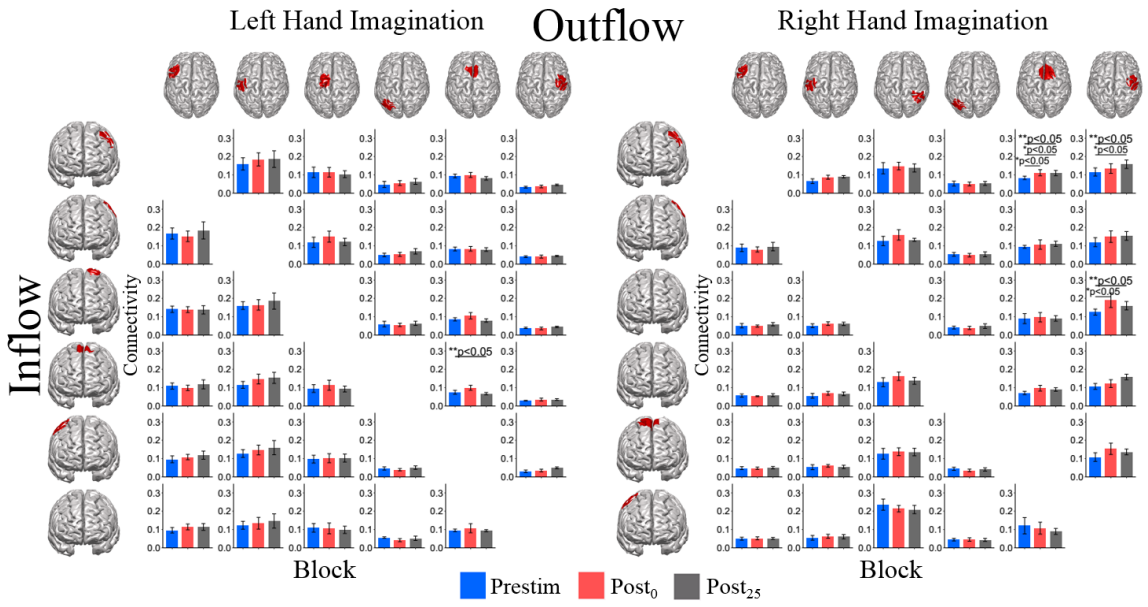

Fig. 16. Alpha band normalized DTF flow between each ROI pair. For left hand imagination (Left) there is a difference in connectivity across session blocks from the SMA to the left PPC. For right hand imagination (Right) there was increased connectivity from the right M1 to right PPC and the left pM following stimulation. There was also increased connectivity from the SMA to the left pM at both time points following stimulation. Bar color indicates the block: pre-stimulation (blue), $Post_0$ (red), and $Post_{25}$ (black). Values are mean across subjects across blocks; error bars are standard error. ** indicates $p<.05$ across blocks, * indicates $p<.05$ FDR corrected post-hoc between blocks between pre-stimulation and post-stimulation blocks.

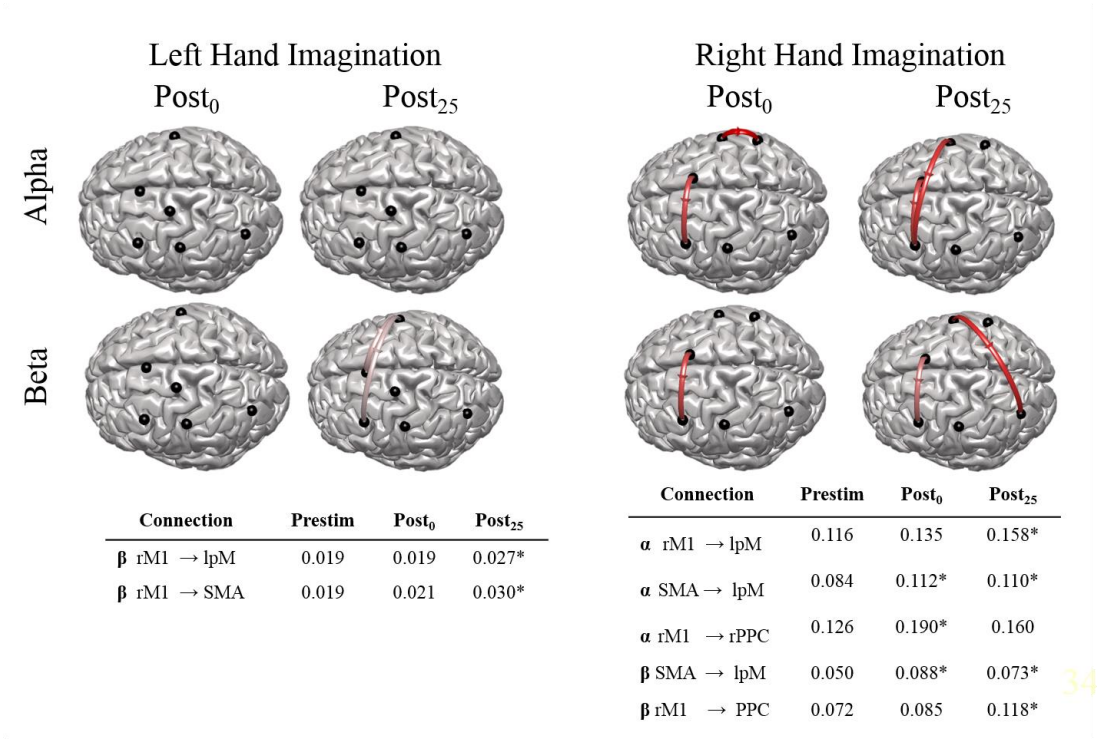

Connection	Prestim	$Post_0$	$Post_{25}$
β rM1 → lpM	0.019	0.019	0.027*
β rM1 → SMA	0.019	0.021	0.030*

Connection	Prestim	$Post_0$	$Post_{25}$
α rM1 → lpM	0.116	0.135	0.158*
α SMA → lpM	0.084	0.112*	0.110*
α rM1 → rPPC	0.126	0.190*	0.160
β SMA → lpM	0.050	0.088*	0.073*
β rM1 → PPC	0.072	0.085	0.118*

Fig. 17. Normalized DTF values across time. Alpha (top) and beta (middle) band changes in connectivity prior to and after stimulation for right and left hand imagination. Red indicates and increase in connectivity based on the values included in the table. Values are mean across subjects across blocks. All included connections had $p<0.05$ across all blocks. * indicates $p < 0.05$ post-hoc between pre-stimulation and post-stimulation blocks.

To evaluate the significance of the connectivity, we calculated, on a trial by trial basis, if each connection was statistically significant based on surrogate phase shuffling. There were significant changes in the number of significant trials following stimulation (**Fig 18**). For left hand imagination, there was a change in statistically significant trials from left mM1 to the left pM and SMA, from left lateral S1 to left PPC, and from SMA

to left pM with trends towards increasing connectivity at $Post_0$ and a return to baseline or decrease at $Post_{25}$. For right hand imagination, there were bidirectional changes between left pM and left SMC with trends towards increased significant trials post-stimulation and from left PPC to left pM and right PPC with a trend towards increased significant trials at $Post_{25}$. There were no significant pairwise post-hoc changes following stimulation.

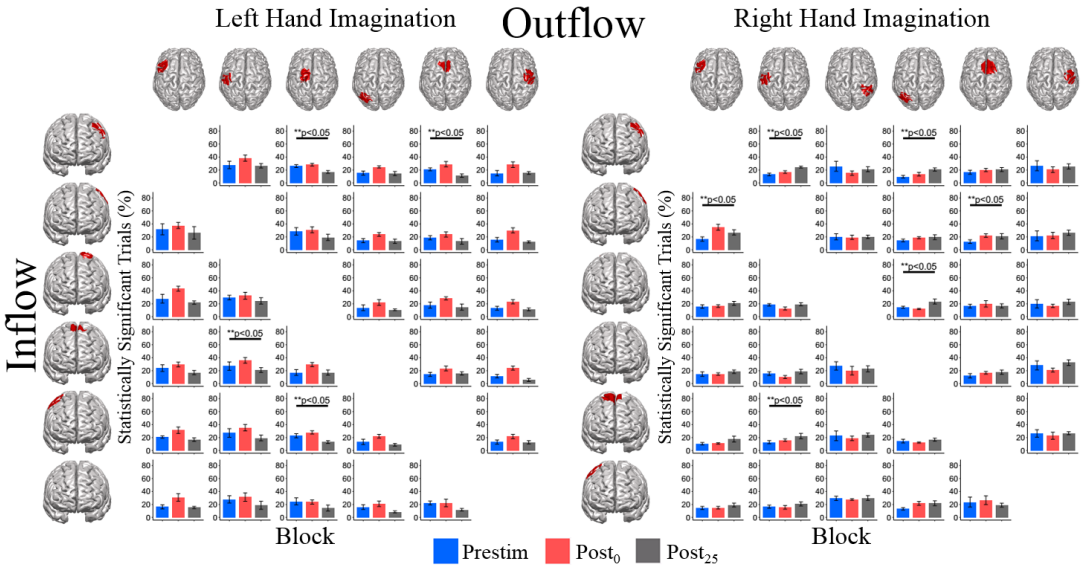

Fig. 18. The percentage trials with significant alpha band connectivity between ROIs. For left hand imagination (Left) there was a change in significant trials from left mM1 to the left pM and SMA, from left lateral S1 to left PPC, and from SMA to left pM. For right hand imagination (Right) there were bidirectional changes between left pM and left SMC and from left PPC to left pM and right PPC. Bar color indicates the block: pre-stimulation (blue), $Post_0$ (red), and $Post_{25}$ (black). Values are mean across subjects across blocks; error bars are standard error. ** indicates $p<.05$ across blocks.

To examine the relationship between alpha band connectivity values and behavioral performance metrics we utilized a generalized linear model with each

normalized connectivity value as a fixed effect within the same model. Overall, specific normalized connectivity values were correlated with behavioral outcome measures. For right hand imagination trials, inflow to SMA was significantly correlated with increased correct trials (β=3.59, $p < 0.01$ FDR corrected). Outflow from left pM (β=-1.54, $p < 0.05$ FDR corrected), left S1 (β=-1.62, $p < 0.05$ FDR corrected), and right PPC (β=-1.21, $p < 0.05$ FDR corrected) correlated with decreased correct trials. For left hand imagination trials, inflow to the left LS1 was correlated with fewer correct trials (β=-1.53, $p < 0.05$ FDR corrected). Outflow from left pM (β=1.57, $p < 0.05$ FDR corrected), left LS1 (β=0.98, $p < 0.05$ FDR corrected), and right M1 (β=2.18, $p < 0.05$ FDR corrected) correlated with an increased number correct. Inflow to right M1 (β=-4072, $p < 0.05$ FDR corrected) and outflow from left PPC (β=5769, $p < 0.05$ FDR corrected) correlated with the time to hit correct targets.

Multiple directed connectivity values for both hand imaginations were correlated with changes in the time to hit correct targets (**Fig. 19**). For left hand motor imagination connections from left LS1 to right M1 correlated with a decreased time to hit while connectivity from left LS1 to left PPC correlated with an increased time to hit. For right hand motor imagination connections from right M1 and PPC to left pM and S1 correlated with an increased time to hit. Bidirectional left PPC-SMA connections correlated with a decreased time to hit. For both hand imaginations connections from ipsilateral pM/M1 to SMA correlated with a decreased time to hit.

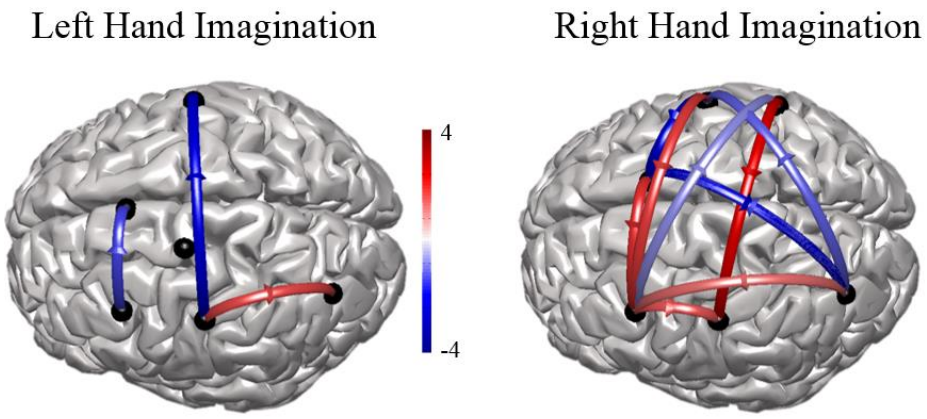

Fig. 19. Beta scores between normalized connectivity values in the alpha band and the time to hit correct trials. For left hand motor imagination (Left) connections from left LS1 to right M1 are correlated with a decreased time to hit while connectivity from left LS1to left PPC correlated with an increased time to hit. For right hand motor imagination (Right) connections from right M1 and PPC to left pM and S1 correlated with an increased time to hit. Input to left pM also correlated with an increased time to hit. Bidirectional left PPC-SMA connections correlated with a decreased time to hit. For both hand imaginations connections from ipsilateral pM/M1 to SMA correlated with a decreased time to hit. Red indicates an increased time to hit, blue indicates a reduced time to hit. $p < 0.05$ for all displayed connections with FDR correction for multiple comparisons.

Data set two

The source distribution of alpha power differs following the different stimulation conditions **(Fig 20)**. When comparing the effect of anodal stimulation between data sets

one and two, there are similarities in an increase in inflow to the left motor and parietal regions and an increase in outflow from the right motor regions. However there are also differences, specifically the inflow and outflow from SMA for the three condition subjects, which shows an increase in inflow and decrease in outflow following stimulation (**Fig. 21)**.

The mean of the baseline subtracted $Post_0$ and $Post_{25}$ connectivity values illustrated the effect of stimulation on motor imagery networks based on laterality of hand imagination (**Fig 22**). Outflow from the left sensorimotor cortex/PPC differed between stimulation types for left hand imagination with the anodal group having significant decreases in outflow compared to sham and cathode. For right hand imagination, the inflow to the left sensorimotor cortex/PPC differed between stimulation conditions, with cathodal stimulation having a significant decrease compared to the anodal stimulation, which showed an increase.

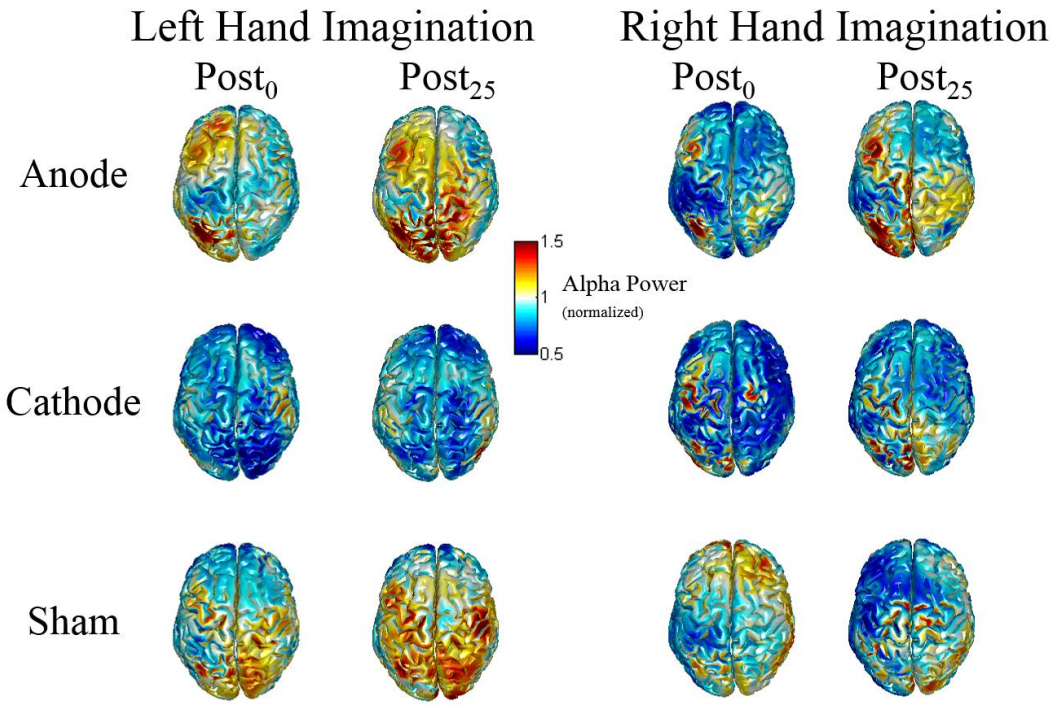

Fig 20. Source distribution of alpha power normalized to pre-stimulation baseline. The stimulation conditions differentially modulate the power in the alpha band following stimulation across the brain bilaterally.

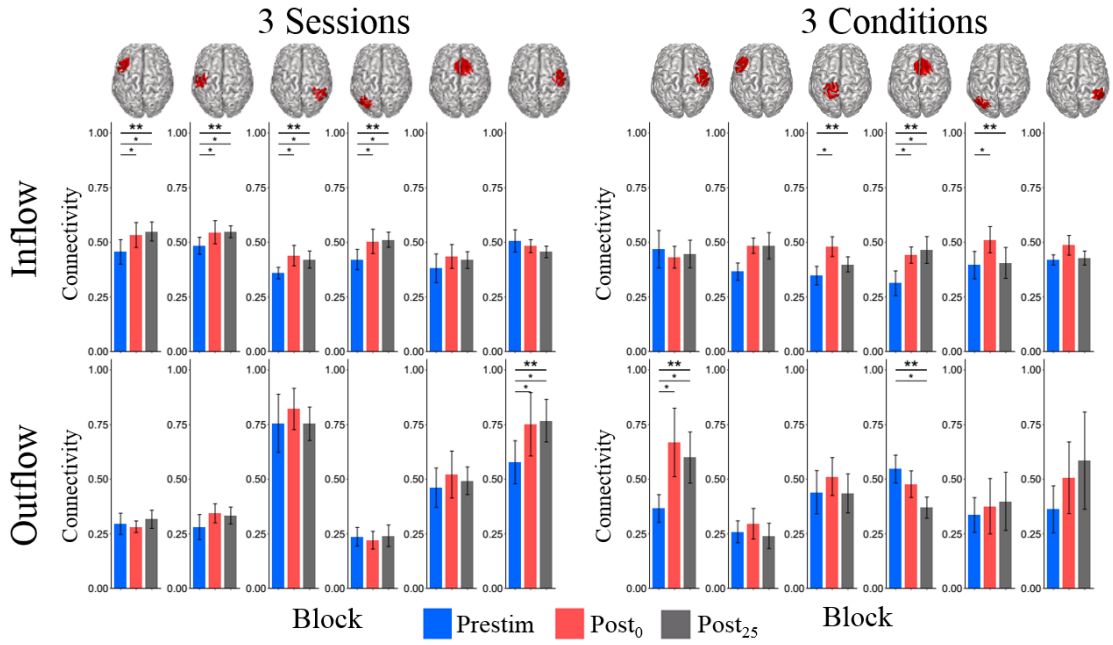

Fig. 21. Comparison of anodal stimulation connectivity between data sets for right hand imagination. Total inflow and outflow to the mean of $Post_0$ and $Post_{25}$ within subjects across anodal (blue), cathodal (red), and sham (black) stimulation between the two data sets with the mean of the Three Sessions subjects (left) and Three Conditions subjects (right). There are similarities with increased inflow to left motor and parietal regions and increased outflow from right motor cortex. However, there is a difference in SMA inflow/outflow. Values: Mean and +/- SE. ** $p < 0.05$ across blocks; *(above) $p < 0.05$ pairwise post-hoc between blocks; *(below) $p < 0.05$ one-sample t-test.

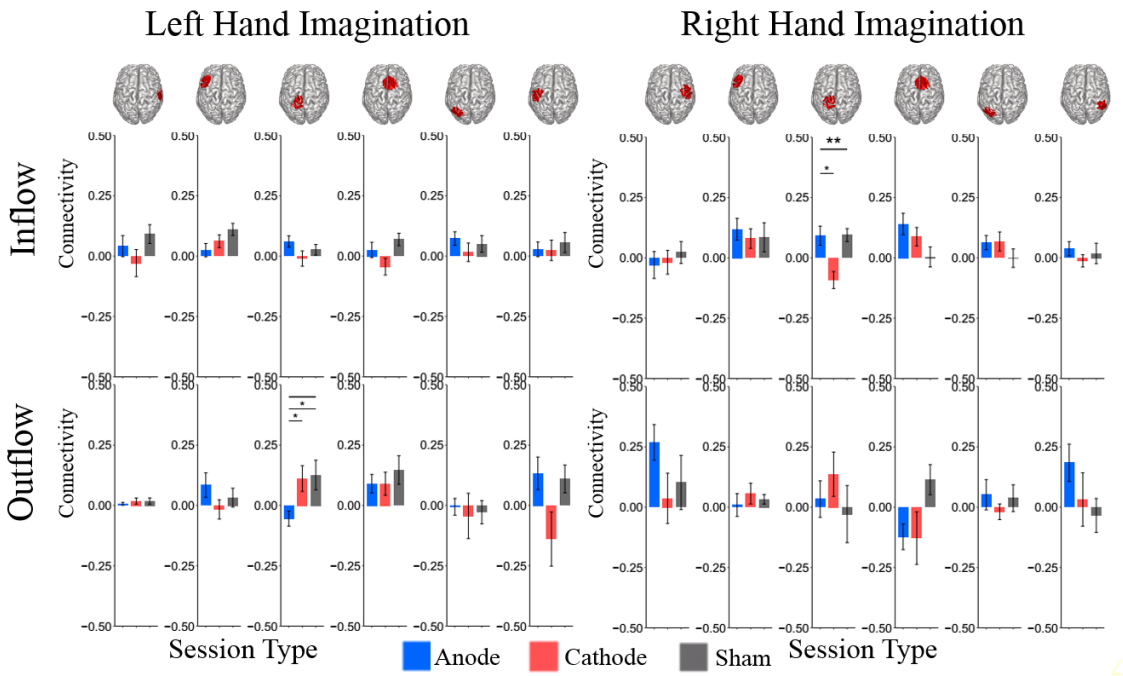

Fig. 22. Change in ROI alpha band total inflow and outflow following stimulation. Baseline subtracted total inflow and outflow to the mean of $Post_0$ and $Post_{25}$ within subjects across anodal (blue), cathodal (red), and sham (black) stimulation. Outflow from left SMC/PPC differed between stimulation types for left hand imagination and inflow differed for right hand imagination. Connections following anodal stimulation differed from baseline more often than following cathodal or sham stimulation. Values: Mean and +/- SE. ** $p < 0.05$ across stimulation types; *(above) $p < 0.05$ pairwise post-hoc between stimulation types; *(below) $p < 0.05$ one-sample t-test.

Data set three

There were differences in total inflow and outflow between motor imagination without feedback and performance of the BCI task with feedback **(Fig. 23)**. During right

hand imagination, MI shows greater outflow from the contralateral hemisphere. During left hand imagination, MI shows greater inflow to the left SMC/PPC. During both imaginations, MI has greater inflow to the left premotor cortex.

There were also differences in the effect of task type in the connectivity response to stimulation. Anodal stimulation has a differential effect on the change in outflow from SMA during left hand imagination, with BCI showing an increase in outflow and MI showing a decrease in outflow. There is also a difference in the left PPC with BCI showing an increase and MI showing a decrease in inflow **(Fig. 24)**. For cathodal stimulation, there is a differential effect on left SMC, with BCI showing a decrease in inflow compared to MI **(Fig. 25)**. There were no significant differences following sham stimulation or for other ROIs.

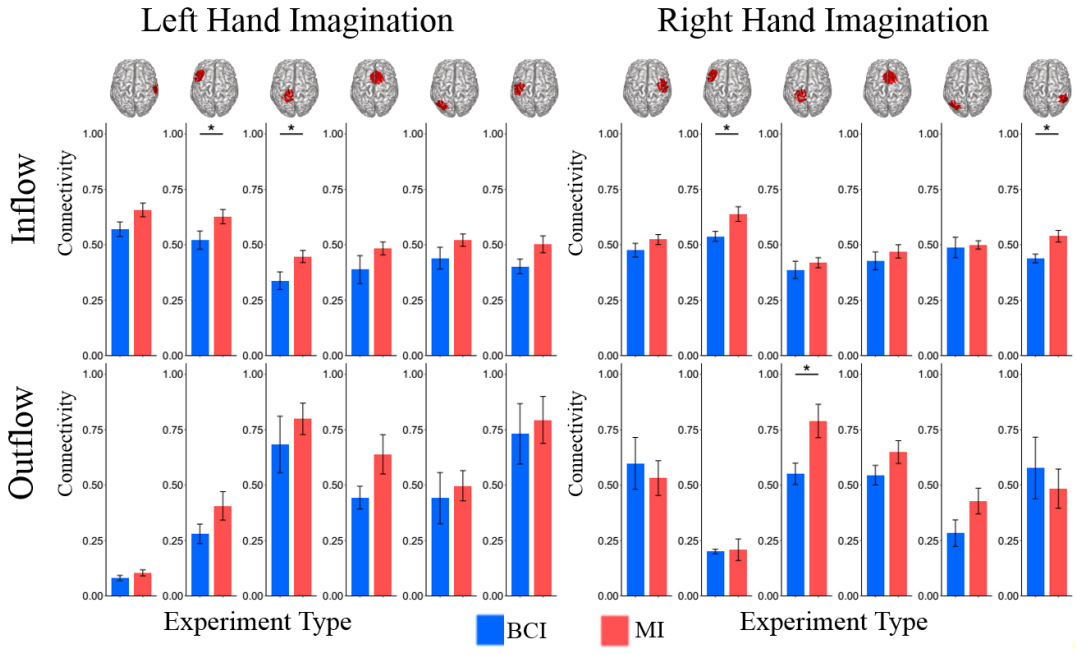

Fig. 23. Comparison of overall connectivity between BCI and MI. There are significant differences between BCI performance of motor imagination with feedback

and MI performance without feedback. During right hand imagination, MI shows greater outflow from the contralateral hemisphere. During left hand imagination, MI shows greater inflow to the left SMC/PPC. During both, MI has greater inflow to the left premotor cortex. BCI (blue) and MI (red). Values: Mean and +/- SE. *p < 0.05 between groups.

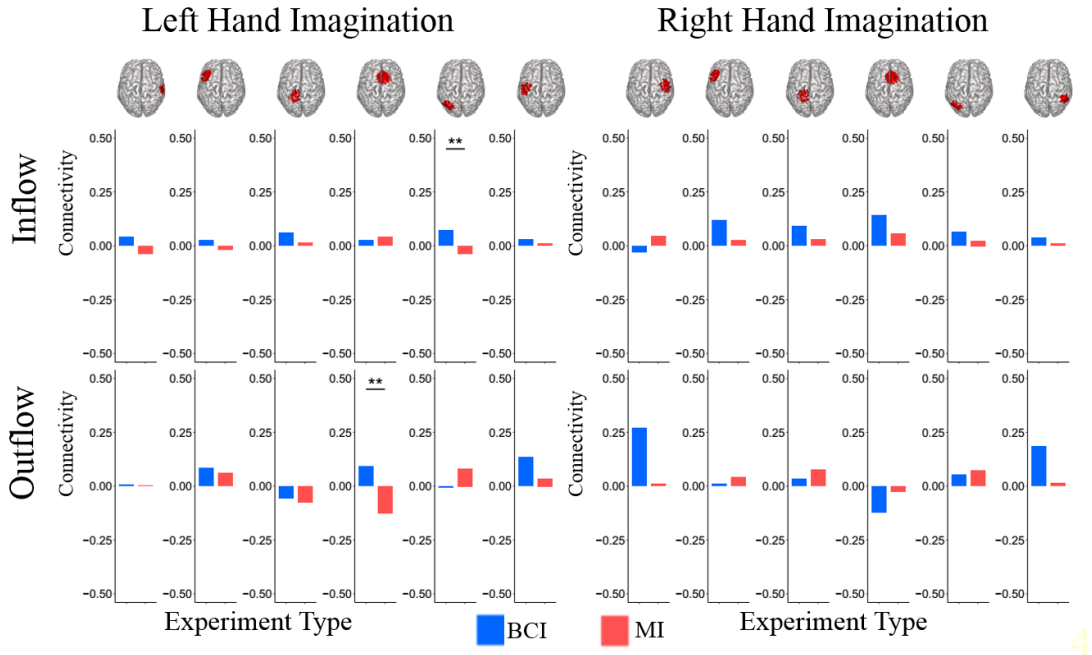

Fig. 24. Comparison between BCI and MI of the change in connectivity following anodal stimulation. During left hand imagination, there are differential effects on the outflow from SMA and inflow to left PPC. During right hand imagination, there are no significant differences between groups. BCI (blue) and MI (red). Values: Mean and +/- SE. **p < 0.05 between groups.

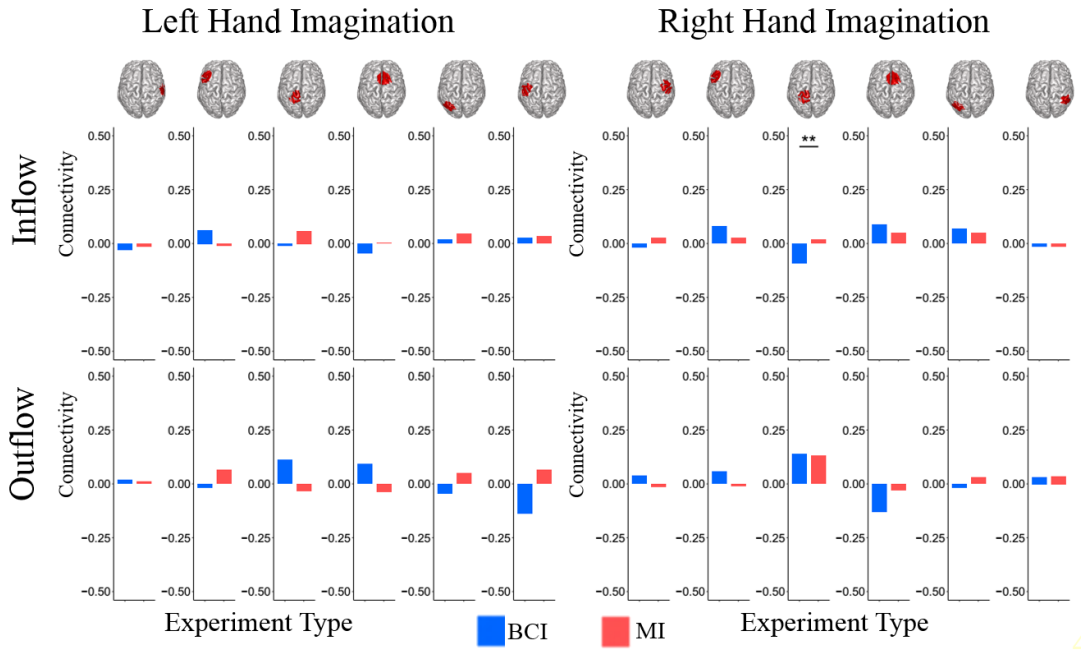

Fig. 25. Comparison between BCI and MI of the change in connectivity following cathodal stimulation. During left hand imagination, there are no significant differences between groups. During right hand imagination, there is a significant difference in inflow to the left SMC between groups, following stimulation. BCI (blue) and MI (red). Values: Mean and +/- SE. *p < 0.05 between groups.

FEM

Qualitative distribution of the current over the cortex illustrates localized targeting of HD-tDCS (**Fig. 26**). Quantitative modeling illustrates the distribution of current density across the skin, skull, CSF, and within the brain. The peak current density calculated within the FEM in grey matter under the electrodes of interest in the left (stimulated) hemisphere: C3: 0.161 A/m^2 CP3: 0.132 A/m^2 PO5: 0.007 A/m^2. Peak

current density in white matter: C3: 0.492 A/m^2 CP3: 0.356 A/m^2 PO5: 0.005 A/m^2 (**Fig. 27**).

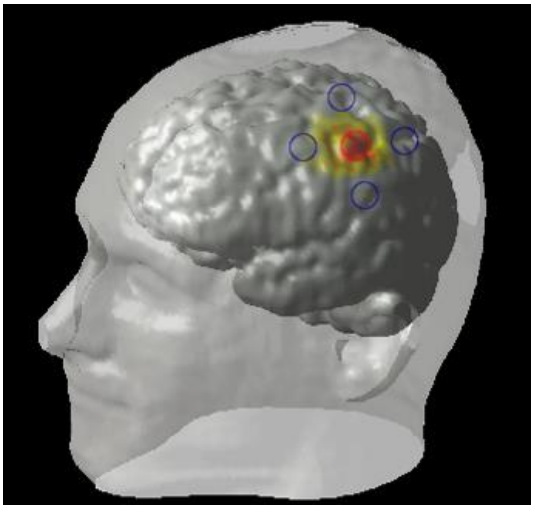

Fig. 26. FEM model of HD-tDCS. Qualitative distribution of current flow during HD-tDCS over the left sensorimotor cortex. Peak currents are confined to cortical regions with the extent of the Laplacian, 4 x 1, spatial configuration. Red circle indicates center active electrode and blue circles represent return electrodes.

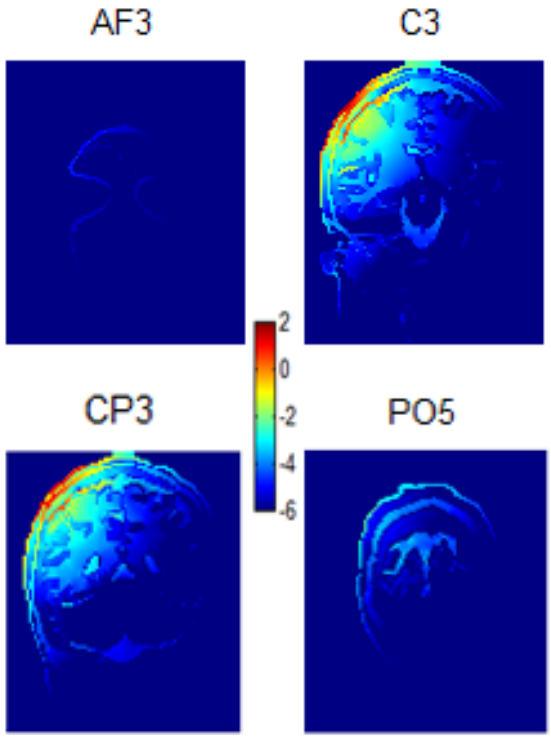

Fig. 27. Coronal sections of quantitative FEM model. The current distribution across head and brain tissues at electrodes from anterior to posterior. C3 and CP3 are within the 4 x1 electrode region. Peak current is at the skin, CSF, and cortical gray matter near the stimulating electrodes. Colors indicate the natural log of total current density within each voxel.

Conclusion

Unilateral high-definition tDCS during motor imagery based brain computer interface performance has bilateral connectivity effects. Connectivity, and these stimulation effects, differ based on the laterality of hand imagination, with an increased effect on connectivity when performing right hand imagination, contralateral to the stimulated hemisphere. These results suggest that tDCS interacts with ongoing

endogenous oscillations and affects communication between brain areas involved in the task being performed.

Directed connectivity measures yield information on total and relative influence between ROIs. During right hand imagination, the left sensorimotor cortex desynchronizes (and vice versa for left hand imagination), which is characterized by a decrease in power in the alpha band. This decrease in power is due to networks within the sensorimotor cortex altering their firing patterns when activated by the motor imagination task, this is referred to as event-related desynchronization (ERD). Concurrent with this ERD, we found a high degree of outflow from within the hemisphere ipsilateral to the motor imagination, from the pM and PPC during right hand imagination and from pM and SMC for left hand imagination. Following stimulation, this outflow increased for right hand imagination and trended towards an increase for left hand imagination. For right hand imagination, there was an increase in inflow to the stimulated hemisphere in the pM and SMC, and increased inflow bilaterally to the PPC. This suggests that the integration of the stimulated sensorimotor cortex, and stimulated hemisphere more generally, into the motor imagination network is increased following anodal stimulation; this increased information flow within the network could lead to previously reported improved behavioral performance, such as reduced time to hit following anodal stimulation (Baxter et al., 2016). This also suggests that the stimulation after-effect is task specific and alters connectivity in a task specific manner, in this case, regardless of the location of the stimulation electrode to the outflow region. It is unclear if the effect is based on the same physiological basis however as the increase in inflow is bilateral in the

right-hand imagination case and unilateral in the left-hand imagination case. These results illustrate the network effects of stimulation on regions not directly targeted and that these effects are use dependent. Using resting state fMRI, Polania and colleagues found increased connectivity between the stimulated left primary motor cortex, and subcortical structures of the ipsilateral thalamus and caudate nucleus (Polanía et al., 2012). As the thalamus has widespread cortico-cortical; connections, this could be a pathway through which the intrahemispheric changes in connectivity occur.

Computational modeling of transcranial direct current stimulation has been extensively performed. Our experimental setup specific model supports previous simulation results (Kuo et al., 2013) where HD-tDCS yields biologically affective cortical distribution of current in the stimulated region with a low level of current also reaching subcortical structures, the contralateral hemisphere and more anterior and posterior electrodes in the prefrontal and co-parietal regions. In addition, it supports the connectivity results in suggesting that there is a network effect due to stimulation rather than a direct effect of the stimulation on distant cortical regions.

Multiple studies have examined the interactions of stimulation with motor execution on connectivity. Polania et al examined connectivity at the EEG sensor level using graph theory measures and found increased connectivity in the alpha band within the left hemisphere during a right hand motor task following anodal stimulation over the left primary motor cortex (Polanía et al., 2011). For right hand imagination, we did not see significant increases in the DTF values within the left hemisphere, but we did see changes in the percentage of trials showing significant connectivity within the left

hemisphere, with a trend towards an increased percentage of significant trials post-stimulation In addition, Polania and colleagues found no change or decreased interhemispheric connectivity based on specific electrodes in the alpha band following stimulation, whereas we report the opposite. Notturno and colleagues examined functional connectivity following tDCS with the active electrode over the left primary motor cortex and found no effect on coherence during motor movement between C3 and any other electrode following 20 minutes of 1mA anodal or cathodal stimulation, though they did not look at pairwise coherence between other electrodes (Notturno et al., 2014). We found an overall increase in inflow to the left SMC during right hand imagination following stimulation, primarily driven by right cortical output. An explanation for the previously found lack of effect by Notturno and colleagues may be the relationship between the timing of stimulation and task performance. These previous studies performed stimulation during rest whereas we had subjects perform the task simultaneous with stimulation. During sensorimotor rhythm modulation for controlling a BCI, the control signal is generated from both hemispheres whereby there may be increased interaction between the two during task performance. Combining this with stimulation may then increase both ipsilateral and contralateral connectivity due to task specific activity. These differences highlight the importance of context with stimulation, whereby differing activity during stimulation leads to differing aftereffects of the stimulation on task specific activity

Within the second data set, we examined differences between anodal, cathodal, and sham stimulation on the same subjects. We report opposing effects of

anodal and cathodal stimulation on the left SMC/PPC, a region directly affected by stimulation, which suggests differential interactions of the stimulated network with laterality of hand imagination. The region is synchronized with left hand imagination and desynchronized with right hand imagination and these results suggest the stimulation is interacting to affect this network based on the underlying activity. Anodal stimulation increases information flow to the area during right hand imagination, when sub-networks within the cortex are not synchronously active, while it decreases outflow when the networks are synchronous; the opposite is true for cathodal stimulation, which suggests an impairment of differential connectivity to/from the stimulated area with cathodal stimulation.

During motor imagination during the peak control period, we found changes in connectivity both intra and interhemispherically. The connectivity of motor imagination during BCI varies based on the laterality of imagination. These differences and connectivity patterns are likely due to event related synchronization and desynchronization across the motor cortex and these interactions with the rest of the motor imagery network through cortico-cortical connections both intrahemispherically and across the corpus callosum between the two hemispheres connecting the motor and parietal cortices (Feurra et al., 2011; Gao, Duan, & Chen, 2011; Karabanov, Chao, Paine, & Hallett, 2013). There are many regions showing increased BOLD during motor imagination (Hétu et al., 2013) and there is a large degree of interconnectivity within the sensorimotor cortex bilaterally, including the premotor, motor, and parietal cortices (Gao et al., 2011). Our results show similar relative connectivity when examining the

normalized inflow and outflow compared to the work of Gao et al. We see similar trends for right hand motor imagination with high inflow compared to outflow to the left M1 and S1 and a greater amount of outflow compared to inflow for the right M1 and pM. For left hand imagination, we see higher inflow to the right M1 than outflow, and see higher outflow for the pM and SMC. Other work primarily examined changes in connectivity between rest and motor imagination. During right hand motor execution, Notturno et al. found increased coherence compared to rest in the low alpha band between left M1 and right S1 and left M1 and left pM, reduced coherence between left M1 and left PPC, and increased high alpha and beta coherence between left M1 and the contralateral cortex (Notturno et al., 2014). Kus et al. found a decrease in beta outflow from sensorimotor cortex contralateral to finger execution or imagination during task performance compared to baseline (Kus et al., 2006). Athanasiou et al. examined connectivity in the alpha band during motor imagination and found information flow from contralateral to ipsilateral M1 and SMA to ipsilateral M1 (Athanasiou, Lithari, Kalogianni, Klados, & Bamidis, 2012). We did not compare rest to task performance so we cannot directly compare these changes in connectivity, however we see an opposite pattern of high connectivity both pre- and post- stimulation, from the ipsilateral to contralateral SMC and from SMA to the contralateral M1.

A significant difference between previous studies examining the connectivity during motor imagination is that, in this current study, subjects received feedback during the imagination performance. In addition, we examined the connectivity at the peak control signal time window for each trial, when the alpha power difference between the two

hemispheres is largest. With this, we do not assume that the subject is performing the motor imagination robustly over the entire control time window, and empirically, with untrained subjects it is unlikely that they are performing the imagination for the entire available time period. Within this time window of peak difference, we find high influence from ipsilateral to the contralateral hemisphere, from the region of high synchrony to that of low synchrony. The outflow from the ipsilateral hemisphere is different between motor imagination and SMR-BCI with feedback, where we see an increase outflow from the ipsilateral hemisphere and decreased outflow from the contralateral hemisphere with feedback. We cannot differentiate the driver of this difference, if it is learning or feedback specific, but there is a difference between these two experimental paradigms where the underlying task is the same. This difference in overall connectivity between the tasks also suggests reasoning behind a differential effect of stimulation on connectivity during these tasks.

Differential changes between motor imagination and SMR-BCI were evident after cathodal and anodal stimulation. Bortoletto and colleagues examined performance and MEP size following a left thumb abduction task, where the effect of anodal stimulation on fast, with learning, vs. slow, without learning, abduction were differentiated. They argued that the effect differed due to the task specific learning, and found a decrease in MEP size when combining learning with anodal stimulation and the opposite effect when combining anodal stimulation with activation without learning (Bortoletto, Pellicciari, Rodella, & Miniussi, 2015). Bortoletto and colleagues argue their results support a neural noise hypothesis of stimulation whereby during the task without learning, anodal

stimulation increases the signal, and with learning, the signal is already high and anodal stimulation reduces this. While we do not examine excitability directly, we do see increased outflow during motor imagination without learning, which, if it is taken as a measure of excitability, would parallel the results seen by this previous study. However, there are significant differences between these studies as in this current study, subjects only receive feedback within the BCI condition, whereas in the study by Bortoletto and colleagues, subjects received feedback in both conditions.

From present knowledge of connectivity during motor imagination we know the primary motor cortex as well as the supplementary motor area, and parietal cortex, are involved in motor imagination and this network may include prefrontal cortex as well, in particular, when receiving feedback. How an increase in connectivity amongst these areas inform the behavior is unclear as the connection from SMA to sensorimotor and premotor areas are suggested to influence the inhibition of movement execution during motor imagination (Kasess et al., 2008). The parietal areas are involved in attention as well as visual motor transformation or performing visual motor tasks (Andersen & Buneo, 2002). We instructed subjects to perform kinesthetic imagination but they may also perform visual imagination which may involve a more complex motor task; for example, throwing a ball, opening a door handle, or any task that additionally involves the imagination of the upper limb and some type of object may involve parietal areas. Andersen et al. have developed brain computer interface devices using parietal reach and grasp areas in non-human primates as well as initial work with humans showing that subjects can control a

robotic device based on movement, intention, and imagination using solely parietal areas (Aflalo et al., 2015; Hauschild, Mulliken, Fineman, Loeb, & Andersen, 2012).

We found specific connectivity features to correlate with change in performance as measured by the number of correct trials and the time to hit correct targets. For both left and right hand imagination, connectivity from ipsilateral premotor/motor to SMA correlate with a decreased time to hit. For left hand motor imagination connections from left lateral sensorimotor to right motor correlates with a decreased time to hit whereas for right hand motor imagination connections from right motor and sensorimotor cortices to left premotor and sensorimotor correlate with an increased time to hit. This non-symmetric effect may reflect specific connections due to the right handedness of subjects studied where the left hemisphere is dominant and contralateral influence impairs motor imagery performance. Bidirectional left parietal-SMA connections and left parietal to right motor correlate with a decreased time to hit, whereas output from left parietal to left premotor correlates with an increased time to hit illustrating the differential effects of the parietal cortex on the motor imagination network. To the best of our knowledge, this is the first study examining connectivity change following tDCS and correlating connectivity to behavioral performance to examine how planned targeting of the network with stimulation could be used improve performance.

Using directed network connectivity there are strong correlation between connection in the parietal cortex and imagination and timing of correct trials. We do not attempt to predict performance based on these connectivity measures but rather use this correlation to examine how the network interacts at this peak control signal and how that

correlates timing and performance for the trial overall. Previous work examined offline motor imagery classification between right hand and foot imagery of features derived from independent component using connectivity, frequency, and power-based metrics and found that connectivity features presented similar discriminatory performance as frequency based metrics and found little difference between different connectivity measures including directed transfer function, coherence, partial directed coherence among others (Billinger et al., 2013). This study did not report specific connectivity features used for classification so we were unable to compare connectivity results. In addition, this work did not examine the relationship between connectivity and subsequent BCI performance using band power features. Overall, previous work has not examined the interaction of connectivity measures with performance but has rather examined how connectivity changes during task performance and if connectivity based classifiers can be used to improve classification accuracy.

Our results support the hypothesis that tDCS interacts with ongoing endogenous brain activity in an activity/task-specific manner. During motor imagination, there is a decrease in alpha power in the contralateral sensorimotor cortex due to a desynchronization in the underlying networks, with areas involved in the imagination decoupling from surrounding areas. Based on unilateral sensorimotor stimulation, we see differing interactions of the stimulation aftereffects on network connectivity based on the laterality of hand imagination. The effects of targeting network connections and the most efficacious methodology to do this using TCS is still unclear. We may hypothesize that regions that we aim to increase connectivity between should be stimulated via anodal

stimulation, to increase excitation and therefore increase the probability of correlating the firing in these areas, however the timing of the firing is of importance as the timing of input onto a neuron and subsequent firing of that neuron can induce long-term potentiation or long-term depression, other parameters being equal (Müller-Dahlhaus & Ziemann, 2015). Future work to examine the time dynamics of connectivity and behavioral output will be useful in determining stimulation strategies to optimize performance and develop closed-loop bidirectional BCIs.

Conclusion and Future Directions

The results of this work suggest a way forward using a combination of electrophysiology and noninvasive neuromodulation to target local activity and network connections. A combination of modeling and network analysis during brain states of interest, be they task specific or symptomatic, with stimulation likely will lead to local and network effects that improve the behavioral outcome be it due to inhibition or potentiation of local and network neural activity. Using this approach, computational psychiatry has been proposed to improve patient symptoms and outcomes though much work is still required to validate this proposed framework for neuropsychiatric illnesses and the maximum possible effect size and optimal treatment regimens are unknown (Huys, Maia, & Frank, 2016; Stephan et al., 2015).

Closed-loop targeting based on local activity and network connections in which a control system uses ongoing electrophysiological recordings to direct and trigger simulation are beginning to be proposed following the lead of deep brain stimulation (Afshar et al., 2012; Dangi, Orsborn, Moorman, & Carmena, 2013; Herron, Denison, & Chizeck, 2015; Little & Brown, 2012; Priori, Foffani, Rossi, & Marceglia, 2013). Commercial products have already been developed by device manufacturers with the capability of combining EEG and TCS, though there have not yet been published peer-reviewed studies using these devices for closed-loop stimulation.

The combined possibilities of using multifocal targeting of network activity and connections for specific tasks with closed-loop stimulation will yield an increased understanding of brain dynamics across brain states, from behavioral task performance to

neuropsychiatric disorders, and should open new approached to treating these disorders, possibly when combined with cognitive training. While the current results illustrate how tDCS interacts and alters endogenous oscillatory activity, using a similar strategy with tACS expands targeting possibilities, and parameter space, to specific frequencies. While current distribution during tDCS is highest in the cortex, tACS has recently been shown to allow for targeting deeper structures without affecting surface tissue (Grossman et al., 2017). While the recent era of noninvasive neuromodulation spans from the introduction of TMS in the early 1980s to the rediscovery of TCS in the late 1990s, the potential of the field to improve patient quality of life has been demonstrated in the past decade. Combining this stimulation with BCIs to provide feedback will allow for functional targeting of task specific brain regions and connectivity for rehabilitation and possibly enhancement of performance. With ongoing studies and further refinement of techniques, we will likely be able to optimize stimulation for individual subjects with specific conditions to target specific symptoms.

Bibliography

Aflalo, T., Kellis, S., Klaes, C., Lee, B., Shi, Y., Pejsa, K., … Andersen, R. A. (2015). Decoding motor imagery from the posterior parietal cortex of a tetraplegic human. *Science*, *348*(6237), 906–910. http://doi.org/10.1126/science.aaa5417

Afshar, P., Khambhati, A., Stanslaski, S., Carlson, D., Jensen, R., Linde, D., … Denison, T. (2012). A translational platform for prototyping closed-loop neuromodulation systems. *Frontiers in Neural Circuits*, *6*(January), 117. http://doi.org/10.3389/fncir.2012.00117

Allison, B. Z., Brunner, C., Kaiser, V., Müller-Putz, G. R., Neuper, C., & Pfurtscheller, G. (2010). Toward a hybrid brain-computer interface based on imagined movement and visual attention. *Journal of Neural Engineering*, *7*(2), 26007. http://doi.org/10.1088/1741-2560/7/2/026007

Amadi, U., Ilie, A., Johansen-Berg, H., & Stagg, C. J. (2014). Polarity-specific effects of motor transcranial direct current stimulation on fMRI resting state networks. *NeuroImage*, *88*, 155–161. http://doi.org/10.1016/j.neuroimage.2013.11.037

Ammann, C., Lindquist, M. A., & Celnik, P. A. (2016). Response variability of different anodal transcranial direct current stimulation intensities across multiple sessions. *Brain Stimulation*, 1–7. http://doi.org/10.1016/j.brs.2017.04.003

Andersen, R. A., & Buneo, C. A. (2002). Intentional Maps in Posterior Parietal Cortex. *Annual Review of Neuroscience*, *25*(1), 189–220. http://doi.org/10.1146/annurev.neuro.25.112701.142922

Antal, A., Boros, K., Poreisz, C., Chaieb, L., Terney, D., & Paulus, W. (2008). Comparatively weak after-effects of transcranial alternating current stimulation (tACS) on cortical excitability in humans. *Brain Stimulation*, *1*(2), 97–105. http://doi.org/10.1016/j.brs.2007.10.001

Antal, A., Chaieb, L., Moliadze, V., Monte-Silva, K., Poreisz, C., Thirugnanasambandam, N., … Paulus, W. (2010). Brain-derived neurotrophic factor (BDNF) gene polymorphisms shape cortical plasticity in humans. *Brain Stimulation*, *3*(4), 230–7. http://doi.org/10.1016/j.brs.2009.12.003

Antal, A., & Paulus, W. (2013). Transcranial alternating current stimulation (tACS). *Frontiers in Human Neuroscience*, *7*(June), 317. http://doi.org/10.3389/fnhum.2013.00317

Astolfi, L., Cincotti, F., Mattia, D., Marciani, M. G., Baccala, L. A., Fallani, F. D. V., … Babiloni, F. (2007). Comparison of different cortical connectivity estimators for high-resolution EEG recordings. *Human Brain Mapping*, *28*(2), 143–157. http://doi.org/10.1002/hbm.20263

Athanasiou, A., Lithari, C., Kalogianni, K., Klados, M. A., & Bamidis, P. D. (2012). Source detection and functional connectivity of the sensorimotor cortex during actual and imaginary limb movement: A preliminary study on the implementation of econnectome in motor imagery protocols. *Advances in Human-Computer Interaction*, *2012*. http://doi.org/10.1155/2012/127627

Ball, T., Demandt, E., Mutschler, I., Neitzel, E., Mehring, C., Vogt, K., … Schulze-Bonhage, A. (2008). Movement related activity in the high gamma range of the

human EEG. *NeuroImage*, *41*(2), 302–10. http://doi.org/10.1016/j.neuroimage.2008.02.032

Baxter, B. S., Decker, A., & He, B. (2013). Noninvasive control of a robotic arm in multiple dimensions using scalp electroencephalogram. In *International IEEE/EMBS Conference on Neural Engineering, NER*. http://doi.org/10.1109/NER.2013.6695867

Baxter, B. S., Edelman, B. J., Nesbitt, N., & He, B. (2016). Sensorimotor Rhythm BCI with Simultaneous High Definition-Transcranial Direct Current Stimulation Alters Task Performance. *Brain Stimulation*, *9*(6), 834–841. http://doi.org/10.1016/j.brs.2016.07.003

Berardi, N., Pizzorusso, T., & Maffei, L. (2000). Critical periods during sensory development. *Current Opinion in Neurobiology*. http://doi.org/10.1016/S0959-4388(99)00047-1

Berger, H. (1929). Uber das Elektroenkephalogramm des Menschen. *Archiv Fur Psychatrie*, *87*, 527–570.

Bergmann, T. O., Karabanov, A., Hartwigsen, G., Thielscher, A., & Siebner, H. R. (2016). Combining non-invasive transcranial brain stimulation with neuroimaging and electrophysiology: Current approaches and future perspectives. *NeuroImage*, *140*, 4–19. http://doi.org/10.1016/j.neuroimage.2016.02.012

Berker, A. O. de, Bikson, M., Bestmann, S., de Berker, A. O., Bikson, M., & Bestmann, S. (2013). Predicting the behavioral impact of transcranial direct current stimulation: issues and limitations. *Frontiers in Human Neuroscience*, *7*(October), 613. http://doi.org/10.3389/fnhum.2013.00613

Bestmann, S., de Berker, A. O., & Bonaiuto, J. (2015). Understanding the behavioural consequences of noninvasive brain stimulation. *Trends in Cognitive Sciences*, *19*(1), 13–20. http://doi.org/10.1016/j.tics.2014.10.003

Bikson, M., Inoue, M., Akiyama, H., Deans, J. K., Fox, J. E., Miyakawa, H., & Jefferys, J. G. R. (2004). Effects of uniform extracellular DC electric fields on excitability in rat hippocampal slices *in vitro*. *The Journal of Physiology*, *557*(1), 175–190. http://doi.org/10.1113/jphysiol.2003.055772

Bikson, M., & Rahman, A. (2013). Origins of specificity during tDCS: anatomical, activity-selective, and input-bias mechanisms. *Frontiers in Human Neuroscience*, *7*(October), 1–5. http://doi.org/10.3389/fnhum.2013.00688

Billinger, M., Brunner, C., & Müller-Putz, G. R. (2013). Single-trial connectivity estimation for classification of motor imagery data. *Journal of Neural Engineering*, *10*(4), 46006. http://doi.org/10.1088/1741-2560/10/4/046006

Blankertz, B., Sannelli, C., Halder, S., Hammer, E. M., Kübler, A., Müller, K.-R., … Dickhaus, T. (2010). Neurophysiological predictor of SMR-based BCI performance. *NeuroImage*, *51*(4), 1303–9. http://doi.org/10.1016/j.neuroimage.2010.03.022

Bortoletto, M., Pellicciari, M. C., Rodella, C., & Miniussi, C. (2015). The interaction with task-induced activity is more important than polarization: A tDCS study. *Brain Stimulation*, *8*(2), 269–276. http://doi.org/10.1016/j.brs.2014.11.006

Bouton, C. E., Shaikhouni, A., Annetta, N. V., Bockbrader, M. A., Friedenberg, D. A., Nielson, D. M., … Rezai, A. R. (2016). Restoring cortical control of functional

movement in a human with quadriplegia. *Nature*, *533*(7602), 247–250. http://doi.org/10.1038/nature17435

Bradberry, T. J., Gentili, R. J., & Contreras-Vidal, J. L. (2010). Reconstructing three-dimensional hand movements from noninvasive electroencephalographic signals. *The Journal of Neuroscience*, *30*(9), 3432–7. http://doi.org/10.1523/JNEUROSCI.6107-09.2010

Brunner, P., Bianchi, L., Guger, C., Cincotti, F., & Schalk, G. (2011). Current trends in hardware and software for brain-computer interfaces (BCIs). *Journal of Neural Engineering*, *8*(2), 25001. http://doi.org/10.1088/1741-2560/8/2/025001

Brunoni, A., & Boggio, P. (2014). *Clinical use of Transcranial Direct Current Stimulation in Psychiatry*. *The Stimulated Brain: Cognitive Enhancement Using Non-Invasive Brain Stimulation*. Elsevier Inc. http://doi.org/10.1016/B978-0-12-404704-4.00014-4

Brunoni, A., Fregni, F., & Pagano, R. L. (2011). Translational research in transcranial direct current stimulation (tDCS): a systematic review of studies in animals. *Reviews in the Neurosciences*, *22*(4), 471–81. http://doi.org/10.1515/RNS.2011.042

Brunoni, A. R., Nitsche, M. A., Bolognini, N., Bikson, M., Wagner, T., Merabet, L., … Boggio, P. S. (2012). Clinical research with transcranial direct current stimulation (tDCS): Challenges and future directions. *Brain Stimulation*, *5*(3), 175–195. http://doi.org/10.1016/j.brs.2011.03.002

Buch, E. R., Santarnecchi, E., Antal, A., Born, J., Celnik, P. A., Classen, J., … Cohen, L. G. (2017). Effects of tDCS on motor learning and memory formation: A consensus and critical position paper. *Clinical Neurophysiology*, *128*(4), 589–603. http://doi.org/10.1016/j.clinph.2017.01.004

Bundy, D. T., Wronkiewicz, M., Sharma, M., Moran, D. W., Corbetta, M., & Leuthardt, E. C. (2012). Using ipsilateral motor signals in the unaffected cerebral hemisphere as a signal platform for brain-computer interfaces in hemiplegic stroke survivors. *Journal of Neural Engineering*, *9*(3), 36011. http://doi.org/10.1088/1741-2560/9/3/036011

Bütefisch, C. M. (2004). Plasticity in the human cerebral cortex: lessons from the normal brain and from stroke. *The Neuroscientist : A Review Journal Bringing Neurobiology, Neurology and Psychiatry*, *10*(2), 163–73. http://doi.org/10.1177/1073858403262152

Buzsáki, G., Anastassiou, C. a, & Koch, C. (2012). The origin of extracellular fields and currents--EEG, ECoG, LFP and spikes. *Nature Reviews. Neuroscience*, *13*(6), 407–20. http://doi.org/10.1038/nrn3241

Cassady, K., You, A., Doud, A., & He, B. (2014). The impact of mind-body awareness training on the early learning of a brain-computer interface. *TECHNOLOGY*, *2*(3), 254–260. http://doi.org/10.1142/S233954781450023X

Christ, A., Kainz, W., Hahn, E. G., Honegger, K., Zefferer, M., Neufeld, E., … Kuster, N. (2010). The Virtual Family--development of surface-based anatomical models of two adults and two children for dosimetric simulations. *Physics in Medicine and Biology*, *55*(2), N23-38. http://doi.org/10.1088/0031-9155/55/2/N01

Cincotti, F., Mattia, D., Aloise, F., Bufalari, S., Astolfi, L., De Vico Fallani, F., …

Babiloni, F. (2008). High-resolution EEG techniques for brain-computer interface applications. *Journal of Neuroscience Methods*, *167*(1), 31–42. http://doi.org/10.1016/j.jneumeth.2007.06.031

Clark, V. P., Coffman, B. A., Mayer, A. R., Weisend, M. P., Lane, T. D. R., Calhoun, V. D., … Wassermann, E. M. (2012). TDCS guided using fMRI significantly accelerates learning to identify concealed objects. *NeuroImage*, *59*(1), 117–28. http://doi.org/10.1016/j.neuroimage.2010.11.036

Coffman, B. A., Clark, V. P., & Parasuraman, R. (2014). Battery powered thought: Enhancement of attention, learning, and memory in healthy adults using transcranial direct current stimulation. *NeuroImage*, *85*, 895–908. http://doi.org/10.1016/j.neuroimage.2013.07.083

Cohen Kadosh, R., Levy, N., O'Shea, J., Shea, N., & Savulescu, J. (2012). The neuroethics of non-invasive brain stimulation. *Current Biology*, *22*(4), R108–R111.

Collinger, J. L., Wodlinger, B., Downey, J. E., Wang, W., Tyler-Kabara, E. C., Weber, D. J., … Schwartz, A. B. (2012). High-performance neuroprosthetic control by an individual with tetraplegia. *The Lancet*, *6736*(12), 1–8. http://doi.org/10.1016/S0140-6736(12)61816-9

Cramer, S. C., Sur, M., Dobkin, B. H., O'Brien, C., Sanger, T. D., Trojanowski, J. Q., … Vinogradov, S. (2011). Harnessing neuroplasticity for clinical applications. *Brain*, *134*(6), 1591–1609. http://doi.org/10.1093/brain/awr039

Daly, J. J., Cheng, R., Rogers, J., Litinas, K., Hrovat, K., & Dohring, M. (2009). Feasibility of a new application of noninvasive Brain Computer Interface (BCI): a case study of training for recovery of volitional motor control after stroke. *Journal of Neurologic Physical Therapy : JNPT*, *33*(4), 203–11. http://doi.org/10.1097/NPT.0b013e3181c1fc0b

Dangi, S., Orsborn, A. L., Moorman, H. G., & Carmena, J. M. (2013). Design and analysis of closed-loop decoder adaptation algorithms for brain-machine interfaces. *Neural Computation*, *25*(7), 1693–731. http://doi.org/10.1162/NECO_a_00460

Darvas, F., Scherer, R., Ojemann, J. G., Rao, R. P., Miller, K. J., & Sorensen, L. B. (2010). High gamma mapping using EEG. *NeuroImage*, *49*(1), 930–8. http://doi.org/10.1016/j.neuroimage.2009.08.041

Dayan, E., & Cohen, L. G. (2011). Neuroplasticity subserving motor skill learning. *Neuron*, *72*(3), 443–54. http://doi.org/10.1016/j.neuron.2011.10.008

de Vries, S., & Mulder, T. (2007). Motor imagery and stroke rehabilitation: a critical discussion. *Journal of Rehabilitation Medicine : Official Journal of the UEMS European Board of Physical and Rehabilitation Medicine*, *39*(1), 5–13. http://doi.org/10.2340/16501977-0020

Delorme, A., & Makeig, S. (2004). EEGLAB: an open source toolbox for analysis of single-trial EEG dynamics including independent component analysis. *Journal of Neuroscience Methods*, *134*(1), 9–21. http://doi.org/10.1016/j.jneumeth.2003.10.009

Ding, M., Bressler, S. L., Yang, W., & Liang, H. (2000). Short-window spectral analysis of cortical event-related potentials by adaptive multivariate autoregressive modeling: data preprocessing, model validation, and variability assessment. *Biological Cybernetics*, *83*(1), 35–45. http://doi.org/10.1007/s004229900137

Dmochowski, J. P., Datta, A., Bikson, M., Su, Y., & Parra, L. C. (2011). Optimized multi-electrode stimulation increases focality and intensity at target. *Journal of Neural Engineering*, *8*(4), 46011. http://doi.org/10.1088/1741-2560/8/4/046011

Doud, A. J., Lucas, J. P., Pisansky, M. T., & He, B. (2011). Continuous three-dimensional control of a virtual helicopter using a motor imagery based brain-computer interface. *PloS One*, *6*(10). http://doi.org/10.1371/journal.pone.0026322

Dubljević, V., Saigle, V., & Racine, E. (2014). The Rising Tide of tDCS in the Media and Academic Literature. *Neuron*, *82*(4), 731–736. http://doi.org/10.1016/j.neuron.2014.05.003

Edelman, B. J., Baxter, B., & He, B. (2016). EEG Source Imaging Enhances the Decoding of Complex Right-Hand Motor Imagery Tasks. *IEEE Transactions on Biomedical Engineering*, *63*(1), 4–14. http://doi.org/10.1109/TBME.2015.2467312

Edelman, B. J., Johnson, N., Sohrabpour, A., Tong, S., Thakor, N., & He, B. (2015). Systems Neuroengineering: Understanding and Interacting with the Brain. *Engineering*, *1*(3), 292. http://doi.org/10.15302/J-ENG-2015078

Edwards, D., Cortes, M., Datta, A., Minhas, P., Wassermann, E. M., & Bikson, M. (2013). Physiological and modeling evidence for focal transcranial electrical brain stimulation in humans: A basis for high-definition tDCS. *NeuroImage*, 1–10. http://doi.org/10.1016/j.neuroimage.2013.01.042

Engel, A. K., & Fries, P. (2010). Beta-band oscillations — signalling the status quo ?, 156–165. http://doi.org/10.1016/j.conb.2010.02.015

Famm, K., Litt, B., Tracey, K. J., Boyden, E. S., & Slaoui, M. (2013). Drug discovery: A jump-start for electroceuticals. *Nature*, *496*(7444), 159–161. http://doi.org/10.1038/496159a

Fetz, E. E. (2007). Volitional control of neural activity: implications for brain-computer interfaces. *The Journal of Physiology*, *579*(Pt 3), 571–9. http://doi.org/10.1113/jphysiol.2006.127142

Feurra, M., Bianco, G., Polizzotto, N. R., Innocenti, I., Rossi, A., & Rossi, S. (2011). Cortico-Cortical Connectivity between Right Parietal and Bilateral Primary Motor Cortices during Imagined and Observed Actions: A Combined TMS/tDCS Study. *Frontiers in Neural Circuits*, *5*(August), 1–9. http://doi.org/10.3389/fncir.2011.00010

Fischer, D. B., Fried, P. J., Ruffini, G., Ripolles, O., Salvador, R., Banus, J., … Fox, M. D. (2017). Multifocal tDCS targeting the resting state motor network increases cortical excitability beyond traditional tDCS targeting unilateral motor cortex. *NeuroImage*, *157*(May), 34–44. http://doi.org/10.1016/j.neuroimage.2017.05.060

Flöel, A. (2014). NeuroImage tDCS-enhanced motor and cognitive function in neurological diseases. *NeuroImage*, *85*, 934–947. http://doi.org/10.1016/j.neuroimage.2013.05.098

Fox, M. D., Buckner, R. L., Liu, H., Chakravarty, M. M., Lozano, A. M., & Pascual-Leone, A. (2014). Resting-state networks link invasive and noninvasive brain stimulation across diverse psychiatric and neurological diseases. *Proceedings of the National Academy of Sciences of the United States of America*, *111*(41), E4367-75. http://doi.org/10.1073/pnas.1405003111

Friston, K., Moran, R., & Seth, A. K. (2013). Analysing connectivity with Granger causality and dynamic causal modelling. *Current Opinion in Neurobiology*, *23*(2), 172–8. http://doi.org/10.1016/j.conb.2012.11.010

Fritsch, B., Reis, J., Martinowich, K., Schambra, H. M., Ji, Y., Cohen, L. G., & Lu, B. (2010). Direct current stimulation promotes BDNF-dependent synaptic plasticity: Potential implications for motor learning. *Neuron*, *66*(2), 198–204. http://doi.org/10.1016/j.neuron.2010.03.035

Galán, F., Nuttin, M., Lew, E., Ferrez, P. W., Vanacker, G., Philips, J., & Millán, J. D. R. (2008). A brain-actuated wheelchair: asynchronous and non-invasive Brain-computer interfaces for continuous control of robots. *Clinical Neurophysiology : Official Journal of the International Federation of Clinical Neurophysiology*, *119*(9), 2159–69. http://doi.org/10.1016/j.clinph.2008.06.001

Galea, J. M., Vazquez, A., Pasricha, N., de Xivry, J.-J. O., & Celnik, P. (2011). Dissociating the roles of the cerebellum and motor cortex during adaptive learning: the motor cortex retains what the cerebellum learns. *Cerebral Cortex (New York, N.Y. : 1991)*, *21*(8), 1761–70. http://doi.org/10.1093/cercor/bhq246

Gao, Q., Duan, X., & Chen, H. (2011). Evaluation of effective connectivity of motor areas during motor imagery and execution using conditional Granger causality. *NeuroImage*, *54*(2), 1280–1288. http://doi.org/10.1016/j.neuroimage.2010.08.071

Gramfort, A., Papadopoulo, T., Olivi, E., & Clerc, M. (2010). OpenMEEG: opensource software for quasistatic bioelectromagnetics. *Biomedical Engineering Online*, *9*, 45. http://doi.org/10.1186/1475-925X-9-45

Grech, R., Cassar, T., Muscat, J., Camilleri, K. P., Fabri, S. G., Zervakis, M., … Vanrumste, B. (2008). Review on solving the inverse problem in EEG source analysis. *J Neuroeng Rehabil*, *5*, 25. http://doi.org/10.1186/1743-0003-5-25

Green, A. M., & Kalaska, J. F. (2011). Learning to move machines with the mind. *Trends in Neurosciences*, *34*(2), 61–75. http://doi.org/10.1016/j.tins.2010.11.003

Grossman, N., Bono, D., Dedic, N., Kodandaramaiah, S. B., Rudenko, A., Suk, H.-J., … Boyden, E. S. (2017). Noninvasive Deep Brain Stimulation via Temporally Interfering Electric Fields. *Cell*, *169*(6), 1029–1041.e16. http://doi.org/10.1016/j.cell.2017.05.024

Halko, M. a, Datta, a, Plow, E. B., Scaturro, J., Bikson, M., & Merabet, L. B. (2011). Neuroplastic changes following rehabilitative training correlate with regional electrical field induced with tDCS. *NeuroImage*, *57*(3), 885–91. http://doi.org/10.1016/j.neuroimage.2011.05.026

Hamalainen, M. S., & Sarvas, J. (1989). Realistic conductivity geometry model of the human head for interpretation of neuromagnetic data. *IEEE Transactions on Biomedical Engineering*, *36*, 165–171. http://doi.org/10.1109/10.16463

Hamedi, M., Salleh, S.-H., & Noor, A. M. (2016). Electroencephalographic Motor Imagery Brain Connectivity Analysis for BCI: A Review. *Neural Computation*, *28*(6), 999–1041. http://doi.org/10.1162/NECO_a_00838

Hamilton, R., Messing, S., & Chatterjee, A. (2011). Rethinking the thinking cap: Ethics of neural enhancement using noninvasive brain stimulation. *Neurology*, *76*(2), 187–193. http://doi.org/10.1212/WNL.0b013e318205d50d

Hammer, E. M., Halder, S., Blankertz, B., Sannelli, C., Dickhaus, T., Kleih, S., … Kübler, A. (2012). Psychological predictors of SMR-BCI performance. *Biological Psychology*, *89*(1), 80–6. http://doi.org/10.1016/j.biopsycho.2011.09.006

Haselager, P., Vlek, R., Hill, J., & Nijboer, F. (2009). A note on ethical aspects of BCI. *Neural Networks*, *22*(9), 1352–1357. http://doi.org/10.1016/j.neunet.2009.06.046

Hauschild, M., Mulliken, G. H., Fineman, I., Loeb, G. E., & Andersen, R. A. (2012). Cognitive signals for brain-machine interfaces in posterior parietal cortex include continuous 3D trajectory commands. *Proceedings of the National Academy of Sciences*, *109*(42), 17075–17080. http://doi.org/10.1073/pnas.1215092109

He, B., Baxter, B., Edelman, B. J., Cline, C. C., & Ye, W. W. (2015). Noninvasive brain-computer interfaces based on sensorimotor rhythms. *Proceedings of the IEEE*, *103*(6), 1–19. http://doi.org/10.1109/JPROC.2015.2407272

He, B., Gao, S., Yuan, H., & Wolpaw, J. (2013). Brain-Computer Interface. In B. He (Ed.), *Neural Engineering* (pp. 87–151). Springer.

He, B., Musha, T., Okamoto, Y., Homma, S., Nakajima, Y., & Sato, T. (1987). Electric dipole tracing in the brain by means of the boundary element method and its accuracy. *IEEE Transactions on Bio-Medical Engineering*, *34*(6), 406–14.

Herron, J., Denison, T., & Chizeck, H. J. (2015). Closed-loop DBS with movement intention. *2015 7th International IEEE/EMBS Conference on Neural Engineering (NER)*, 844–847. http://doi.org/10.1109/NER.2015.7146755

Hétu, S., Grégoire, M., Saimpont, A., Coll, M.-P., Eugène, F., Michon, P.-E., & Jackson, P. L. (2013). The neural network of motor imagery: an ALE meta-analysis. *Neuroscience and Biobehavioral Reviews*, *37*(5), 930–49. http://doi.org/10.1016/j.neubiorev.2013.03.017

Hochberg, L. R., Bacher, D., Jarosiewicz, B., Masse, N. Y., Simeral, J. D., Vogel, J., … Donoghue, J. P. (2012). Reach and grasp by people with tetraplegia using a neurally controlled robotic arm. *Nature*, *485*(7398), 372–5. http://doi.org/10.1038/nature11076

Hochberg, L. R., Serruya, M. D., Friehs, G. M., Mukand, J. a, Saleh, M., Caplan, A. H., … Donoghue, J. P. (2006). Neuronal ensemble control of prosthetic devices by a human with tetraplegia. *Nature*, *442*(7099), 164–71. http://doi.org/10.1038/nature04970

Holz, E. M., Kaufmann, T., Desideri, L., Malavasi, M., Hoogerwerf, E., & Andrea, K. (2013). User Centered Design in BCI Development. In B. Z. Allison, S. Dunne, R. Leeb, J. Del R. Millán, & A. Nijholt (Eds.), (pp. 155–172). Berlin, Heidelberg: Springer Berlin Heidelberg. http://doi.org/10.1007/978-3-642-29746-5

Horki, P., Solis-Escalante, T., Neuper, C., & Müller-Putz, G. (2011). Combined motor imagery and SSVEP based BCI control of a 2 DoF artificial upper limb. *Medical & Biological Engineering & Computing*, *49*(5), 567–77. http://doi.org/10.1007/s11517-011-0750-2

Hunter, M. A., Coffman, B. A., Gasparovic, C., Calhoun, V. D., Trumbo, M. C., & Clark, V. P. (2015). Baseline effects of transcranial direct current stimulation on glutamatergic neurotransmission and large-scale network connectivity. *Brain Research*, *1594*, 92–107. http://doi.org/10.1016/j.brainres.2014.09.066

Huys, Q. J. M., Maia, T. V, & Frank, M. J. (2016). Computational psychiatry as a bridge between neuro- science and clinical applications, (February), 1–21. http://doi.org/10.1038/nn.4238

Hyvarinen, A. (1999). Fast and Robust Fixed-Point Algorithm for Independent Component Analysis. *IEEE Trans. Neur. Net.*, *10*(3), 626–634.

Im, C. H., Gururajan, A., Zhang, N., Chen, W., & He, B. (2007). Spatial resolution of EEG cortical source imaging revealed by localization of retinotopic organization in human primary visual cortex. *Journal of Neuroscience Methods*, *161*(1), 142–154. http://doi.org/10.1016/j.jneumeth.2006.10.008

Iuculano, T., & Cohen Kadosh, R. (2013). The Mental Cost of Cognitive Enhancement. *Journal of Neuroscience*, *33*(10), 4482–4486. http://doi.org/10.1523/JNEUROSCI.4927-12.2013

Jackson, A., & Zimmermann, J. B. (2012). Neural interfaces for the brain and spinal cord-restoring motor function. *Nature Reviews. Neurology*. http://doi.org/10.1038/nrneurol.2012.219

Javadi, A. H., Cheng, P., & Walsh, V. (2012). Short duration transcranial direct current stimulation (tDCS) modulates verbal memory. *Brain Stimulation*, *5*(4), 468–74. http://doi.org/10.1016/j.brs.2011.08.003

Johnson, M. D., Lim, H. H., Netoff, T. I., Connolly, A. T., Johnson, N., Roy, A., … He, B. (2013). Neuromodulation for brain disorders: challenges and opportunities. *IEEE Transactions on Bio-Medical Engineering*, *60*(3), 610–24. http://doi.org/10.1109/TBME.2013.2244890

Joundi, R. a, Jenkinson, N., Brittain, J.-S., Aziz, T. Z., & Brown, P. (2012). Driving oscillatory activity in the human cortex enhances motor performance. *Current Biology : CB*, *22*(5), 403–7. http://doi.org/10.1016/j.cub.2012.01.024

Jung, T. P., Makeig, S., Humphries, C., Lee, T. W., McKeown, M. J., Iragui, V., & Sejnowski, T. J. (2000). Removing electroencephalographic artifacts by blind source separation. *Psychophysiology*, *37*(2), 163–78. Retrieved from http://www.ncbi.nlm.nih.gov/pubmed/10731767

Kabakov, A. Y., Muller, P. a, Pascual-Leone, A., Jensen, F. E. F., Rotenberg, A., Antal, A., … Fregni, F. (2012). Contribution of axonal orientation to pathway-dependent modulation of excitatory transmission by direct current stimulation in isolated rat hippocampus. *Journal of Neurophysiology*, *107*(7), 1881–9. http://doi.org/10.1152/jn.00715.2011

Kamiński, M., Ding, M., Truccolo, W. A., & Bressler, S. L. (2001). Evaluating causal relations in neural systems: Granger causality, directed transfer function and statistical assessment of significance. *Biological Cybernetics*, *85*(2), 145–157. http://doi.org/10.1007/s004220000235

Kamiński, M. J., & Blinowska, K. J. (1991). A new method of the description of the information flow in the brain structures. *Biological Cybernetics*, *65*(3), 203–210. http://doi.org/10.1007/BF00198091

Kamousi, B., Amini, A. N., & He, B. (2007). Classification of motor imagery by means of cortical current density estimation and Von Neumann entropy. *Journal of Neural Engineering*, *4*(2), 17–25. http://doi.org/10.1088/1741-2560/4/2/002

Kamousi, B., Liu, Z., & He, B. (2005). Classification of motor imagery tasks for brain-computer interface applications by means of two equivalent dipoles analysis. *IEEE Transactions on Neural Systems and Rehabilitation Engineering : A Publication of the IEEE Engineering in Medicine and Biology Society*, *13*(2), 166–71. http://doi.org/10.1109/TNSRE.2005.847386

Karabanov, A. N., Chao, C. C., Paine, R., & Hallett, M. (2013). Mapping different intra-hemispheric parietal-motor networks using twin coil TMS. *Brain Stimulation*, *6*(3), 384–389. http://doi.org/10.1016/j.brs.2012.08.002

Kasashima, Y., Fujiwara, T., Matsushika, Y., Tsuji, T., Hase, K., Ushiyama, J., … Liu, M. (2012). Modulation of event-related desynchronization during motor imagery with transcranial direct current stimulation (tDCS) in patients with chronic hemiparetic stroke. *Experimental Brain Research*, *221*(3), 263–8. http://doi.org/10.1007/s00221-012-3166-9

Kasess, C. H., Windischberger, C., Cunnington, R., Lanzenberger, R., Pezawas, L., & Moser, E. (2008). The suppressive influence of SMA on M1 in motor imagery revealed by fMRI and dynamic causal modeling. *NeuroImage*, *40*(2), 828–837. http://doi.org/10.1016/j.neuroimage.2007.11.040

Keeser, D., Meindl, T., Bor, J., Palm, U., Pogarell, O., Mulert, C., … Padberg, F. (2011). Prefrontal Transcranial Direct Current Stimulation Changes Connectivity of Resting-State Networks during fMRI. *Journal of Neuroscience*, *31*(43), 15284–15293. http://doi.org/10.1523/JNEUROSCI.0542-11.2011

Krause, B., & Cohen Kadosh, R. (2014). Not all brains are created equal: the relevance of individual differences in responsiveness to transcranial electrical stimulation. *Frontiers in Systems Neuroscience*, *8*(February), 25. http://doi.org/10.3389/fnsys.2014.00025

Krusienski, D. J., Grosse-Wentrup, M., Galán, F., Coyle, D., Miller, K. J., Forney, E., & Anderson, C. W. (2011). Critical issues in state-of-the-art brain-computer interface signal processing. *Journal of Neural Engineering*, *8*(2), 25002. http://doi.org/10.1088/1741-2560/8/2/025002

Kübler, A., Nijboer, F., Mellinger, J., Vaughan, T. M., Pawelzik, H., Schalk, G., … Wolpaw, J. R. (2005). Patients with ALS can use sensorimotor rhythms to operate a brain-computer interface. *Neurology*, *64*(10), 1775–7. http://doi.org/10.1212/01.WNL.0000158616.43002.6D

Kuo, H.-I. I., Bikson, M., Datta, A., Minhas, P., Paulus, W., Kuo, M.-F. F., & Nitsche, M. A. (2013). Comparing cortical plasticity induced by conventional and high-definition 4 ?? 1 ring tDCS: A neurophysiological study. *Brain Stimulation*, *6*(4), 644–648. http://doi.org/10.1016/j.brs.2012.09.010

Kuo, H.-I., Paulus, W., Batsikadze, G., Jamil, A., Kuo, M.-F., & Nitsche, M. A. (2016). Chronic Enhancement of Serotonin Facilitates Excitatory Transcranial Direct Current Stimulation-Induced Neuroplasticity. *Neuropsychopharmacology*, *41*(5), 1223–1230. http://doi.org/10.1038/npp.2015.270

Kuo, M.-F. M. M.-F. M., & Nitsche, M. a. (2012). *Effects of Transcranial Electrical Stimulation on Cognition. Clinical EEG and Neuroscience* (Vol. 43). Elsevier Inc. http://doi.org/10.1177/1550059412444975

Kus, R., Ginter, J. S., & Blinowska, K. J. (2006). Propagation of EEG activity during finger movement and its imagination. *Acta Neurobiologiae Experimentalis*, *66*(3), 195–206.

LaFleur, K., Cassady, K., Doud, A., Shades, K., Rogin, E., & He, B. (2013). Quadcopter control in three-dimensional space using a noninvasive motor imagery-based brain–computer interface. *Journal of Neural Engineering*, *10*(4), 46003. http://doi.org/10.1088/1741-2560/10/4/046003

Lapenta, O. M., Minati, L., Fregni, F., & Boggio, P. S. (2013). Je pense donc je fais: transcranial direct current stimulation modulates brain oscillations associated with motor imagery and movement observation. *Frontiers in Human Neuroscience*, *7*(June), 256. http://doi.org/10.3389/fnhum.2013.00256

Liebetanz, D., Nitsche, M. a, Tergau, F., & Paulus, W. (2002). Pharmacological approach to the mechanisms of transcranial DC-stimulation-induced after-effects of human motor cortex excitability. *Brain : A Journal of Neurology*, *125*(Pt 10), 2238–2247. http://doi.org/10.1093/brain/awf238

Lippold, O. C. J., & Redfearn, J. W. T. (1964). Mental Changes Resulting from the Passage of Small Direct Currents Through the Human Brain. *The British Journal of Psychiatry*, *110*(469), 768–772. Retrieved from http://bjp.rcpsych.org/content/110/469/768

Little, S., & Brown, P. (2012). What brain signals are suitable for feedback control of deep brain stimulation in Parkinson's disease? *Annals of the New York Academy of Sciences*, *1265*, 9–24. http://doi.org/10.1111/j.1749-6632.2012.06650.x

Lotze, M., & Halsband, U. (2006). Motor imagery. *Journal of Physiology, Paris*, *99*(4–6), 386–95. http://doi.org/10.1016/j.jphysparis.2006.03.012

Lotze, M., Montoya, P., Erb, M., Hülsmann, E., Flor, H., Klose, U., … Grodd, W. (1999). Activation of cortical and cerebellar motor areas during executed and imagined hand movements: an fMRI study. *Journal of Cognitive Neuroscience*, *11*(5), 491–501. http://doi.org/10.1162/089892999563553

Luft, C. D. B., Pereda, E., Banissy, M. J., & Bhattacharya, J. (2014). Best of both worlds: promise of combining brain stimulation and brain connectome. *Frontiers in Systems Neuroscience*, *8*(July), 1–15. http://doi.org/10.3389/fnsys.2014.00132

Mabe, R. (2017). What Is It Like to Regain a Sense of Touch, Only to Lose It Again? *The Atlantic*. Retrieved from https://www.theatlantic.com/science/archive/2017/04/mind-controlled-robot-arm/522315/

Madhavan, S., & Shah, B. (2012). Enhancing motor skill learning with transcranial direct current stimulation - a concise review with applications to stroke. *Frontiers in Psychiatry*, *3*(January), 66. http://doi.org/10.3389/fpsyt.2012.00066

Mak, J. N., & Wolpaw, J. R. (2009). Clinical Applications of Brain-Computer Interfaces: Current State and Future Prospects. *IEEE Reviews in Biomedical Engineering*, *2*(1), 187–199. http://doi.org/10.1109/RBME.2009.2035356

Matsumoto, J., Fujiwara, T., Takahashi, O., Liu, M., Kimura, A., & Ushiba, J. (2010). Modulation of mu rhythm desynchronization during motor imagery by transcranial direct current stimulation. *Journal of NeuroEngineering and Rehabilitation*, *7*(1), 27. http://doi.org/10.1186/1743-0003-7-27

McCrimmon, C., Fu, J., Wang, M., Silva Lopes, L., Wang, P., Karimi-Bidhendi, A., … Do, A. (2017). A Portable Brain-Computer Interface Platform for EEG Acquisition and Decoding. *IEEE Transactions on Biomedical Engineering*, *9294*(c), 1–1. http://doi.org/10.1109/TBME.2017.2667579

McFarland, D. J., Sarnacki, W. a, & Wolpaw, J. R. (2010). Electroencephalographic (EEG) control of three-dimensional movement. *Journal of Neural Engineering*, *7*(3), 36007. http://doi.org/10.1088/1741-2560/7/3/036007

McFarland, D. J., & Wolpaw, J. R. (2008). Sensorimotor rhythm-based brain-computer interface (BCI): model order selection for autoregressive spectral analysis. *Journal of Neural Engineering*, *5*(2), 155–62. http://doi.org/10.1088/1741-2560/5/2/006

McFarland, D. J., & Wolpaw, J. R. (2010). Brain – Computer Interfaces for the Operation of Robotic and Prosthetic Devices. *Advances in Computers*, *79*(10), 169–187. http://doi.org/10.1016/S0065-2458(10)79004-5

Meinzer, M., Antonenko, D., Lindenberg, R., Hetzer, S., Ulm, L., Avirame, K., … Flöel, A. (2012). Electrical brain stimulation improves cognitive performance by modulating functional connectivity and task-specific activation. *The Journal of Neuroscience : The Official Journal of the Society for Neuroscience*, *32*(5), 1859–66. http://doi.org/10.1523/JNEUROSCI.4812-11.2012

Michel, C. M., Murray, M. M., Lantz, G., Gonzalez, S., Spinelli, L., & Grave De Peralta, R. (2004). EEG source imaging. *Clinical Neurophysiology*, *115*(10), 2195–2222. http://doi.org/10.1016/j.clinph.2004.06.001

Millán, J. D. R., Rupp, R., Müller-Putz, G. R., Murray-Smith, R., Giugliemma, C., Tangermann, M., … Mattia, D. (2010). Combining Brain-Computer Interfaces and Assistive Technologies: State-of-the-Art and Challenges. *Frontiers in Neuroscience*, *4*(September), 1–15. http://doi.org/10.3389/fnins.2010.00161

Moliadze, V., Atalay, D., Antal, A., & Paulus, W. (2012). Close to threshold transcranial electrical stimulation preferentially activates inhibitory networks before switching to excitation with higher intensities. *Brain Stimulation*, *5*(4), 505–11. http://doi.org/10.1016/j.brs.2011.11.004

Mordillo-Mateos, L., Turpin-Fenoll, L., Millán-Pascual, J., Núñez-Pérez, N., Panyavin, I., Gómez-Argüelles, J. M., … Oliviero, A. (2012). Effects of simultaneous bilateral tDCS of the human motor cortex. *Brain Stimulation*, *5*(3), 214–22. http://doi.org/10.1016/j.brs.2011.05.001

Moskowitz, M. a, Lo, E. H., & Iadecola, C. (2010). The science of stroke: mechanisms in search of treatments. *Neuron*, *67*(2), 181–98. http://doi.org/10.1016/j.neuron.2010.07.002

Müller-Dahlhaus, F., & Ziemann, U. (2015). Metaplasticity in Human Cortex. *The Neuroscientist*, *21*(2), 185–202. http://doi.org/10.1177/1073858414526645

Muller, K.-R., Krauledat, M., Dornhege, G., Curio, G., & Blankertz, B. (2004). Machine learning techniques for brain-computer interfaces. *Biomed Tech*, *49*(1), 11–22.

Nijboer, F., & Broermann, U. (2010). Brain–computer interfaces for communication and control in locked-in patients. *Brain-Computer Interfaces*, 1–20. http://doi.org/10.1007/978-3-642-02091-9

Nijboer, F., Clausen, J., Allison, B. Z., & Haselager, P. (2013). The asilomar survey:

Stakeholders' opinions on ethical issues related to brain-computer interfacing. *Neuroethics*, *6*(3), 541–578. http://doi.org/10.1007/s12152-011-9132-6
Nitsche, M. A., Kuo, M. F., Karrasch, R., Wächter, B., Liebetanz, D., & Paulus, W. (2009). Serotonin Affects Transcranial Direct Current-Induced Neuroplasticity in Humans. *Biological Psychiatry*, *66*(5), 503–508. http://doi.org/10.1016/j.biopsych.2009.03.022
Nitsche, M. A., Schauenburg, A., Lang, N., Liebetanz, D., Exner, C., Paulus, W., & Tergau, F. (2003). Facilitation of implicit motor learning by weak transcranial direct current stimulation of the primary motor cortex in the human. *Journal of Cognitive Neuroscience*, *15*(4), 619–26. http://doi.org/10.1162/089892903321662994
Nitsche, M., & Paulus, W. (2001). Sustained excitability elevations induced by transcranial DC motor cortex stimulation in humans. *Neurology*, *57*(10), 1899–901. Retrieved from http://www.ncbi.nlm.nih.gov/pubmed/11723286
Nitsche, M., & Paulus, W. J. (2000). *Excitability changes induced in the human motor cortex by weak transcranial direct current stimulation. The Journal of physiology* (Vol. 527 Pt 3).
Notturno, F., Marzetti, L., Pizzella, V., Uncini, A., & Zappasodi, F. (2014). Local and remote effects of transcranial direct current stimulation on the electrical activity of the motor cortical network. *Human Brain Mapping*, *35*(5), 2220–2232. http://doi.org/10.1002/hbm.22322
Opitz, A., Falchier, A., Yan, C.-G., Yeagle, E. M., Linn, G. S., Megevand, P., … Schroeder, C. E. (2016). Spatiotemporal structure of intracranial electric fields induced by transcranial electric stimulation in humans and nonhuman primates. *Scientific Reports*, *6*(1), 31236. http://doi.org/10.1038/srep31236
Paulus, W. (2011). Neuropsychological Rehabilitation Transcranial electrical stimulation (tES — tDCS ; tRNS , tACS) methods. *Neuropsychological Rehabilitation*, (September), 37–41. http://doi.org/10.1080/09602011.2011.557292
Paulus, W., Nitsche, M. A., & Antal, A. (2016). Application of transcranial electric stimulation (tDCS, tACS, tRNS): From motor-evoked potentials towards modulation of behaviour. *European Psychologist*. http://doi.org/10.1027/1016-9040/a000242
Paulus, W., & Opitz, A. (2013). Ohm's law and tDCS over the centuries. *Clinical Neurophysiology : Official Journal of the International Federation of Clinical Neurophysiology*, *124*(3), 429–30. http://doi.org/10.1016/j.clinph.2012.08.019
Paulus, W., & Rothwell, J. C. (2016). Membrane resistance and shunting inhibition: where biophysics meets state-dependent human neurophysiology. *The Journal of Physiology*, *594*(10), 2719–2728. http://doi.org/10.1113/JP271452
Peña-Gómez, C., Sala-Lonch, R., Junqué, C., Clemente, I. C., Vidal, D., Bargalló, N., … Bartrés-Faz, D. (2012). Modulation of large-scale brain networks by transcranial direct current stimulation evidenced by resting-state functional MRI. *Brain Stimulation*, *5*(3), 252–263. http://doi.org/10.1016/j.brs.2011.08.006
Pfurtscheller, G., Allison, B. Z., Brunner, C., Bauernfeind, G., Solis-Escalante, T., Scherer, R., … Birbaumer, N. (2010). The hybrid BCI. *Frontiers in Neuroscience*, *4*(April), 30. http://doi.org/10.3389/fnpro.2010.00003
Pfurtscheller, G., & Aranibar, A. (1977). Event-related cortical desynchronization

detected by power measurements of scalp EEG. *Electroencephalography and Clinical Neurophysiology*, *42*(6), 817–826. http://doi.org/10.1016/0013-4694(77)90235-8

Pfurtscheller, G., & Lopes da Silva, F. (1999). Event-related EEG/MEG synchronization and desynchronization: basic principles. *Clinical Neurophysiology : Official Journal of the International Federation of Clinical Neurophysiology*, *110*(11), 1842–57. Retrieved from http://www.ncbi.nlm.nih.gov/pubmed/10576479

Pfurtscheller, G., Neuper, C., Flotzinger, D., & Pregenzer, M. (1997). EEG-based discrimination between imagination of right and left hand movement. *Electroencephalography and Clinical Neurophysiology*, *103*(6), 642–651. http://doi.org/10.1016/S0013-4694(97)00080-1

Philip, N. S., Nelson, B. G., Frohlich, F., Lim, K. O., Widge, A. S., & Carpenter, L. L. (2017). Low-Intensity Transcranial Current Stimulation in Psychiatry. *American Journal of Psychiatry*, appi.ajp.2017.1. http://doi.org/10.1176/appi.ajp.2017.16090996

Polanía, R., Nitsche, M. a, & Paulus, W. (2011). Modulating functional connectivity patterns and topological functional organization of the human brain with transcranial direct current stimulation. *Human Brain Mapping*, *32*(8), 1236–49. http://doi.org/10.1002/hbm.21104

Polanía, R., Paulus, W., & Nitsche, M. a. (2012). Modulating cortico-striatal and thalamo-cortical functional connectivity with transcranial direct current stimulation. *Human Brain Mapping*, *33*(10), 2499–508. http://doi.org/10.1002/hbm.21380

Pope, P. A., & Miall, R. C. (2012). Task-specific facilitation of cognition by cathodal transcranial direct current stimulation of the cerebellum. *Brain Stimulation*, *5*(2), 84–94. http://doi.org/10.1016/j.brs.2012.03.006

Poreisz, C., Boros, K., Antal, A., & Paulus, W. (2007). Safety aspects of transcranial direct current stimulation concerning healthy subjects and patients. *Brain Research Bulletin*, *72*(4–6), 208–214. http://doi.org/10.1016/j.brainresbull.2007.01.004

Presacco, A., Goodman, R., Forrester, L., & Contreras-Vidal, J. L. (2011). Neural decoding of treadmill walking from noninvasive electroencephalographic signals. *Journal of Neurophysiology*, *106*(4), 1875–87. http://doi.org/10.1152/jn.00104.2011

Priori, A. (2003). Brain polarization in humans: a reappraisal of an old tool for prolonged non-invasive modulation of brain excitability. *Clinical Neurophysiology*, *114*(4), 589–595. http://doi.org/10.1016/S1388-2457(02)00437-6

Priori, A., Foffani, G., Rossi, L., & Marceglia, S. (2013). Adaptive deep brain stimulation (aDBS) controlled by local field potential oscillations. *Experimental Neurology*, *245*, 77–86. http://doi.org/10.1016/j.expneurol.2012.09.013

Purpura, D. P., & McMurtry, J. G. (1965). Intracellular Activities and Evoked Potential Changes During Polarization of Motor Cortex. *Journal of Neurophysiology*, *28*(1), 166–85. Retrieved from http://www.ncbi.nlm.nih.gov/pubmed/14244793

Qin, L., Ding, L., & He, B. (2004). Motor imagery classification by means of source analysis for brain–computer interface applications. *Journal of Neural Engineering*, *1*(3), 135–141. http://doi.org/10.1088/1741-2560/1/3/002

Qin, L., & He, B. (2005). A wavelet-based time-frequency analysis approach for

classification of motor imagery for brain-computer interface applications. *Journal of Neural Engineering*, *2*(4), 65–72. http://doi.org/10.1088/1741-2560/2/4/001
Radman, T., Ramos, R. L., Brumberg, J. C., & Bikson, M. (2009). Role of cortical cell type and morphology in subthreshold and suprathreshold uniform electric field stimulation in vitro. *Brain Stimulation*, *2*(4), 215–28, 228–3. http://doi.org/10.1016/j.brs.2009.03.007
Rahman, A., Toshev, P. K., & Bikson, M. (2013). Polarizing cerebellar neurons with transcranial Direct Current Stimulation. *Clinical Neurophysiology*, *125*, 1–4. http://doi.org/10.1016/j.clinph.2013.10.003
Ramos-Murguialday, A., Broetz, D., Rea, M., Läer, L., Yilmaz, O., Brasil, F. L., … Birbaumer, N. (2013). Brain-machine interface in chronic stroke rehabilitation: A controlled study. *Annals of Neurology*, *74*(1), 100–8. http://doi.org/10.1002/ana.23879
Ramoser, H., Müller-Gerking, J., & Pfurtscheller, G. (2000). Optimal spatial filtering of single trial EEG during imagined hand movement. *IEEE Transactions on Rehabilitation Engineering : A Publication of the IEEE Engineering in Medicine and Biology Society*, *8*(4), 441–6. Retrieved from http://www.ncbi.nlm.nih.gov/pubmed/11204034
Reis, J., & Fritsch, B. (2011). Modulation of motor performance and motor learning by transcranial direct current stimulation. *Current Opinion in Neurology*, *24*(6), 590–6. http://doi.org/10.1097/WCO.0b013e32834c3db0
Reis, J., Schambra, H. M., Cohen, L. G., Buch, E. R., Fritsch, B., Zarahn, E., … Krakauer, J. W. (2009). Noninvasive cortical stimulation enhances motor skill acquisition over multiple days through an effect on consolidation. *Proceedings of the National Academy of Sciences of the United States of America*, *106*(5), 1590–5. http://doi.org/10.1073/pnas.0805413106
Roy, A., Baxter, B., & Bin He. (2014). High-Definition Transcranial Direct Current Stimulation Induces Both Acute and Persistent Changes in Broadband Cortical Synchronization: A Simultaneous tDCS-EEG Study. *IEEE Transactions on Biomedical Engineering*, *61*(7), 1967–1978. http://doi.org/10.1109/TBME.2014.2311071
Royer, A. S., & He, B. (2009). Goal selection versus process control in a brain-computer interface based on sensorimotor rhythms. *Journal of Neural Engineering*, *6*(1), 16005. http://doi.org/10.1088/1741-2560/6/1/016005
Ruffini, G., Fox, M. D., Ripolles, O., Miranda, P. C., & Pascual-Leone, A. (2014). Optimization of multifocal transcranial current stimulation for weighted cortical pattern targeting from realistic modeling of electric fields. *NeuroImage*, *89*, 216–225. http://doi.org/10.1016/j.neuroimage.2013.12.002
Sadleir, R. J., Vannorsdall, T. D., Schretlen, D. J., & Gordon, B. (2010). Transcranial direct current stimulation (tDCS) in a realistic head model. *NeuroImage*, *51*(4), 1310–8. http://doi.org/10.1016/j.neuroimage.2010.03.052
Salari, N., Büchel, C., & Rose, M. (2012). Functional dissociation of ongoing oscillatory brain states. *PloS One*, *7*(5), e38090. http://doi.org/10.1371/journal.pone.0038090
Sameshima, K., & Baccala, L. A. (2001). Partial directed coherence: a new concept in

neural structure determination. *Biological Cybernetics*, *84*(6), 463–474. http://doi.org/10.1007/PL00007990

Schalk, G., McFarland, D. J., Hinterberger, T., Birbaumer, N., & Wolpaw, J. R. (2004). BCI2000: a general-purpose brain-computer interface (BCI) system. *IEEE Transactions on Bio-Medical Engineering*, *51*(6), 1034–43. http://doi.org/10.1109/TBME.2004.827072

Scherer, R., & Pfurtscheller, G. (2013). Thought-based interaction with the physical world. *Trends in Cognitive Sciences*, *17*(10), 490–2. http://doi.org/10.1016/j.tics.2013.08.004

Schneider, T., & Neumaier, A. (2001). Algorithm 808: ARfit---a matlab package for the estimation of parameters and eigenmodes of multivariate autoregressive models. *ACM Transactions on Mathematical Software*, *27*(1), 58–65. http://doi.org/10.1145/382043.382316

Schomer, D. L., & Lopes da Silva, F. (2010). *Niedermeyer's Electroencephalography: Basic Principles, Clinical Applications, and Related Fields*. *Book* (Vol. 1). Retrieved from http://books.google.com/books?hl=fr&lr=&id=xSKqZxXOlukC&pgis=1

Sehm, B., Schäfer, A., Kipping, J., Margulies, D., Conde, V., Taubert, M., … Ragert, P. (2012). Dynamic modulation of intrinsic functional connectivity by transcranial direct current stimulation. *Journal of Neurophysiology*, *108*(12), 3253–63. http://doi.org/10.1152/jn.00606.2012

Sellers, E. W., Mcfarland, D. J., Vaughan, T. M., & Wolpaw, J. R. (2010). BCIs in the Laboratory and at Home : The Wadsworth Research Program. *New York*, 97–111. http://doi.org/10.1007/978-3-642-02091-9

Sellers, E. W., Vaughan, T. M., & Wolpaw, J. R. (2010). A brain-computer interface for long-term independent home use. *Amyotrophic Lateral Sclerosis : Official Publication of the World Federation of Neurology Research Group on Motor Neuron Diseases*, *11*(5), 449–55. http://doi.org/10.3109/17482961003777470

Silvester, P. P., & Ferrari, R. L. (1996). *Finite Elements for Electrical Engineers*. Cambridge, UK: Cambridge University Press.

Silvoni, S., Ramos-Murguialday, a., Cavinato, M., Volpato, C., Cisotto, G., Turolla, a., … Birbaumer, N. (2011). Brain-Computer Interface in Stroke: A Review of Progress. *Clinical EEG and Neuroscience*, *42*(4), 245–252. http://doi.org/10.1177/155005941104200410

Soekadar, S. R., Birbaumer, N., & Cohen, L. G. (2011). Brain – Computer Interfaces in the Rehabilitation of Stroke and Neurotrauma. *Stroke*, 3–18. http://doi.org/10.1007/978-4-431-54008-3

Soekadar, S. R., Witkowski, M., Cossio, E. G., Birbaumer, N., & Cohen, L. G. (2014). Learned EEG-based brain self-regulation of motor-related oscillations during application of transcranial electric brain stimulation: feasibility and limitations. *Frontiers in Behavioral Neuroscience*, *8*(March), 93. http://doi.org/10.3389/fnbeh.2014.00093

Soekadar, S. R., Witkowski, M., Cossio, E. G., Birbaumer, N., Robinson, S. E., & Cohen, L. G. (2013). In vivo assessment of human brain oscillations during application of

transcranial electric currents. *Nature Communications*, *4*(May), 2032. http://doi.org/10.1038/ncomms3032

Stagg, C., Jayaram, G., Pastor, D., Kincses, Z. T., Matthews, P. M., & Johansen-Berg, H. (2011). Polarity and timing-dependent effects of transcranial direct current stimulation in explicit motor learning. *Neuropsychologia*, *49*(5), 800–4. http://doi.org/10.1016/j.neuropsychologia.2011.02.009

Stagg, C., & Nitsche, M. (2011). Physiological basis of transcranial direct current stimulation. *The Neuroscientist*, *17*(1), 37–53. http://doi.org/10.1177/1073858410386614

Stephan, K. E., Schlagenhauf, F., Huys, Q. J. M., Raman, S., Aponte, E. A., Brodersen, K. H., … Heinz, A. (2015). Computational neuroimaging strategies for single patient predictions. *NeuroImage*. http://doi.org/10.1016/j.neuroimage.2016.06.038

Strickland, E. (2017). Facebook Announces "Typing-by-Brain" Project. Retrieved January 6, 2017, from http://spectrum.ieee.org/the-human-os/biomedical/bionics/facebook-announces-typing-by-brain-project

Tadel, F., Baillet, S., Mosher, J. C., Pantazis, D., & Leahy, R. M. (2011). Brainstorm: A user-friendly application for MEG/EEG analysis. *Computational Intelligence and Neuroscience*, *2011*. http://doi.org/10.1155/2011/879716

Terney, D., Chaieb, L., Moliadze, V., Antal, A., & Paulus, W. (2008). Increasing human brain excitability by transcranial high-frequency random noise stimulation. *The Journal of Neuroscience : The Official Journal of the Society for Neuroscience*, *28*(52), 14147–55. http://doi.org/10.1523/JNEUROSCI.4248-08.2008

van Wijk, B. C. M., Beek, P. J., & Daffertshofer, A. (2012). Neural synchrony within the motor system: what have we learned so far? *Frontiers in Human Neuroscience*, *6*(September), 252. http://doi.org/10.3389/fnhum.2012.00252

Velliste, M., Perel, S., Spalding, M. C., Whitford, A. S., & Schwartz, A. B. (2008). Cortical control of a prosthetic arm for self-feeding. *Nature*, *453*(7198), 1098–101. http://doi.org/10.1038/nature06996

Wang, C., Xia, B., Li, J., Yang, W., Xiao, D., Velez, A. C., & Yang, H. (2011). Motor Imagery BCI-based robot arm system. In *Motor Imagery BCI-based robot arm system* (pp. 181–184). IEEE.

Wei, P., He, W., Zhou, Y., & Wang, L. (2013). Performance of motor imagery brain-computer interface based on anodal transcranial direct current stimulation modulation. *IEEE Transactions on Neural Systems and Rehabilitation Engineering*, *21*(3), 404–15. http://doi.org/10.1109/TNSRE.2013.2249111

Wiethoff, S., Hamada, M., & Rothwell, J. C. (2014). Variability in response to transcranial direct current stimulation of the motor cortex. *Brain Stimulation*, *7*(3), 468–475. http://doi.org/10.1016/j.brs.2014.02.003

Wolpaw, J., Birbaumer, N., McFarland, D., Pfurtscheller, G., & Vaughan, T. (2002). Brain-computer interfaces for communication and control. *Clinical Neurophysiology*, *113*(6), 767–91. Retrieved from http://www.ncbi.nlm.nih.gov/pubmed/12048038

Wolpaw, J., & Boulay, C. (2010). *Brain-Computer Interfaces*. (B. Graimann, G. Pfurtscheller, & B. Allison, Eds.)*New York*. Berlin, Heidelberg: Springer Berlin

Heidelberg. http://doi.org/10.1007/978-3-642-02091-9
Wolpaw, J. R., & McFarland, D. J. (2004). Control of a two-dimensional movement signal by a noninvasive brain-computer interface in humans. *Proceedings of the National Academy of Sciences of the United States of America*, *101*(51), 17849–54. http://doi.org/10.1073/pnas.0403504101
Wolpaw, J. R., McFarland, D. J., Neat, G. W., & Forneris, C. A. (1991). An EEG-based brain-computer interface for cursor control. *Electroencephalography and Clinical Neurophysiology*, *78*, 252–259. http://doi.org/10.1016/0013-4694(91)90040-B
Wolpaw, J., & Wolpaw, E. W. (2012). *Brain Computer Interfaces: Principles and Practice*. Oxford University Press.
Wurzman, R., Hamilton, R., Pascual-Leone, A., & Fox, M. (2016). An open letter concerning do-it-yourself (DIY) users of transcranial direct current stimulation (tDCS). *Annals of Neurology*, 1–4. http://doi.org/10.1002/ana.24689
Yuan, H., Doud, A., Gururajan, A., & He, B. (2008). Cortical imaging of event-related (de)synchronization during online control of brain-computer interface using minimum-norm estimates in frequency domain. *IEEE Transactions on Neural Systems and Rehabilitation Engineering*, *16*(5), 425–31. http://doi.org/10.1109/TNSRE.2008.2003384
Yuan, H., & He, B. (2014). Brain-Computer Interfaces Using Sensorimotor Rhythms: Current State and Future Perspectives. *IEEE Transactions on Biomedical Engineering*, *61*(5), 1425–1435. http://doi.org/10.1109/TBME.2014.2312397
Zaghi, S., Acar, M., Hultgren, B., Boggio, P. S., & Fregni, F. (2010). Noninvasive brain stimulation with low-intensity electrical currents: putative mechanisms of action for direct and alternating current stimulation. *The Neuroscientist : A Review Journal Bringing Neurobiology, Neurology and Psychiatry*, *16*(3), 285–307. http://doi.org/10.1177/1073858409336227
Zander, T. O., & Kothe, C. (2011). Towards passive brain-computer interfaces: applying brain-computer interface technology to human-machine systems in general. *Journal of Neural Engineering*, *8*(2), 25005. http://doi.org/10.1088/1741-2560/8/2/025005
Zhang, X., Zhu, S., & He, B. (2010). Imaging Electric Properties of Biological Tissues by RF Field Mapping in MRI. *IEEE Transactions on Medical Imaging*, *29*(2), 474–481. http://doi.org/10.1109/TMI.2009.2036843
Zimerman, M., & Hummel, F. C. (2014). *Brain Stimulation and its Role in Neurological Diseases*. *The Stimulated Brain*. Elsevier Inc. http://doi.org/10.1016/B978-0-12-404704-4.00012-0